Supporting Information

Systematic study of the synthesis and coordination of 2-(1,2,3-triazol-4-yl)-pyridine to Fe(II), Ni(II) and Zn(II); ion-induced folding into helicates, mesocates and larger architectures, and application to magnetism and self-selection

Nan Wu, Caroline F. C. Melan, Kristina A. Stevenson, Olivier Fleischel, Huan Guo, Fatemah Habib, Rebecca J. Holmberg, Muralee Murugesu, Nicholas J. Mosey, Hélène Nierengarten and Anne Petitjean*

Table of contents

p 2-13 Experimental synthetic details for the **synthesis** of ligands and complexes

p 14-22 Copy of **^{1}H** and **^{13}C NMR spectra** of new **organic compounds**

p 23-31 **NMR** data of **Fe(II) complexes** (stacked 1D plots, COSY, ageing, ^{19}F)

p 32-44 **UV-vis data** of Fe(II), Ni(II) and selected Zn (II) complexes

p 45-48 Details on **DFT calculations**: methods, spectra, transitions and molecular orbitals

p 49-51 **Mass spectrometry** analyses

p 51 **Vapour pressure osmometry** analysis

p 52 Details on **magnetic studies**

p 53-54 **Models**

p 54-81 **Revised crystallographic data** for $[Fe_2(\mathbf{L3})_3](BF_4)_4$ [CCDC# 1057879]

A. Synthesis

Materials and methods: Commercially available compounds were used as received. Deuterated solvents were used as received, except for $CDCl_3$ which was neutralized by passing through a short column of basic alumina (such treated $CDCl_3$ is signaled below by an asterisk, *i.e.,* '$CDCl_3$*'). ^{1}H NMR and ^{13}C NMR were performed using 300 MHz, 400 MHz and 500 MHz Bruker instruments. Peak listings for all NMR spectra are given in ppm and referenced against the solvent residual signal. UV-vis spectra were recorded on a Cary 50 spectrometer (200-1100 nm). Column chromatography was performed on silica gel with a particle size of 40-63 µm and a pore diameter of 60 Å. **Caution:** organic azides are potentially explosive. Handle with care.

A.1. Ligands

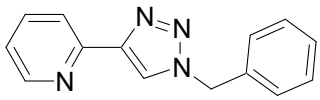

L1

2-Benzyl-1*H*-[1,2,3]triazol-4-yl-pyridine (L1):[1] Benzylazide (68 mg, 0.48 mmol, 1.0 equiv.) and 2-ethynylpyridine (50 mg, 0.48 mmol, 1.0 equiv.) were dissolved in *t*-BuOH (1 mL) into a microwave vial. A 10 mL solution of copper(II) sulphate pentahydrate (7.6 mg, 10 mol%) was prepared and 1 mL of this solution was used to dissolve sodium ascorbate (9.5 mg, 10 mol%). The latter solution was transferred to the starting microwave vial. The reaction mixture was stirred at 125°C using a 100 W irradiation power for 30 min. Upon cooling to room temperature, water (10 mL) was added to the homogeneous orange solution. The precipitate was filtered and washed with water (3 × 10 mL). The crude solid was stirred in water at room temperature and the aqueous solution filtered to give the expected compound as a white solid (90 mg, 80%). ^{1}H NMR ($CDCl_3$*, 300 MHz, 25°C): 8.55 (d, ^3J = 4.2 Hz, 1 H), 8.19 (d, ^3J = 8.1 Hz, 1 H), 8.06 (s, 1 H), 7.78 (dt, ^3J = 8.0 Hz, ^4J = 1.5 Hz, 1 H), 7.37 (m, 5 H), 7.22 (m, 1 H), 5.60 (s, 2 H). Mp: 110-112 °C; lit.: 110-112°C.[1]

2-Ethynyl-6-methylpyridine was prepared from 2-bromo-6-methylpyridine by Sonogashira coupling and deprotection (K_2CO_3, CH_3OH/CH_2Cl_2) according to literature protocols.[2]

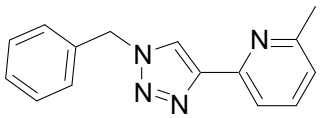

L1M

2-Benzyl-1*H*-[1,2,3]triazol-4-yl)-6-methylpyridine (L1M): Benzylbromide (210 mg, 1.23 mmol) was stirred in the presence of sodium azide (85 mg, 1.31 mmol, 1.1 equiv.) in DMF (20 mL) at room temperature for three days. To this solution were added 2-ethynyl-6-methylpyridine [2] (145 mg, 1.24 mmol, 1.0 equiv.), copper(II) sulfate pentahydrate

(122 mg, 0.49 mmol, 0.4 equiv.), sodium ascorbate (440 mg, 2.22 mmol, 1.8 equiv.) and water (5 mL). The mixture was stirred at room temperature for two days. To the resulting mixture were added water (70 mL) and a solution of saturated aqueous ethylenediaminetetraacetic acid/ammonia (16 mL/16 mL) and the mixture stirred. The resulting white precipitate was filtered, washed with water and dried. Purification by column chromatography (silica, 1:10 acetone/DCM) gave a white solid (243 mg, 80%). ^{1}H NMR ($CDCl_3$*, 400 MHz, 25°C): 8.05 (s, 1 H), 7.96 (d, ^{3}J = 7.8 Hz, 1 H), 7.63 (t, ^{3}J = 7.8 Hz, 1 H), 7.3-7.4 (m, 5 H), 7.06 (d, ^{3}J = 7.6 Hz, 1 H), 5.57 (s, 2 H), 2.52 (s, 2 H). ^{13}C NMR ($CDCl_3$*, 100 MHz): 158.3, 149.8, 138.1, 134.7, 129.3, 128.9, 122.5, 122.0, 117.4, 54.5, 24.6. R_f (SiO_2, 1:10 acetone:DCM) = 0.3. EA: *calc*. for $C_{15}H_{14}N_4$, % C 71.98, % H 5.64, % N 22.38, *found*, % C 71.91, % H 5.57, % N 22.48. EI-MS (+): 250.12 [M^+], 221.11 [$(M-N_2)^+$]. Mp: 140-142 °C.

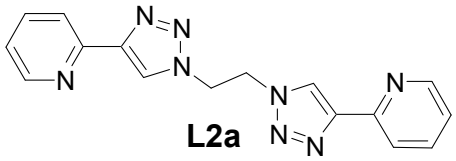

L2a

L2a: To a stirred solution of dibromoethane (135 µL, 1.57 mmol) in dimethylformamide (5 mL) and water (1 mL) were added sodium azide (238 mg, 3.6 mmol, 2.3 equiv.), copper(II) sulfate pentahydrate (161 mg, 0.63 mmol, 0.4 equiv.), sodium ascorbate (250 mg, 1.26 mmol, 0.8 equiv.) and 2-ethynylpyridine (404 µL, 4.00 mmol, 2.55 equiv.). The resulting orange mixture was stirred at room temperature overnight under argon and was then heated at 90 °C for 24 h. To the resulting mixture was added a solution of saturated aqueous ethylenediaminetetraacetic acid/ammonia (25 mL/15 mL) followed by ethyl acetate (100 mL). The organic layer was separated and washed with a mixture of saturated aqueous ethylenediaminetetraacetic acid/ammonia (10 mL/5 mL). The combined aqueous layers were extracted with ethyl acetate. The combined organic layers were dried with sodium sulfate and concentrated in vacuum. Recrystallization from 95% ethanol gave the expected compound with an overall yield of 50%. ^{1}H NMR (400 MHz, $CDCl_3$*): 8.51 (d, ^{3}J = 4.8 Hz, 2 H), 8.11 (d, ^{3}J = 7.8 Hz, 2 H), 8.03 (s, 2 H), 7.74 (td, ^{3}J = 7.7 Hz, ^{4}J = 1.5 Hz, 2 H), 7.20 (m, 2 H), 5.04 (s, 4 H). ^{13}C NMR (100 MHz, $CDCl_3$*): 149.9, 149.5, 148.9, 137.0, 123.2 (2 C), 120.5, 49.7. R_f (SiO_2, 1.0:0.8 CH_2Cl_2/acetone) = 0.27. EA: *calc*. for $C_{16}H_{14}N_8 \cdot 0.6\ H_2O$ % C 58.39, % H 4.65, % N 34.04, *found*, % C 58.69, % H 4.38, % N 33.70. EI-MS (+): 318.13 [M^+], 289.11 [$(M-N_2)^+$], 261.11 [$(M-2\ N_2)^+$]. Mp: 205 °C.

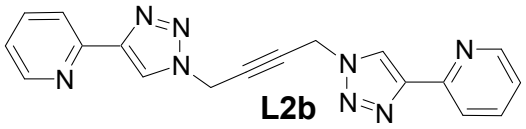

L2b

L2b: To a stirred solution of 1,4-dichlorobut-2-yne[3] (250 mg, 2.03 mmol) in dimethylformamide (2 mL) was added sodium azide (303 mg, 4.7 mmol, 2.3 equiv.). The light orange mixture was stirred at room temperature for 2 h. To the beige/orange mixture were added water (0. 8 mL), copper(II) sulfate pentahydrate (122 mg, 7.6×10^{-4} mol, 0.38 equiv.), sodium ascorbate (307 mg, 1.55 mmol, 0.76 equiv.) and 2-ethynylpyridine (420 µL, 4.2 mmol, 2.05 equiv.). The resulting mixture was stirred at room temperature under argon for 17 h. To the mixture were added a solution of saturated aqueous EDTA (15 mL), ammonia (5 mL) and water (30 mL). The resulting suspension was stirred vigorously in air for 20 h. The solid was filtered, washed with water and air-dried to yield the expected product as an off-white powder (635 mg, 91%). ^{1}H NMR (400 MHz, $CDCl_3$*): 8.58 (d, ^3J = 3.8 Hz, 2 H), 8.39 (s, 2 H), 8.17 (d, ^3J = 7.8 Hz, 2 H), 7.78 (td, ^3J = 7.6 Hz, ^4J = 1.6 Hz, 2 H), 7.24 (m, 2 H), 5.33 (s, 4 H). ^{13}C NMR (400 MHz, $CDCl_3$*): 150.0, 149.6, 149.0, 137.2, 123.2, 122.0, 120.5, 79.1, 40.2. EA: *calc*. for $C_{18}H_{14}N_8\cdot0.2\ H_2O$, % C 62.49, % H 4.20, % N 32.39, *found*, % C 62.48, % H 4.13, % N 32.31. EI-MS (+): 342.13 [M^+], 313.12 [$(M-N_2)^+$], 285.11 [$(M- 2\ N_2)^+$]. Mp: 235 °C (decomp.).

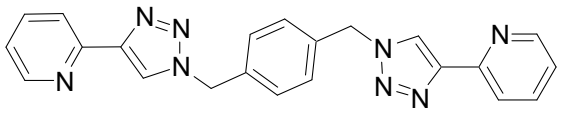

L2c

L2c:[4] To a stirred solution of *p*-dibromoxylene (455 mg, 1.72 mmol) in dimethylformamide (5 mL) and water (1 mL) was added sodium azide (257 mg, 3.96 mmol, 2.3 equiv.), copper(II) sulfate pentahydrate (175 mg, 0.69 mmol, 0.4 equiv.), sodium ascorbate (309 mg, 1.55 mmol, 0.9 equiv.) and 2-ethynylpyridine (380 µL, 3.78 mmol, 2.05 equiv.). The beige suspension was left to stir at room temperature under argon for three days. Concentrated aqueous ammonia (5 mL), saturated aqueous EDTA (5 mL) and water (40 mL) were added to the reaction mixture. The heterogeneous mixture was stirred vigorously in air until the yellow solid turned white and the solution turned dark green. The white precipitate was then filtered, washed with water, dried in air and recrystallized from hot 95% ethanol. The off-white precipitate was filtered and washed with cold ethanol to yield 576 mg of pure **L2**. A second crop of 33 mg was collected after cooling the filtrate in the freezer for two days, leading to an overall yield of 90 %. ^{1}H NMR (300

MHz, $CDCl_3$*): 8.54 (d, ^3J = 4.8 Hz, 2 H), 8.17 (d, ^3J = 7.9 Hz, 2 H), 8.06 (s, 2 H), 7.78 (td, ^3J = 7.6 Hz, ^4J = 1.5 Hz, 2 H), 7.35 (s, 4 H), 7.22 (m, 2 H), 5.59 (s, 4 H).[2] R_f (SiO_2, 1.0:0.8 CH_2Cl_2/acetone) = 0.39.

2,2-Bisbromomethylnaphthalene was prepared according to literature procedures by $LiAlH_4$ reduction of the commercially available diester[5] followed by bromination with PBr_3.[5]

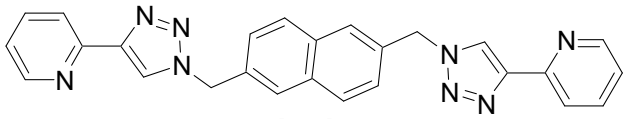

L2d

L2d: To a stirred solution of 2,2-bisbromomethylnaphthalene (300 mg, 0.95 mmol) in dimethylformamide (12 mL) was added sodium azide (180 mg, 2.77 mmol, 2.90 equiv.). The mixture was stirred at room temperature for 5 h. Then were added water (3 mL), copper(II) sulfate pentahydrate (95 mg, 0.38 mmol, 0.4 equiv.), sodium ascorbate (170 mg, 0.85 mmol, 0.9 equiv.) and 2-ethynylpyridine (207 µL, 2.04 mmol, 2.15 equiv.). The resulting mixture was stirred at room temperature under argon for 20 h. To the mixture were added a solution of saturated aqueous EDTA (6 mL), ammonia (6 mL) and water (30 mL). The resulting suspension was stirred vigorously in air until the solution became dark green and the precipitate white. The solid was filtered, washed with water, air-dried and purified by recrystallization from hot 95% ethanol to give pure **L2b** as a white powder with an overall yield of 74%. ^{1}H NMR (500 MHz, $CDCl_3$*): 8.52 (br d, ^3J = 4 Hz, 2 H), 8.18 (d, ^3J = 7.8 Hz, 2 H), 8.08 (s, 2 H), 7.84 (d, ^3J = 8.6 Hz, 2 H), 7.80 (s, 2 H), 7.77 (td, ^3J = 7.8 Hz, 2 H), 7.45 (d, ^3J = 8.2 Hz, 2 H), 7.20 (dd, ^3J = 7 Hz, ^3J = 5 Hz, 2 H), 5.76 (s, 4 H). ^{13}C NMR (100 MHz, $CDCl_3$*): 150.5, 149.7, 149.2, 137.2, 133.47, 133.12, 129.62, 127.8, 126.7, 123.3, 122.39, 120.64, 54.7. R_f (SiO_2, 1:1 DCM/acetone) = 0.56. EA: *calc*. for $C_{26}H_{20}N_8 \cdot 0.25\ H_2O$, % C 69.55, % H 4.60, % N 24.96, *found*, % C 69.76, % H 4.50, % N 24.70. EI-MS (+): 444.18 [M^+], 416.17 [$(M-N_2)^+$]. Mp: 233-235 °C.

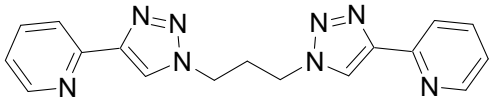

L3

L3:[4] To a stirred solution of dibromopropane (153 µL, 1.51 mmol) in dimethylformamide (2 mL) was added sodium azide (233 mg, 3.47 mmol, 2.3 equiv.). The mixture was stirred at 80 °C for 24 h. Then were added dimethylformamide (0.5 mL) and water (0.5 mL), copper(II) sulfate pentahydrate (153 mg, 0.6 mmol, 0.4 equiv.), sodium ascorbate (243 mg, 1.21 mmol, 0.8 equiv.) and 2-ethynylpyridine (313 µL, 3.10 mmol, 2.05 equiv.). The

resulting mixture was stirred at room temperature under argon for 20 h. To the mixture were added a solution of saturated aqueous EDTA (5 mL), ammonia (5 mL) and water (15 mL). The resulting suspension was stirred vigorously in air until the solution became dark green and the precipitate white. The solid was filtered, washed with water, air-dried and purified by flash column chromatography on silica gel (dichloromethane/acetone/chloroform) to give pure **L3** as a white powder with an overall yield of 83%. ^{1}H NMR (300 MHz, $CDCl_3$*): 8.60 (d, ^{3}J = 4.8 Hz, 2 H), 8.24 (s, 2 H), 8.17 (d, ^{3}J = 7.9 Hz, 2 H), 7.79 (td, ^{3}J = 7.7 Hz, ^{4}J = 1.7 Hz, 2 H), 7.24 (m, 2 H), 4.52 (t, ^{3}J = 6.4 Hz, 4 H), 2.68 (q, 2 H). ^{13}C NMR (400 MHz, $CDCl_3$*): 149.98, 149.44, 148.65, 136.93, 122.99, 122.67, 120.25, 46.95, 30.58. R_f (SiO_2, 1.0:1.2 DCM/acetone) = 0.36. Mp: 193 °C; lit.: 184 °C (decomp.).[4]

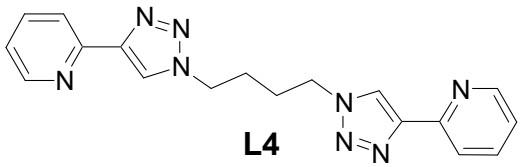

L4

L4: To a stirred solution of 1,4-dibromobutane (180 µL, 1.51 mmol) in dimethylformamide (2.5 mL) was added sodium azide (226 mg, 3.47 mmol, 2.30 equiv.). The mixture was stirred at 80°C for 24 h. Then were added dimethylformamide (0.6 mL), water (0.6 mL), copper(II) sulfate pentahydrate (153 mg, 0.60 mmol, 0.4 equiv.), sodium ascorbate (145 mg, 1.36 mmol, 0.9 equiv.) and 2-ethynylpyridine (330 µL, 3.25 mmol, 2.15 equiv.). The resulting mixture was stirred at room temperature under argon for 20 h. To the mixture were added a solution of saturated aqueous EDTA (5 mL), ammonia (5 mL) and water (15 mL). The resulting suspension was stirred vigorously in air until the solution became dark green and the precipitate white. The solid was filtered, washed with water, air-dried and purified by recrystallization from hot 95% ethanol to give pure **L4** as a white powder with an overall yield of 73%. The product was further purified using column chromatography using 0.5:1 dichloromethane: acetone as the eluent. This afforded white powdered crystals in 70% yield. ^{1}H NMR (400 MHz, $CDCl_3$*): 8.57 (br d, ^{3}J = 5 Hz, 2 H), 8.18 (d, ^{3}J = 7.8 Hz, 2 H), 8.14 (s, 2 H), 7.79 (td, ^{3}J = 7.7 Hz, ^{4}J =1.5 Hz, 2 H), 7.24 (br t, 2 H), 4.48 (br m, 4 H), 2.03 (br m, 4 H). ^{13}C NMR (100 MHz, $CDCl_3$*, signals read from HSQC and HMBC, as the ligand was not soluble enough to collect 1D ^{13}C NMR data): 150.0, 148.8, 148.8, 137.8, 123.1, 122.4, 121.0, 49.9, 27.5. R_f (SiO_2, 1:2 CH_2Cl_2/acetone) = 0.23. EA: *calc*. for $C_{18}H_{18}N_8$ 0.05 CH_2Cl_2 % C 61.83, % H 5.20, % N 31.96, *found*, % C 61.84, % H 5.17, % N

32.28. EI-MS (+): 346.16 [M^+], 318.16 [$(M-N_2)^+$], 201.11 [(M-triazolopyridine)$^+$], 159.09 [(triazolopyridine-CH_2)$^+$]. Mp: 223-224 °C.

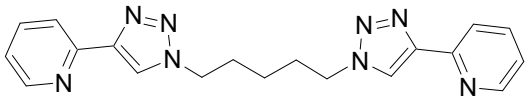

L5

L5: To a stirred solution of 1,5-dibromopentane (180 µL, 1.32 mmol) in dimethylformamide (2.2 mL) was added sodium azide (198 mg, 3.04 mmol, 2.30 equiv.). The mixture was stirred at 80°C for 24 h. Then were added dimethylformamide (0.5 mL), water (0.5 mL), copper(II) sulfate pentahydrate (132 mg, 0.53 mmol, 0.9 equiv.), sodium ascorbate (236 mg, 1.19 mmol, 0.9 equiv.) and 2-ethynylpyridine (290 µL, 2.84 mmol, 2.15 equiv.). The resulting mixture was stirred at room temperature under argon for 20 h. To the mixture were added a solution of saturated aqueous EDTA (4.5 mL), ammonia (4.5 mL) and water (15 mL). The resulting suspension was stirred vigorously in air until the solution became dark green and the precipitate white. The solid was filtered, washed with water, air-dried and purified by recrystallization from hot 95% ethanol to give pure **C5** as a white powder with an overall yield of 77%. The product was further purified using column chromatography using 0.5:1 dichloromethane: acetone as the eluent. This afforded white powdered crystals in 74% yield. ^{1}H NMR (400 MHz, $CDCl_3$*): 8.57 (d, ^3J = 4.6 Hz, 2 H), 8.17 (d, ^3J = 8.1 Hz, 2 H), 8.11 (s, 2 H), 7.77 (td, ^3J = 7.7 Hz, ^4J = 1.6 Hz, 2 H), 7.23 (dd, ^3J = 7.2 Hz, ^4J = 4.9 Hz, 2 H), 4.42 (t, ^3J = 7.1 Hz, 4 H), 2.03 (quin, ^3J = 7.4 Hz, 4 H), 1.43 (m, 2 H). ^{13}C NMR (100 MHz, $CDCl_3$*): 150.6, 149.8, 148.9, 137.2, 123.5, 122.2, 120.6, 50.4, 30.0, 23.8. R_f (SiO_2, 1:2 CH_2Cl_2/acetone) = 0.32. EA: *calc*. for $C_{19}H_{20}N_8$, % C 63.32, % H 5.59, % N 31.09, *found*, % C 63.34, % H 5.54, % N 31.22. EI-MS (+): 360.18 [M^+], 215.13 [(M-triazolopyridine)$^+$]. Mp: 184-185 °C.

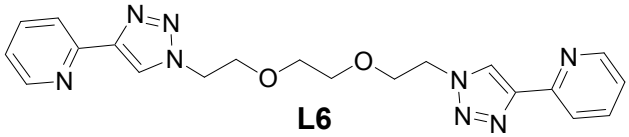

L6

L6 was prepared from the isolated bis azide reagent (1-azido-2-[2-(2-azidoethoxy)-ethoxy]-ethane). 1-Azido-2-[2-(2-azido-ethoxy)-ethoxy]-ethane was prepared from 1-chloro-2-[2-(2-chloroethoxy)-ethoxy]-ethane according to reference 6.[6] **L6** was then prepared under microwave conditions. Into a microwave vial were introduced 1.0 mL of a 5.0 mM copper(II) sulfate solution (5.0 µmol, 0.01 equiv.), sodium ascorbate (9.9 mg, 50 µmol, 0.1 equiv.), 1-azido-2-[2-(2-azidoethoxy)-ethoxy]-ethane (100 mg, 0.5 mmol), 2-ethynylpyridine (108 mg, 1.05 mmol, 2.1 equiv.) and tert-butanol (1.0

mL). The microwave vial was sealed and subjected to a 100 W power and 125 °C for 30 minutes. Water (10 mL) was then added and the solution extracted with dichloromethane (5×5 mL). The combined organic layers were dried on sodium sulfate, filtered and evaporated to dryness to give a brown oil that slowly crystallized. Recrystallization from chloroform and hexane gave the desired product (170 mg, 80% yield) as light colorless needles. ^{1}H NMR (400 MHz, 1:1 $CDCl_3$* / CD_3CN): 8.51 (br m, 2 H), 8.33 (s, 2 H), 8.03 (d, ^{3}J = 7.8 Hz, 2 H), 7.76 (t, ^{3}J = 7.8 Hz, ^{4}J = 1.6 Hz, 2 H), 7.22 (m, 2 H), 4.58 (t, ^{3}J = 5.0 Hz, 4 H), 3.86 (t, ^{3}J = 5.0 Hz, 4 H), 3.58 (s, 4 H). ^{13}C NMR (100 MHz, $CDCl_3$*): 150.7, 149.6, 148.6, 137.1, 123.5, 123.0, 120.4, 70.7, 69.7, 50.6. EA: *calc*. for $C_{20}H_{22}N_8O_2$, % C 59.10, % H 5.46, % N 27.57, *found*, % C 59.17, % H 5.43, % N 27.56. EI-MS (+): 406.19 [M^+], 378.18 [$(M-N_2)^+$], 285.11 [$(M- 2 N_2)^+$]. Mp: 92.0-92.5 °C.

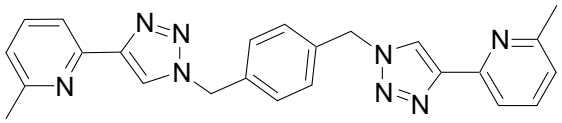

L2cM

L2cM: A mixture of α,α'-dibromo-*p*-xylene (145 mg, 0.55 mmol) and sodium azide (79 mg, 1.2 mmol, 2.2 equiv.) in dimethylformamide (10 mL) was stirred at room temperature for 3 h. Then were added water (4.5 mL), copper(II) sulfate pentahydrate (55 mg, 0.22 mmol, 0.4 equiv.), sodium ascorbate (207 mg, 1.05 mmol, 1.9 equiv.) and 2-ethynyl-6-methylpyridine[2] (143 mg , 1.22 mmol, 2.15 equiv.). The resulting solution was degassed and stirred at room temperature under argon for 40 h. A solution of saturated aqueous EDTA (8 mL), ammonia (8 mL) and water (35 mL) were added and the resulting suspension was stirred vigorously in air until the solution became dark green and the precipitate white. The solid was filtered, washed with water, air-dried and purified by recrystallization (hot ethanol) to give pure **L2cM** as an off-white powder with an overall yield of 54%. ^{1}H NMR (400 MHz, $CDCl_3$*): 8.08 (s, 2 H), 7.94 (d, ^{3}J = 7.8 Hz, 2 H), 7.63 (t, ^{3}J = 7.8 Hz, 2 H), 7.32 (s, 4 H), 7.06 (d, ^{3}J = 7.8 Hz, 2 H), 5.58 (s, 4 H), 2.51 (s, 6 H). ^{13}C NMR (100 MHz, $CDCl_3$*): 158.6, 149.8, 149.5, 137.4, 135.6 , 129.2, 122.9, 122.3, 117.7, 54.1, 24.8. EA: *calc*. for $C_{24}H_{22}N_8 \cdot 1.3\ H_2O$ % C 64.65, % H 5.56, % N 25.13, *found*, % C 64.65, % H 5.45, % N 25.14. EI-MS (+): 422.20 [M^+]. Mp: 195-196 °C.

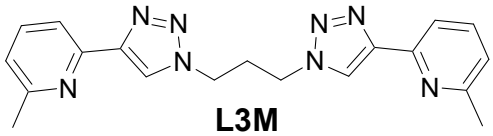

L3M

L3M: A mixture of 1,3-dibromopropane (118 mg, 0.58 mmol) and sodium azide (85 mg, 1.29 mmol, 2.2 equiv.) in dimethylformamide (12 mL) was stirred at room temperature for 20 h. Then were added water (3 mL), copper(II) sulfate pentahydrate (55

mg, 0.22 mmol, 0.4 equiv.), sodium ascorbate (214 mg, 1.08 mmol, 1.86 equiv.) and 2-ethynyl-6-methylpyridine[2] (148 mg , 1.26 mmol, 2.16 equiv.). The resulting mixture was stirred at room temperature under argon for 70 h. A solution of saturated aqueous EDTA (8 mL), ammonia (8 mL) and water (35 mL) were added and the resulting suspension was stirred vigorously in air until the solution became dark green and the precipitate white. The solid was filtered, washed with water, air-dried and purified by column (5:1 to 1:1 CH_2Cl_2/acetone) to give pure **L3M** as shiny white crystals with an overall yield of 78%. ^{1}H NMR (400 MHz, $CDCl_3$*): 8.24 (s, 2 H), 7.95 (d, ^3J = 7.6 Hz, 2 H), 7.66 (t, ^3J = 7.7 Hz, 2 H), 7.10 (d, ^3J = 7.6 Hz, 2 H), 4.49 (t, ^3J = 6.5 Hz, 4 H), 2.7 (quint.,^3J = 6.4 Hz, 2 H), 2.57 (s, 3 H). ^{13}C NMR (100 MHz, $CDCl_3$*): 158.7, 149.7, 149.3, 137.3, 122.9, 122.8, 117.5, 47.2, 31.0, 24.8. R_f (SiO_2, 1:1 CH_2Cl_2/acetone) = 0.27. EA: *calc*. for $C_{19}H_{20}N_8$, % C 63.32, % H 5.59, % N 31.09, *found*, % C 63.41, % H 5.64, % N 31.18. EI-MS (+): 360.18 [M^+], 201.11 [(M-triazolomethylpyridine)$^+$], 172.1 [(triazolomethyl-pyridine-CH_2)$^+$], 159.17 [(triazolomethyl-pyridine)$^+$]. Mp: 125.5-126.7 °C.

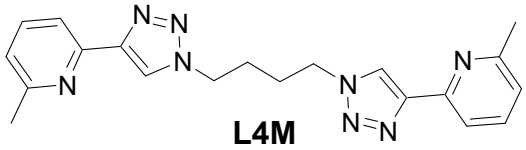

L4M: A mixture of 1,4-dibromobutane (99 mg, 0.46 mmol) and sodium azide (73 mg, 1.1 mmol, 2.4 equiv.) in dimethylformamide (10 mL) was stirred at 60 °C for 20 h. Then were added water (3 mL), copper(II) sulfate pentahydrate (54 mg, 0.22 mmol, 0.5 equiv.), sodium ascorbate (210 mg, 1.06 mmol, 2.3 equiv.) and 2-ethynyl-6-methylpyridine[2] (117 mg , 1.0 mmol, 2.2 equiv.). The resulting mixture was stirred at room temperature under argon for 48 h. After adding a solution of saturated aqueous EDTA (8 mL), ammonia (8 mL) and water (36 mL), the resulting suspension was stirred vigorously in air until the solution became dark green and the precipitate white. The solid was filtered, washed with water, air-dried and purified by column (5:1 to 1:1 CH_2Cl_2 / acetone) to give pure **L4M** as a white powder with an overall yield of 73%. ^{1}H NMR (400 MHz, $CDCl_3$*): 8.12 (s, 2 H), 7.94 (d, ^3J = 7.8 Hz, 2 H), 7.64 (t, ^3J = 7.7 Hz, 2 H), 7.1 (d, ^3J = 7.8 Hz, 2 H), 4.45 (br m, 4 H), 2.55 (s, 6 H), 2.02 (br m, 4 H). ^{13}C NMR (100 MHz, $CDCl_3$*): 158.6, 149.8, 149.3, 137.4, 122.8, 122.2, 117.6, 49.7, 27.4, 24.9. R_f (SiO_2, 1:1 CH_2Cl_2/acetone) = 0.27. EA: *calc*. for $C_{20}H_{22}N_8$, % C 64.15, % H 5.92, % N 29.93, *found*, % C 64.06, % H 5.93, % N 29.94. EI-MS (+): 374.19 [M^+], 215.13 [(M-triazolomethylpyridine)$^+$], 173.10 [(triazolomethyl-pyridine-CH_2)$^+$]. Mp: 185-187 °C.

A.2. Complexes

- M(**L1**)$_3^{2+}$: Nickel (II) and iron (II) complexes of ligand **L1** were obtained by mixing 1 equiv. of metal salt $[Ni(H_2O)_6](BF_4)_2$ and $[Fe(H_2O)_6](BF_4)_2$ respectively; typically 7×10^{-5} mol) with 3 equiv. of ligand **L1** in a mixture of dichloromethane and acetonitrile (typically 5 mL total), yielding a pink and dark orange solution, respectively. Very slowly vapour diffusion of diethylether led to the formation of single crystals.

- M_2(**L2a,c-L5**)$_3^{2+}$: Nickel(II) and iron(II) complexes of ligands **L2a-c**, **L3**, **L4** and **L5** were obtained by mixing 2 equiv. of metal salt $[Ni(H_2O)_6](BF_4)_2$ and $[Fe(H_2O)_6](BF_4)_2$ respectively; ~ 7×10^{-5} mol) with 3 equiv. of ligands **L2c** or **L5** in a mixture of dichloromethane or chloroform and acetonitrile (typically 5-7 mL total), yielding a pink or dark orange solution respectively. Very slowly vapour diffusion of diethyl ether led to the formation of bright single crystals or powders. In all cases, recovery yields were between 74 and 95%. Complexes of **L3** with iron(II) were prepared in degassed solvents and crystallized under argon to ensure no contamination with iron(III) which may interfere with the study of their magnetic behaviour. As discussed in the text, the other ligands bound to iron(II) only form low spin complexes, and no oxidation was observed neither in the crystal nor in solution, even after an extended period of time. Hence their preparation was conducted in non-degassed solvent, without the precaution of an inert gas atmosphere. *Note*: (i) gentle heating may be required to solubilize the reagents; (ii) any trace of unreacted ligand or metal ion was remove by filtration prior to diffusion of diethylether.

- M_2(**L3M**, **L4M**)$_3^{2+}$: Nickel(II) and iron(II) complexes of ligands **L3M**, **L4M** were obtained by mixing 2 equiv. of metal salt $[Ni(H_2O)_6](BF_4)_2$ and $[Fe(H_2O)_6](BF_4)_2$ respectively (typically 10^{-5} mol) with 3.0 equiv. of ligand in acetonitrile (1 mL). After sonication, solutions were obtained and were concentrated to dryness. The residue was then refluxed in CH_2Cl_2 (3 mL) for 2 h. The solid was filtered, washed with dichloromethane and dried in vacuo (typical yields are 51-55% of a bright yellow powders for the iron (II) complexes, and blue/purple powders for the nickel (II) complexes).

[Fe(**L1**)$_3$[(BF$_4$)$_2$: ^{1}H NMR (CD_3CN, 300 MHz, 25º C): 8.76 (br s, 3 H), 8.16 (br d, ^3J ~ 7.5 Hz, 3 H), 7.99 (br t, ^3J ~ 7 Hz, 3 H), 7.74 (br s, 3 H), 7.4 (br m, 12 H), 7.2 (br m, 8 H), 5.63 (br s, 8 H). UV-vis (CH_3CN; λ_{max} (nm) [$\log_{10}(\varepsilon)$]) 240 [4.6], 280 [4.6], 315 [3.7], 368 [sh; 3.6], 426 [3.9].

EA: $C_{42}H_{36}N_{12}FeB_2F_8 \cdot 0.55\ H_2O$, *calc.*: %C 53.20, %H 3.94, %N 17.73; *found*: %C 53.58, %H 4.32, %N 17.90.

[Fe(**L1M**)$_3$][(BF$_4$)$_2$: ^{1}H NMR (CD_3CN, 300 MHz, 25º C): broad signals 6-7 and 2-3.5 ppm. UV-vis (CH_3CN; λ_{max} (nm) [$\log_{10}(\varepsilon)$]) 242 [4.6], 290 [4.5], 294 [sh, 4.4], 302 [sh, 4.1]. EA: $C_{45}H_{42}N_{12}FeB_2F_8 \cdot 1.05\ H_2O$, *calc.*: %C 54.09, %H 4.45, %N 16.82; *found*: %C 54.23, %H 4.39, %N 16.68.

Iron complex(es) of **L2a**: mixtures of $[Fe(H_2O)_6](BF_4)_2$ (2 equiv.) and **L2a** (3 equiv.) gave ^{1}H NMR (CD_3CN, 300 MHz, 25 º C): broad signals mixed with sharp signals from a well defined structure (see stacked ^{1}H NMR spectra below); UV-vis (CH_3CN; λ_{max} (nm) [$\log_{10}(\varepsilon)$]): 240 [4.8], 280 [4.9], 315 [sh, 3.9], 370 [sh; 3.9], 420 [4.1].

[Fe$_2$(**L2b**)$_3$](BF$_4$)$_4$: ^{1}H NMR (CD_3CN, 300 MHz, 25 º C, *in situ* preparation): 8.84 (br s, 6 H), 8.22 (br d, ^3J = 7.3 Hz, 6 H); 8.07 (br t, 6 H), 7.61 (br d, 6 H), 7.38 (br t, 6 H), 5.37 (d, ^2J = 17 Hz, 6 H), 5.26 (d, ^2J = 17 Hz, 6 H). UV-vis (CH_3CN; λ_{max} (nm) [$\log_{10}(\varepsilon)$]) 240 [4.8], 280 [4.9], 320 [4.0], 370 [sh; 4.0], 420 [4.1].

[Fe$_2$(**L2c**)$_3$](BF$_4$)$_4$: ^{1}H NMR (CD_3CN, 300 MHz, 25 º C, *in situ* preparation): 8.82 (br s, 6 H), 8.15 (br d, ^3J = 7.4 Hz, 6 H); 8.08 (br t, ^3J = 7.4 Hz, 6 H), 7.80 (br d, ^3J = 5 Hz, 6 H), 7.4 (br m, 6 H), 7.26 (br s, 12 H), 5.50 (d, ^2J = 15 Hz, 6 H), 5.33 (d, ^2J = 15 Hz, 6 H). UV-vis (CH_3CN; λ_{max} (nm) [$\log_{10}(\varepsilon)$]) 241 [4.9], 281 [4.9], 314 [4.0], 371 [sh; 4.0], 428 [4.2]. EA: $C_{66}H_{54}N_{24}Fe_2B_4F_{16} \cdot 4.75\ H_2O$, *calc.*: %C 45.88, %H 3.70, %N 19.46; *found*: %C 46.27, %H 4.09, %N 19.56.

[Fe$_2$(**L2d**)$_3$](BF$_4$)$_4$: ^{1}H NMR (CD_3CN, 300 MHz, 25 º C, *in situ* preparation): 8.84 (br s, 6 H), 8.17 (br d, ^3J = 7.6 Hz, 6 H); 8.08 (br t, ^3J = 7.3 Hz, 6 H), 7.84 (br d, ^3J = 4 Hz, 6 H), 7.53 (br s, 6 H), 7.43 (br t, ^3J = 6 Hz, 6 H), 7.34 (br d, ^3J = 8 Hz, 6 H), 6.76 (br d, ^3J = 8 Hz, 6 H), 5.59 (d, ^2J = 15 Hz, 6 H), 5.32 (d, ^2J = 15 Hz, 6 H). UV-vis (CH_3CN; λ_{max} (nm) [$\log_{10}(\varepsilon)$]) 224 [5.2], 278 [4.9], 322 [3.9], 370 [sh; 3.8], 426 [4.0]. EA: $C_{78}H_{60}N_{24}Fe_2B_4F_{16} \cdot 3.6\ H_2O$, *calc.*: %C 50.44, %H 3.65, %N 18.10; *found*: %C 50.21, %H 3.39, %N 17.90.

[Fe$_2$(**L3**)$_3$](BF$_4$)$_4$: ^{1}H NMR (CD_3CN, 300 MHz, 25º C, *in situ* preparation): 8.69 (s, 6 H), 8.15 (br d, ^3J = 7 Hz, 6 H), 8.05 (br t, ^3J = 7 Hz, 6 H), 7.83 (br d, ^3J = 3 Hz, 6 H), 4.1-4.5 (br m, 12 H), 2.2-2.6 (br m, 6 H). UV-vis (CH_3CN; from titration data) λ_{max} (nm) [$\log_{10}(\varepsilon)$]) 240 [4.9], 280 [5.0], 320 [4.0], 376 [4.0], 414 [sh; 4.2], 426 [4.2]. EA: $C_{51}H_{48}N_{24}Fe_2B_4F_{16} \cdot 1.85\ CHCl_3$, *calc.*: %C 37.86, %H 3.00, %N 20.05; *found*: %C 37.60, %H 3.16, %N 20.29.

[Fe_2(**L4**)$_3$](BF$_4$)$_4$: ^{1}H NMR (CD_3CN, 400 MHz, 25º C, *in situ* preparation): 8.74 (s, 6 H), 8.15 (br d, ^3J = 7.9 Hz, 6 H), 8.07 (br t, ^3J = 7.5 Hz, 6 H), 7.83 (br m, 6 H), 7.43 (br t, 6 H), 4.2-4.5 (br m, 12 H), 1.6-1.8 (br m, 6 H). UV-vis (CH_3CN): λ_{max} (nm) [$\log_{10}(\varepsilon)$]) 240 [4.8], 280 [4.9], 320 [3.9], 370 [3.9], 425 [4.1]. EA: $C_{54}H_{54}B_4F_{16}Fe_2N_{24}$ · 5.7 H_2O, *calc*.: %C 40.52, %H 4.12, %N 21.00; *found*: %C 40.49, %H 3.91, %N 20.80.

[Fe_2(**L5**)$_3$](BF$_4$)$_4$: ^{1}H NMR (CD_3CN, 500 MHz, 25º C, *in situ* preparation): 8.70 (s, 6 H, 33%), 8.65 (s, 6 H, 66%), 8.08-8.18 (br m, 6 H, 100%), 8.00-8.8 (br t, 6 H, 100%), 7.87 (br d, ^3J = 3 Hz, 6 H, 66%), 7.8 (br d, 6 H, 33 %), 7.3-7.45 (br m, 6 H, 100%), 4.3-4.45 (br m, 12 H, 50 %), 4.2-4.3 (br m, 12 H, 50%), 1.9-2.0 (br s, mixed with solvent peak), 1.7-1.9 (br m, 12 H, 100%), 1.35-1.45 (br m, 3 H, 33%), 1.25-1.45 (br m, 3 H, 33%), 1.15-1.25 (br m, 6 H, 33 %). UV-vis (CH_3CN): λ_{max} (nm) [$\log_{10}(\varepsilon)$]) 240 [4.8], 280 [4.9], 320 [sh, 3.9], 370 [sh, 3.9], 430 [4.2]; EA: $C_{57}H_{60}B_4F_{16}Fe_2N_{24}$ · 4.5 H_2O, *calc*.: %C 42.23, %H 4.29, %N 20.73; *found*: %C 42.33, %H 4.41, %N 20.62.

[Fe_2(**L3M**)$_3$](BF$_4$)$_4$: ^{1}H NMR (CD_3CN, 300 MHz, 25º C, *in situ* preparation): very broad signals over 0-55 ppm. UV-vis (CH_3CN; from titration data): λ_{max} (nm) [$\log_{10}(\varepsilon)$]) 242 [4.7], 290 [4.8], 362 [2.9]. EA: $C_{57}H_{60}N_{24}Fe_2B_4F_{16}$·2.85 H_2O *calc*.: %C 43.02, %H 4.16, %N 21.12; *found*: %C 43.21, %H 4.03, %N 20.92.

[Fe_2(**L4M**)$_3$](BF$_4$)$_4$: ^{1}H NMR (CD_3CN, 300 MHz, 25º C, *in situ* preparation): very broad signals over 0-55 ppm. UV-vis (CH_3CN; from titration data): λ_{max} (nm) [$\log_{10}(\varepsilon)$]) 244 [4.8], 292 [4.8], 358 [3.2]. EA: $C_{60}H_{66}B_4F_{16}Fe_2N_{24}$ · 2.45 H_2O · 0.45 EtOAc *calc*.: %C 44.55, %H 4.51, %N 20.18; *found*: %C 44.51, %H 4.43, %N 20.11.

[Ni(**L1**)$_3$](BF$_4$)$_2$: UV-vis (CH_3CN; λ_{max} (nm) [$\log_{10}(\varepsilon)$]) 239 nm [4.6], 285 [4.4], 532 [1.1], 730 [sh], 796 [0.95], 864 [1.0]; EA: $C_{42}H_{36}N_{12}NiB_2F_8$·0.1 $CHCl_3$·0.1 H_2O, *calc*.: %C 52.96, %H 3.83, %N 17.60; *found*: %C 52.86, %H 4.05, %N 17.81.

[Ni(**L1M**)$_3$](BF$_4$)$_2$: UV-vis (CH_3CN; λ_{max} (nm) [$\log_{10}(\varepsilon)$]) 242 [4.6], 250 [sh, 4.5], 290 [4.5], 302 [sh, 4.3], 585 [1.0], 960 [1.4]. EA: $C_{45}H_{42}N_{12}NiB_2F_8$·2 H_2O·0.25 EtOAc, *calc*.: %C 53.06, %H 4.65, %N 16.14; *found*: %C 53.02, %H 4.57, %N 16.10.

[Ni_2(**L2c**)$_3$](BF$_4$)$_4$: UV-vis (CH_3CN; λ_{max} (nm) [$\log_{10}(\varepsilon)$]) 238 nm [4.9], 287 [4.8], 528 [1.4], 793 [1.3], 860 [1.3]; EA: $C_{66}H_{54}N_{24}Ni_2B_4F_{16}$·4.75 H_2O, *calc*.: %C 45.73, %H 3.69, %N 19.39; *found*: %C 45.84, %H 3.67, %N 19.29.

[Ni_2(**L2d**)$_3$](BF_4)$_4$: UV-vis (CH_3CN; λ_{max} (nm) [$\log_{10}(\varepsilon)$]) 226 nm [5.3], 284 [4.8], 514 [1.8], 790 [1.4], 850 [1.4]; EA: $C_{78}H_{60}N_{24}Ni_2B_4F_{16}\cdot 1.2\ CHCl_3\cdot 5.85\ H_2O$, *calc*.: %C 46.48, %H 3.59, %N 16.42; *found*: %C 46.51, %H 3.63, %N 16.45.

[Ni_2(**L3**)$_3$](BF_4)$_4$: UV-vis (CH_3CN; λ_{max} (nm) [$\log_{10}(\varepsilon)$]) 238 nm [4.8], 284 [4.7], 296 [sh], 534 [1.5], 720 [sh], 790 [1.3], 860 [1.3]; EA: $C_{51}H_{48}N_{24}Ni_2B_4F_{16}\cdot 0.6\ CHCl_3$, *calc*.: %C 40.42, %H 3.19, %N 21.92; *found*: %C 40.15, %H 3.52, %N 21.74.

[Ni_2(**L4**)$_3$](BF_4)$_4$: UV-vis (CH_3CN; λ_{max} (nm) [$\log_{10}(\varepsilon)$]) 242 nm [4.7], 287 [4.6], 294 [sh, 4.6], 532 [1.4], 800 [1.3], 855 [1.3]; EA: $C_{54}H_{54}N_{24}Ni_2B_4F_{16}\cdot 8.8\ H_2O\cdot 1.45$ EtOAc, *calc*.: %C 40.42, %H 4.68, %N 18.78; *found*: %C 40.04, %H 4.50, %N 18.60.

[Ni_2(**L5**)$_3$](BF_4)$_4$: UV-vis (CH_3CN; λ_{max} (nm) [$\log_{10}(\varepsilon)$]) 238 [4.8], 252 [sh, 4.6], 286 [4.6], 296 [sh, 4.5], 528 [1.4], 800 [1.3], 855 [1.3]; EA: $C_{57}H_{60}N_{24}Ni_2B_4F_{16}\cdot 4.9\ H_2O\cdot 0.4$ EtOAc, *calc*.: %C 42.16, %H 4.41, %N 20.14; *found*: %C 42.09, %H 4.22, %N 19.95.

[Ni_2(**L3M**)$_3$](BF_4)$_4$: UV-vis (CH_3CN; λ_{max} (nm) [$\log_{10}(\varepsilon)$]) 240 nm [4.8], 252 [sh, 4.7], 294 [4.8], 304 [sh, 4.7], 365 [sh, 1.6], 580 [1.2], 930 [1.6], 965 [1.6]; EA: $C_{57}H_{60}N_{24}Ni_2B_4F_{16}\cdot 2.3\ H_2O$ *calc*.: %C 43.13, %H 4.1, %N 21.18; *found*: %C 42.84, %H 4.35, %N 21.18.

[Ni_2(**L4M**)$_3$](BF_4)$_4$: UV-vis (CH_3CN; λ_{max} (nm) [$\log_{10}(\varepsilon)$]) 240 nm [4.7], 252 [sh, 4.5], 294 [4.7], 304 [sh, 4.6], 365 [sh, 1.7], 580 [1.4], 965 [1.6]; EA: $C_{60}H_{66}N_{24}Ni_2B_4F_{16}\cdot 4.1\ H_2O$, *calc*.: %C 43.37, %H 4.50, %N 20.23; *found*: %C 43.47, %H 4.38, %N 20.10.

[Cu_2(**L3M**)$_2$](BF_4)$_2$: To a solution of ligand **L3M** (5.2 mg, 1.4×10^{-5} mol) in degassed CD_3CN (480 µL) was added a solution of [$Cu(CH_3CN)_4$]BF_4 in CD_3CN (186 µL of a 78 mM solution in CD_3CN, 1.5×10^{-5} mol, 1.0 equiv.). Within 10 minutes, a yellow precipitate formed and was filtered, washed with CH_3CN, CH_2Cl_2, and dried under vacuum to yield 4 mg of a bright yellow, air stable powder. EA: $C_{38}H_{40}N_{16}Cu_2B_2F_8$, *calc*.: %C 44.68, %H 3.95, %N 21.94; *found*: %C 44.65, %H 3.78, %N 21.58.

References: [1] Z. Gonda, Z. Novák, *Dalton Trans*. **2010**, *39*, 726-729. [2] D. Alagille, R. M. Baldwin, B. L. Roth, J. T. Wroblewski, E. Grajkowska , G. D. Tamagnan, *Bioorg. Med. Chem.* **2005**, *13*, 197-210. [3] A. W. Johnson, *J. Chem. Soc*. **1946**, 1009-1014. [4] J. D. Crowley, P. H. Bandeen, *Dalton Trans*. **2010**, *39*, 612-623. [5] J. Campos Rosa, D. Galanakis, G. Robin, P.M. Dunn, *J. Med. Chem.* **1996**, *39*, 4247-4254. [6] A. B. J. Withey, G. Chen, T. L. Uyen Nguyen, M. H. Stenzel, *Biomacromolecules* **2009**, *10*, 3215-3226.

B. ^{1}H and ^{13}C NMR spectra of the ligands

L1M

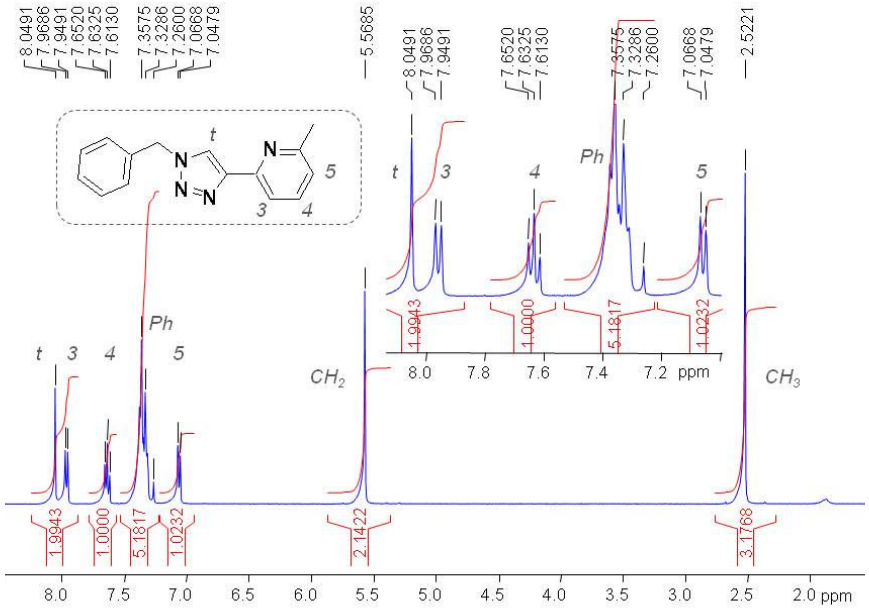

Figure S1: ^{1}H NMR of **L1M** in $CDCl_3$* (400 MHz, 25°C).

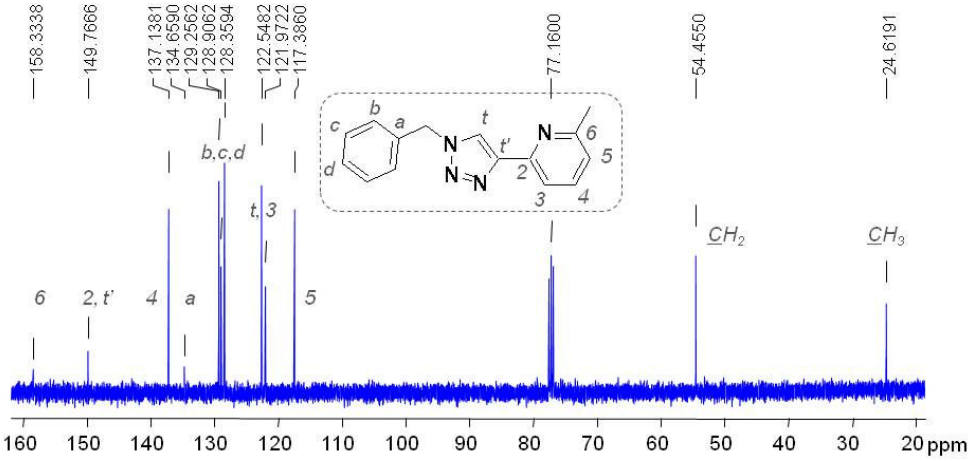

Figure S2: ^{13}C NMR of **L1M** in $CDCl_3$* (100 MHz, 25°C).

L2a

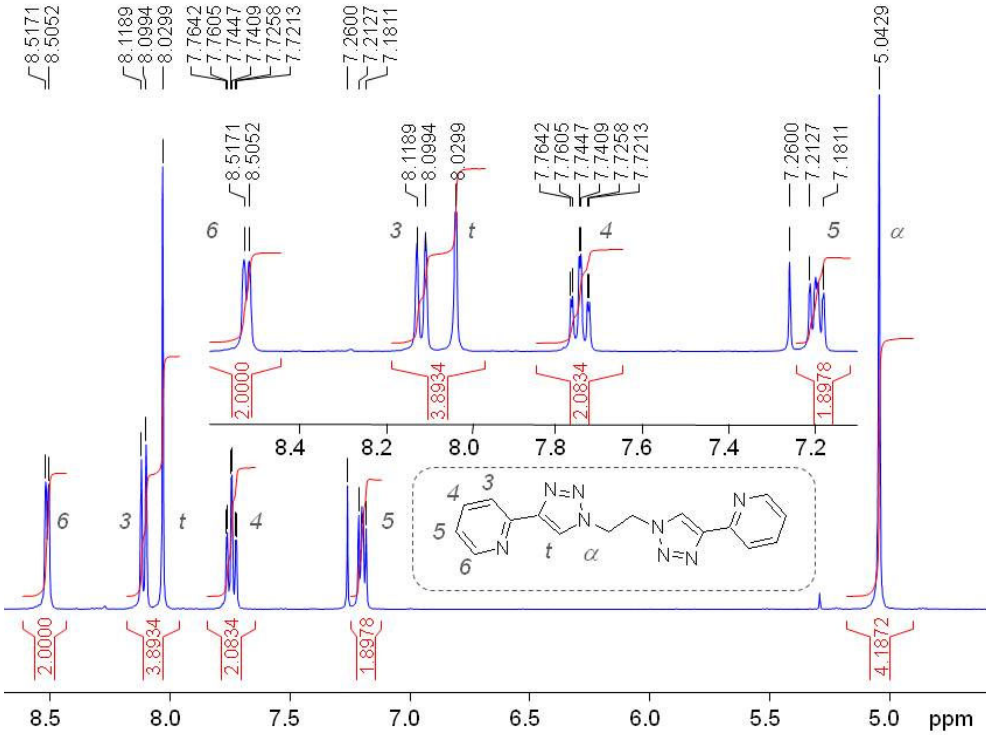

Figure S3: ^{1}H NMR of **L2a** in $CDCl_3$* (400 MHz, 25°C).

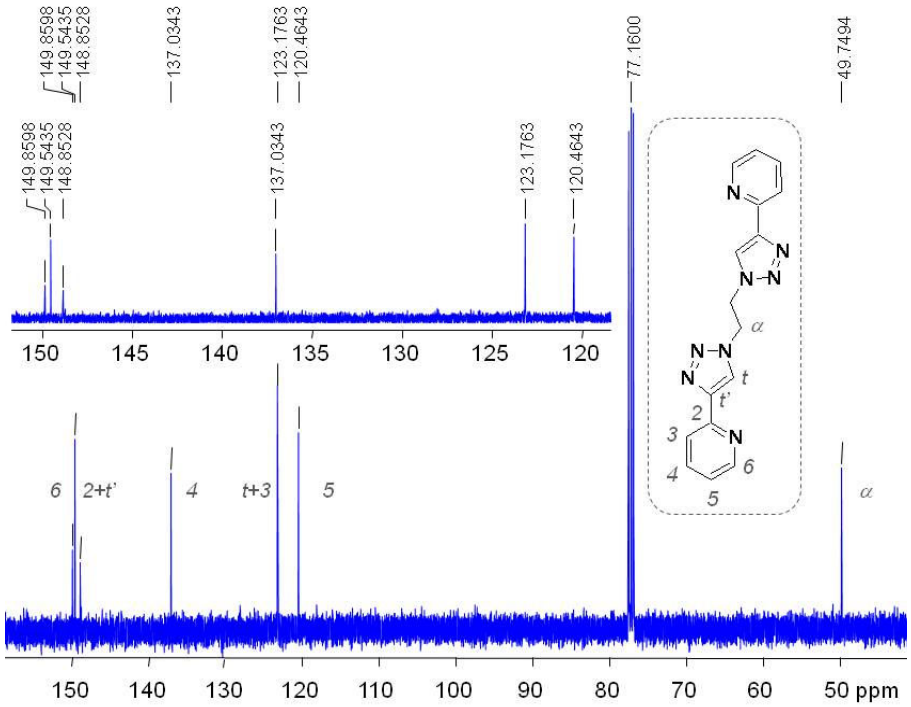

Figure S4: ^{13}C NMR of **L2a** in $CDCl_3$* (100 MHz, 25°C).

L2b

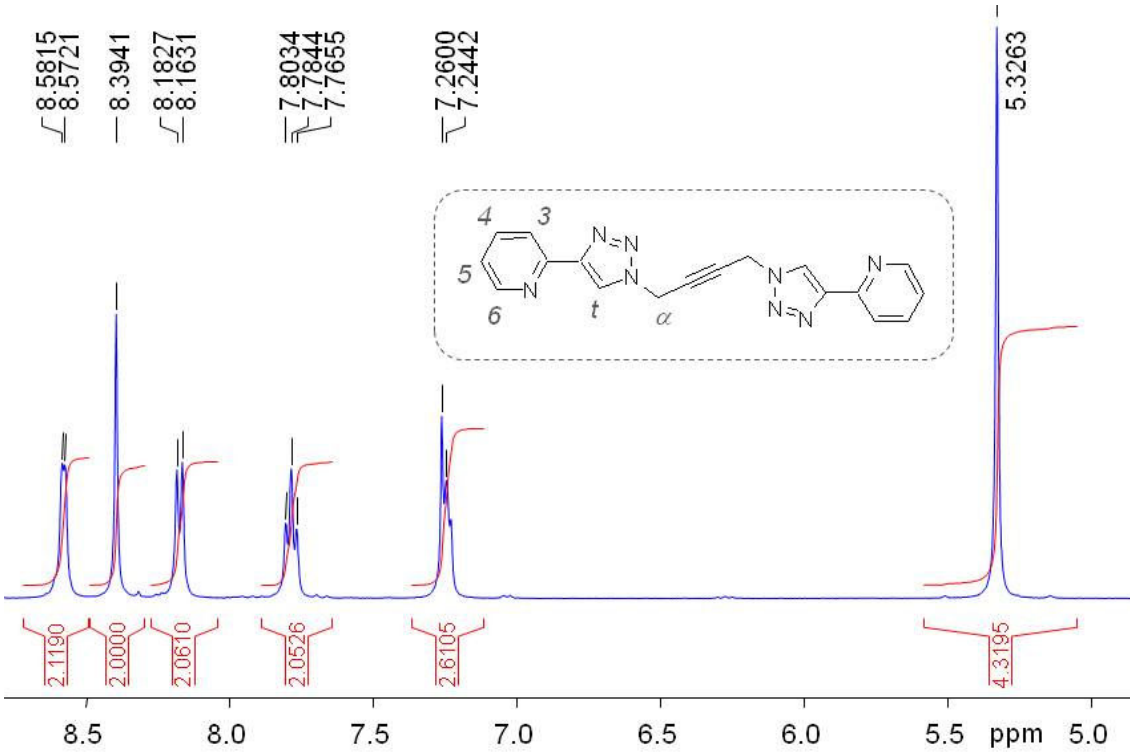

Figure S5: ^{1}H NMR of **L2b** in $CDCl_3$* (400 MHz, 25°C).

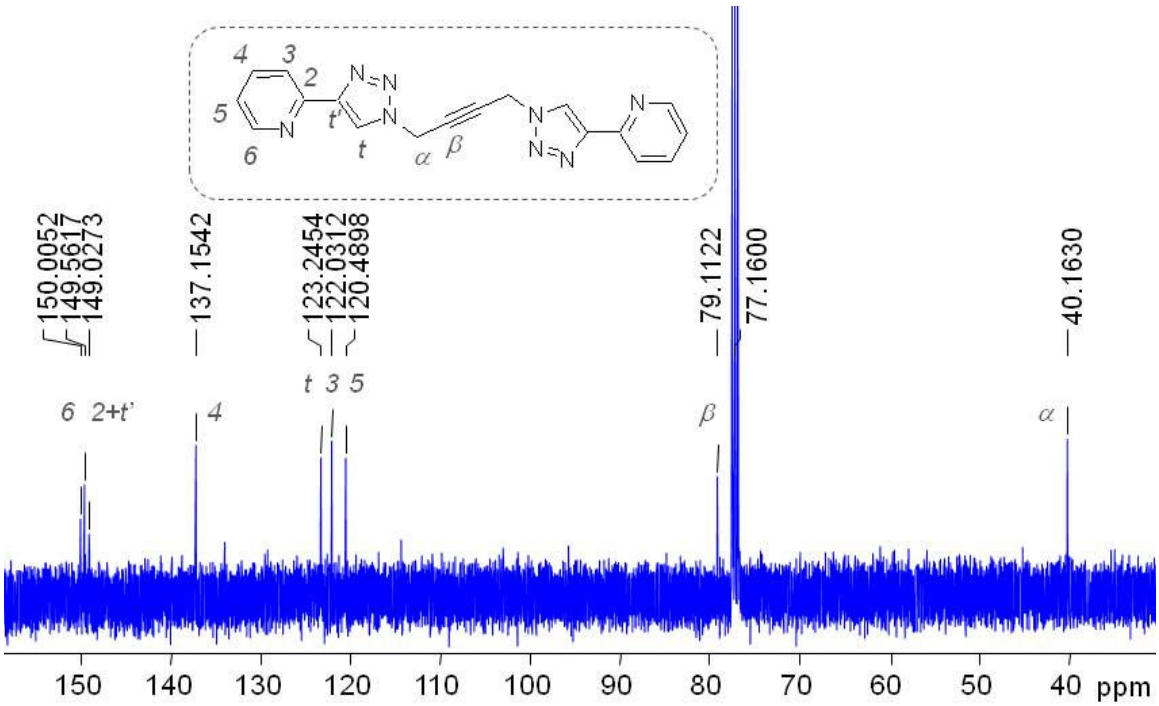

Figure S6: ^{13}C NMR of **L2b** in $CDCl_3$* (100 MHz, 25°C).

L4

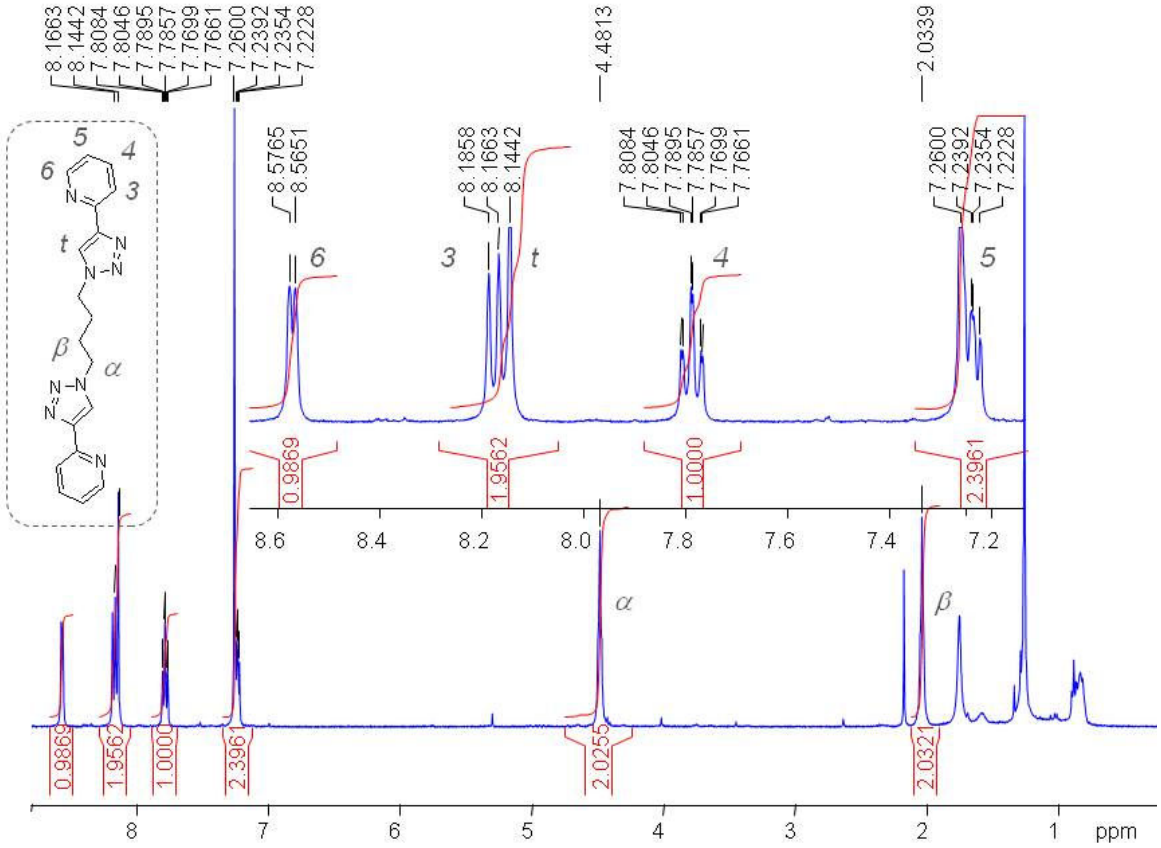

Figure S7: ^{1}H NMR of **L4** in $CDCl_3$* (400 MHz, 25°C).

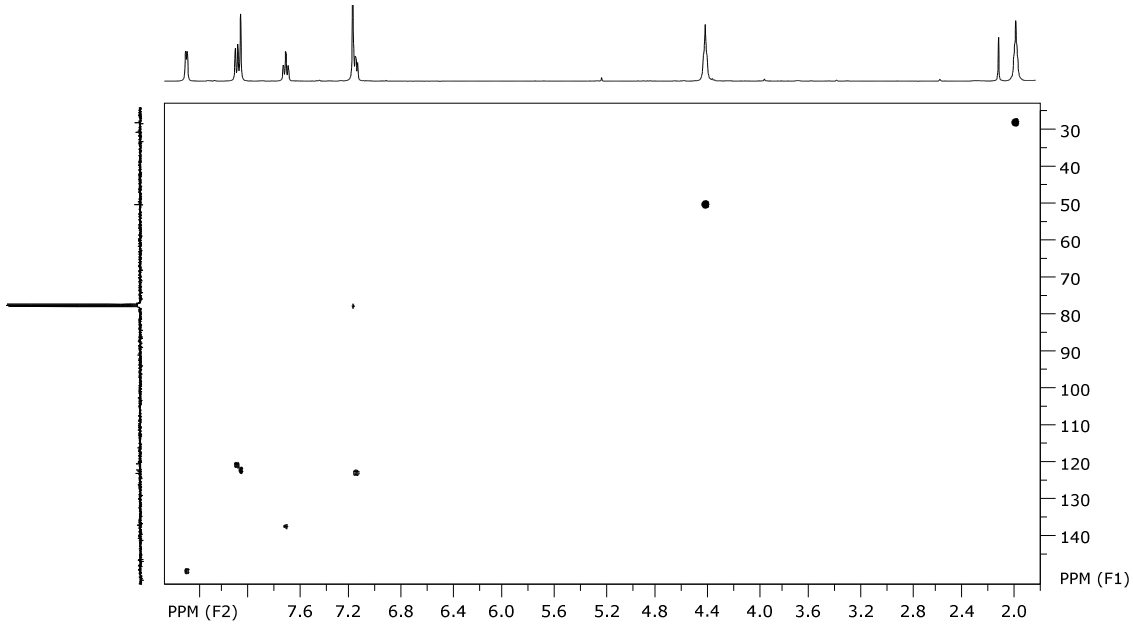

Figure S8: ^{13}C-^{1}H HSQC NMR of **L4** in $CDCl_3$* (400 MHz, 25°C).

L5

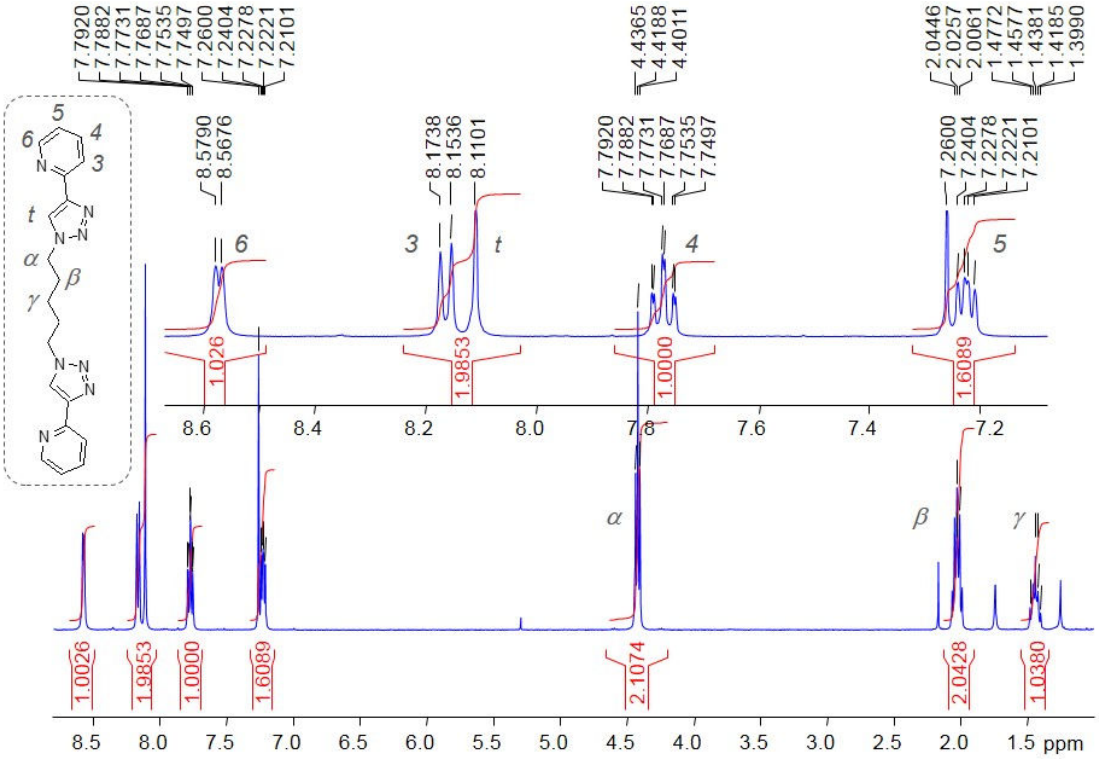

Figure S9: ^{1}H NMR of **L5** in $CDCl_3$* (400 MHz, 25°C).

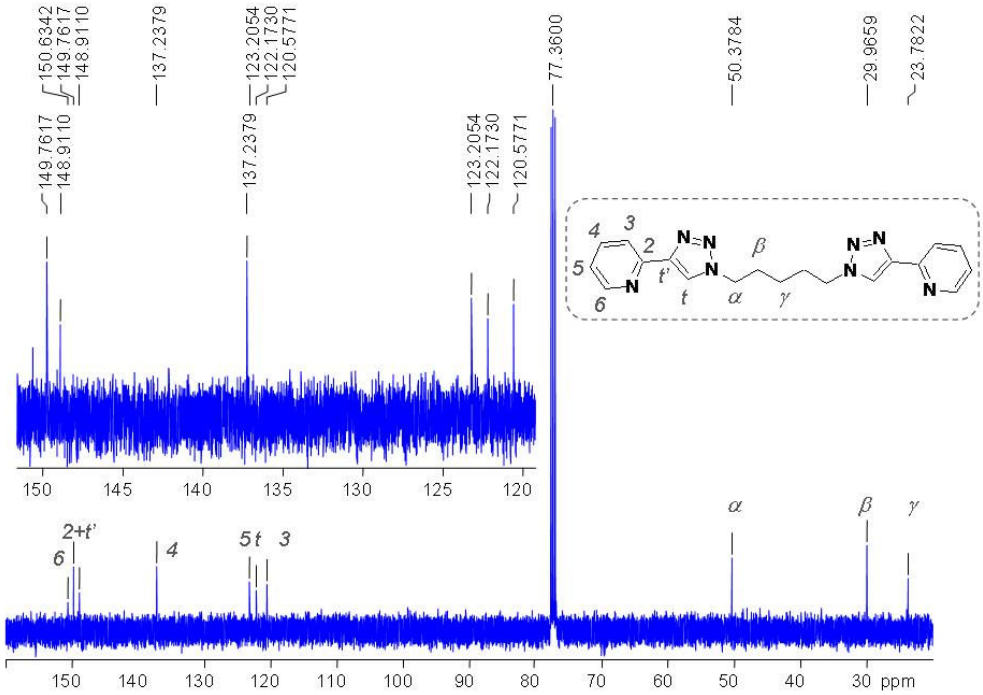

Figure S10: ^{13}C NMR of **L5** in $CDCl_3$* (100 MHz, 25°C).

L6

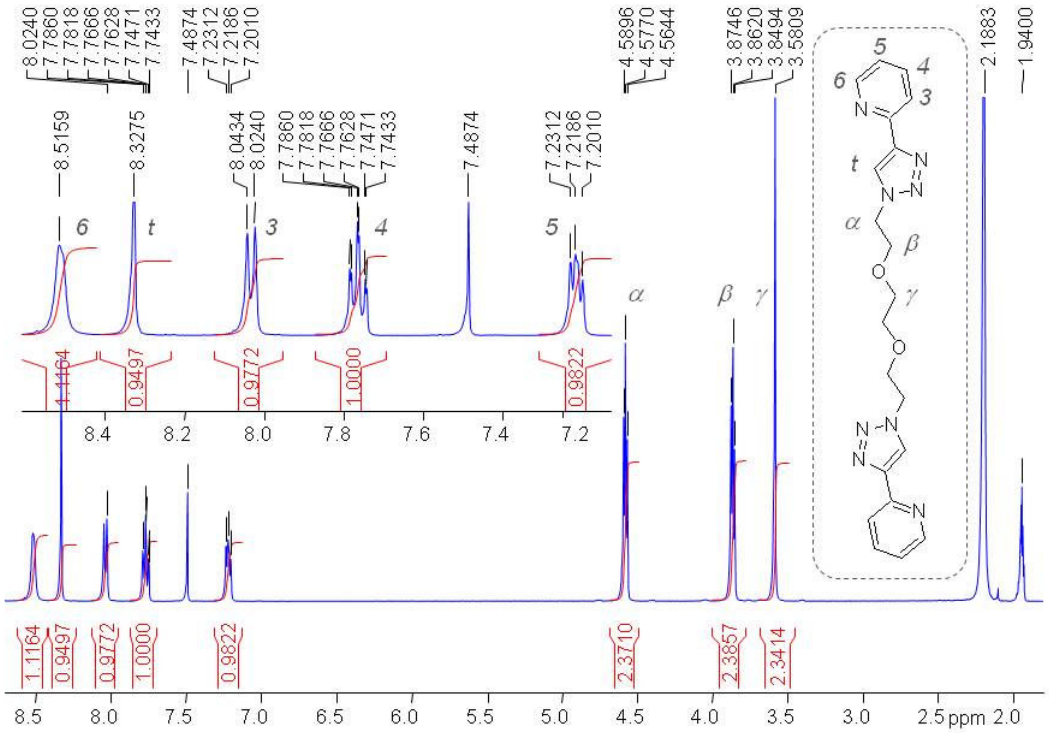

Figure S11: ^{1}H NMR of **L6** in 1:1 $CDCl_3$*/CD_3CN (400 MHz, 25°C; calibrated on CH_3CN at 1.94 ppm).

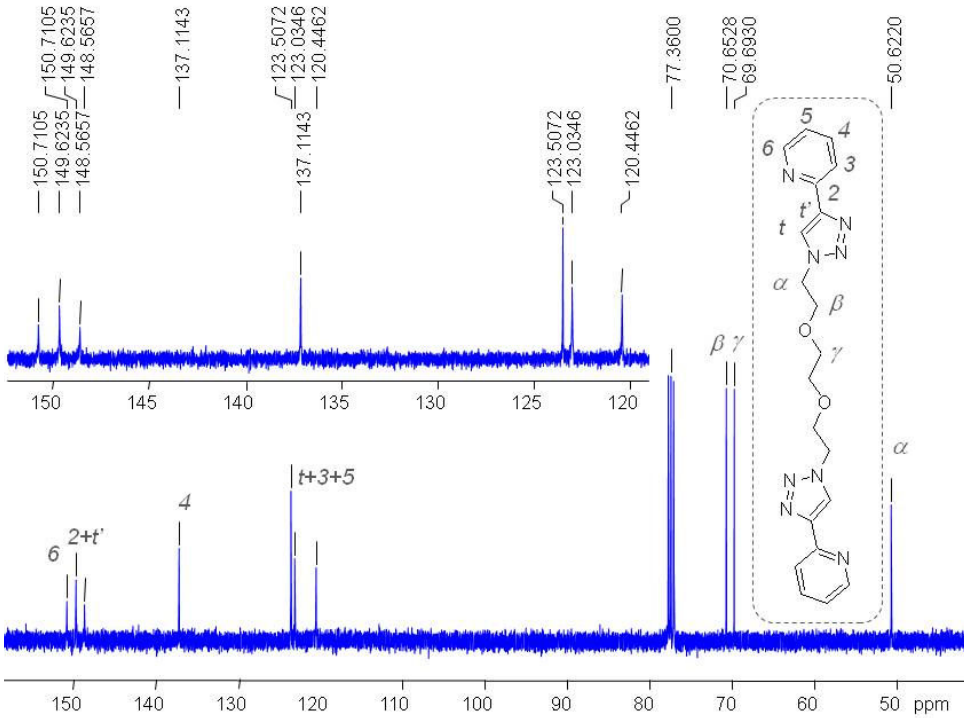

Figure S12: ^{13}C NMR of **L6** in $CDCl_3$* (100 MHz, 25°C).

L3M

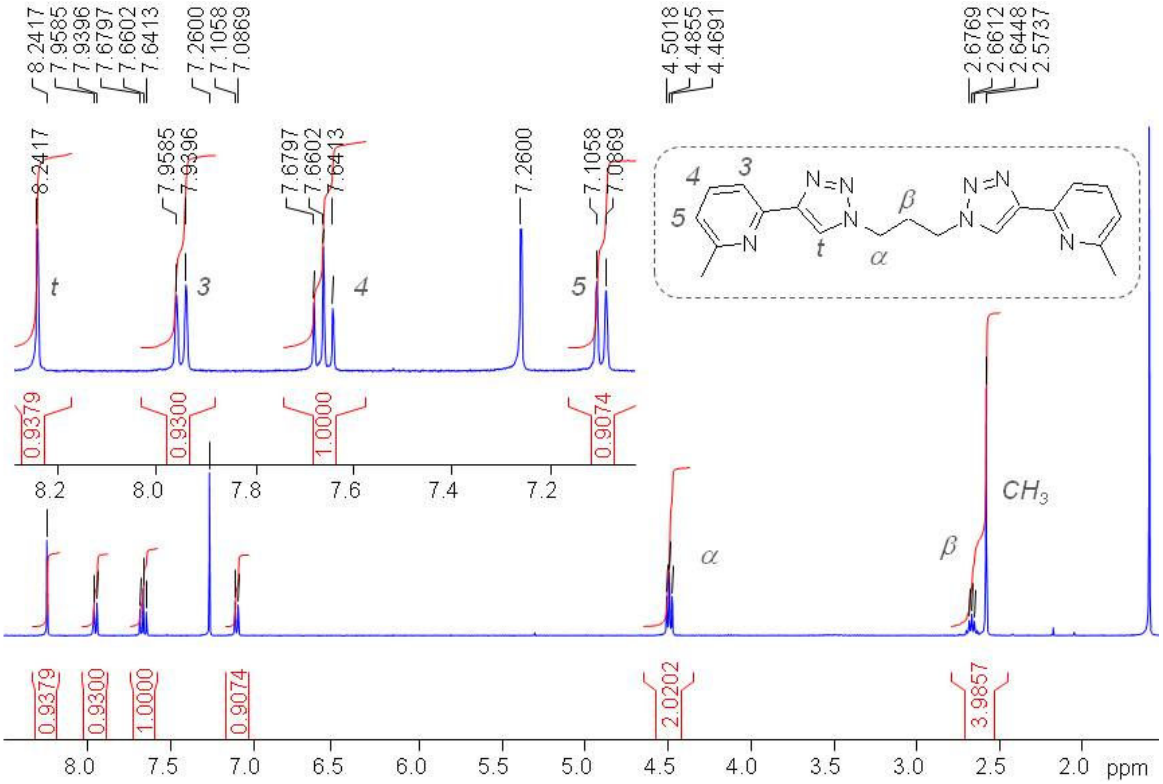

Figure S13: ^{1}H NMR of **L3M** in $CDCl_3$* (400 MHz, 25°C).

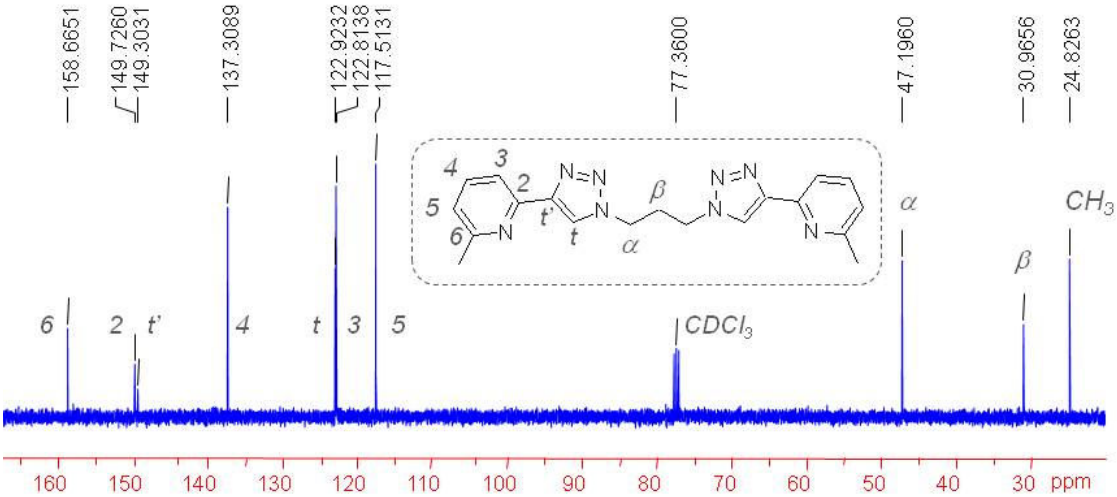

Figure S14: ^{13}C NMR of **L3M** in $CDCl_3$* (100 MHz, 25°C).

L4M

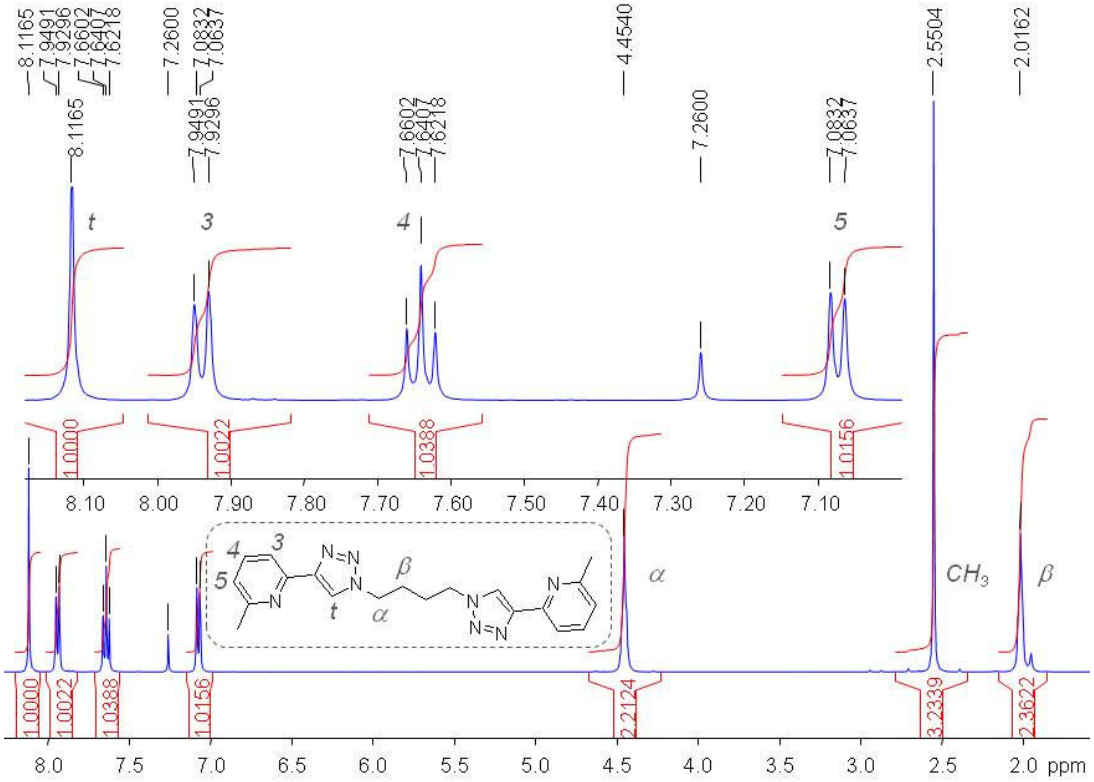

Figure S15: ^{1}H NMR of **L4M** in $CDCl_3$* (400 MHz, 25°C).

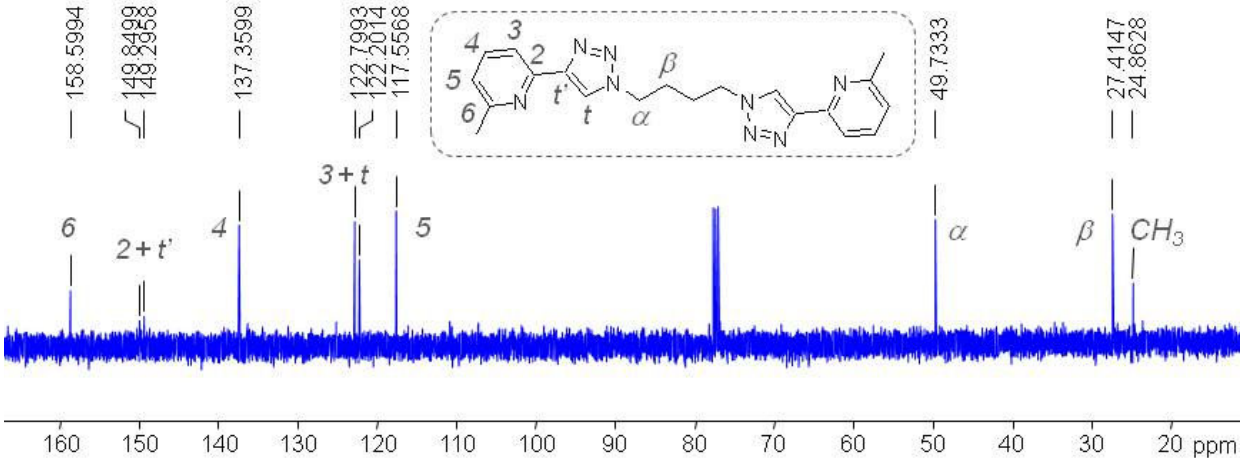

Figure S16: ^{13}C NMR of **L4M** in $CDCl_3$* (100 MHz, 25°C).

L2cM

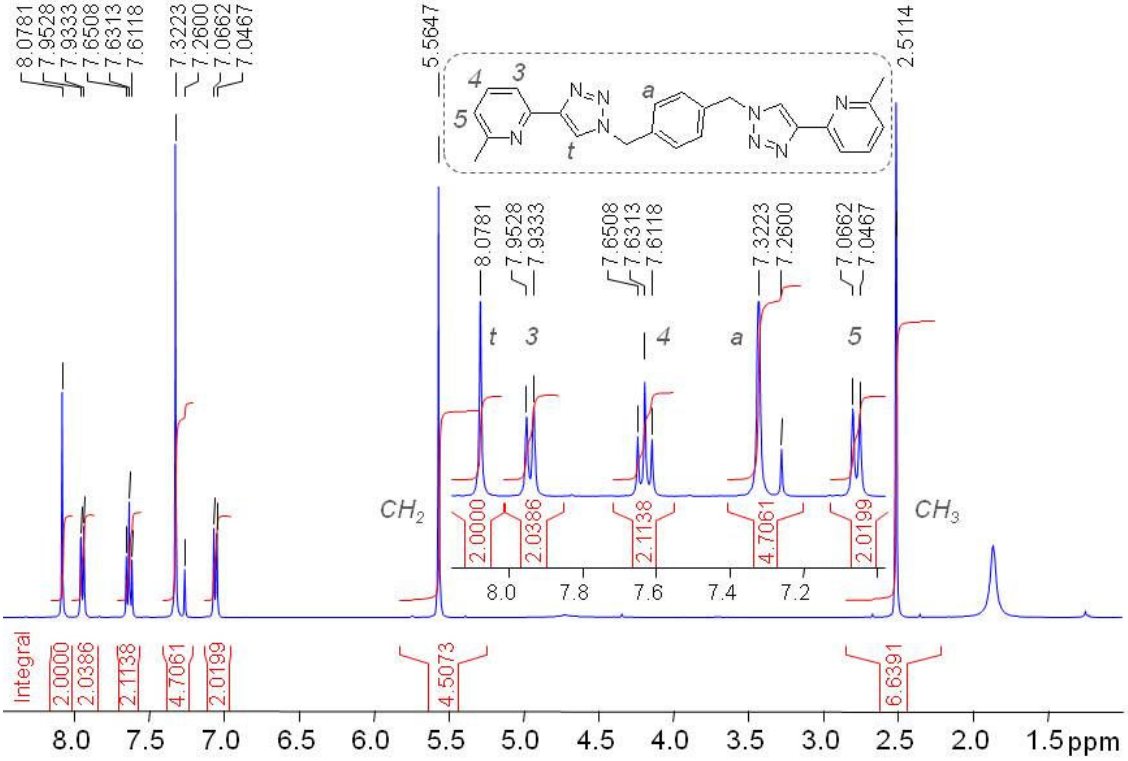

Figure S17: ^{1}H NMR of **L2cM** in $CDCl_3$* (400 MHz, 25°C).

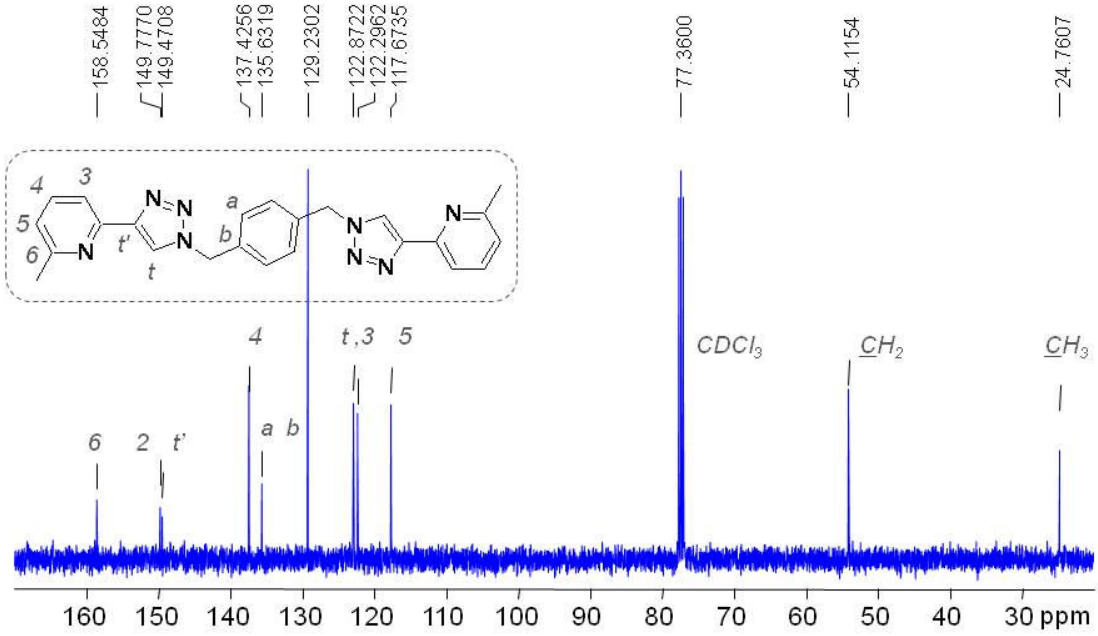

Figure S18: ^{13}C NMR of **L2cM** in $CDCl_3$* (100 MHz, 25°C).

C. ^{1}H NMR spectroscopy of the complexes

1) Iron complexes of **L1**, **L2a,b,c,d**, **L3**, **L4** and **L5** (CD_3CN): Stacked plots

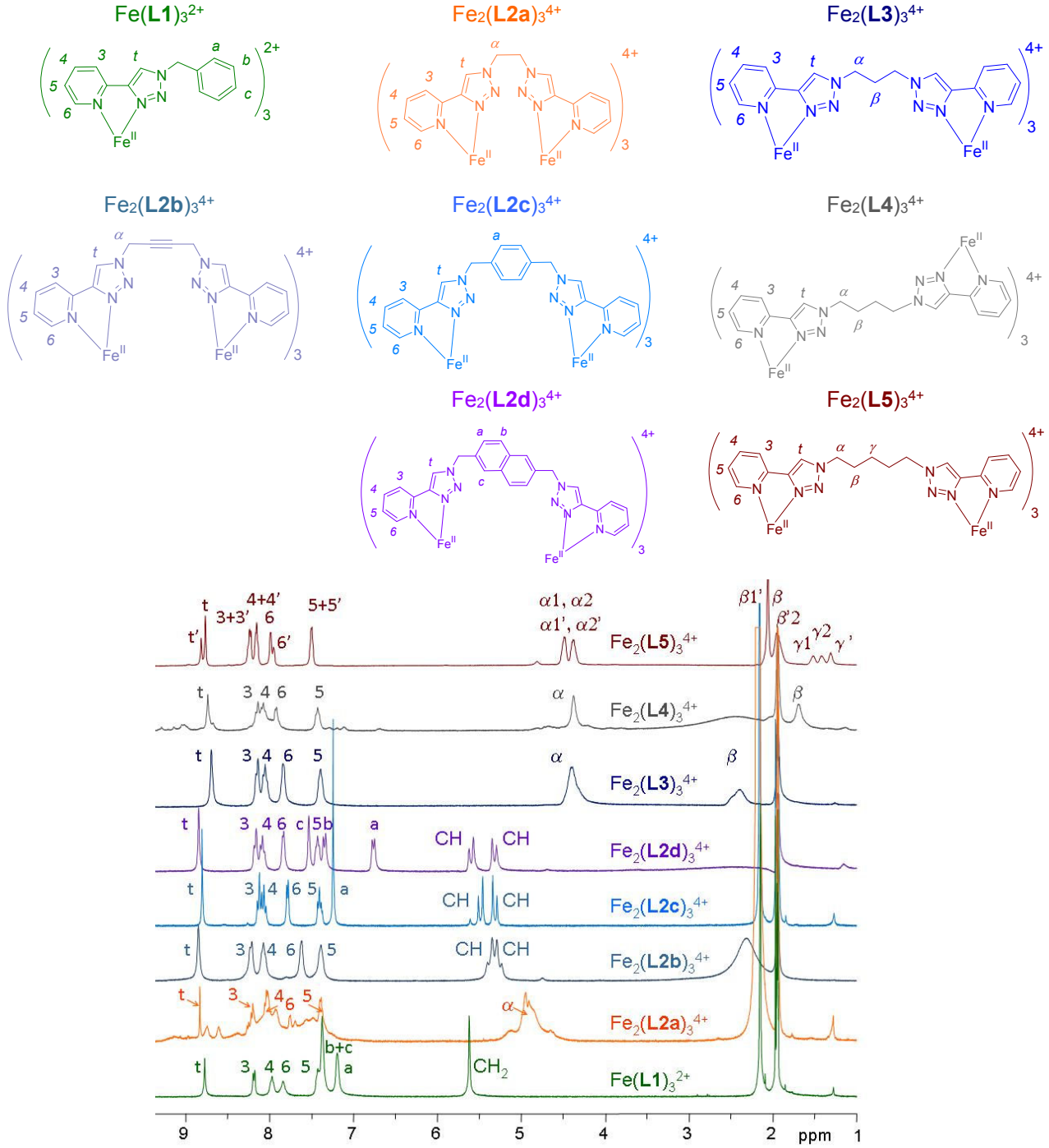

Figure S19: Stacked ^{1}H NMR spectra of Fe(**L1**)$_3^{2+}$, Fe$_2$(**L2a**)$_3^{4+}$ (400 MHz), Fe$_2$(**L2b**)$_3^{4+}$, Fe$_2$(**L2c**)$_3^{4+}$, Fe$_2$(**L2d**)$_3^{4+}$, Fe$_2$(**L3**)$_3^{4+}$, Fe$_2$(**L4**)$_3^{4+}$ (300 MHz) and Fe$_2$(**L5**)$_3^{4+}$ (500 MHz) in CD_3CN, 25ºC (c ~ 1-10 mM), prepared *in situ* by mixing $[Fe(H_2O)_6](BF_4)_2$ and ligand in 2/3 ratio (1/3 ratio for Fe(**L1**)$_3^{2+}$).

2) COSY spectra of the iron complexes of **L1**, **L2a-d**, **L3**, **L4** and **L5** (CD_3CN)

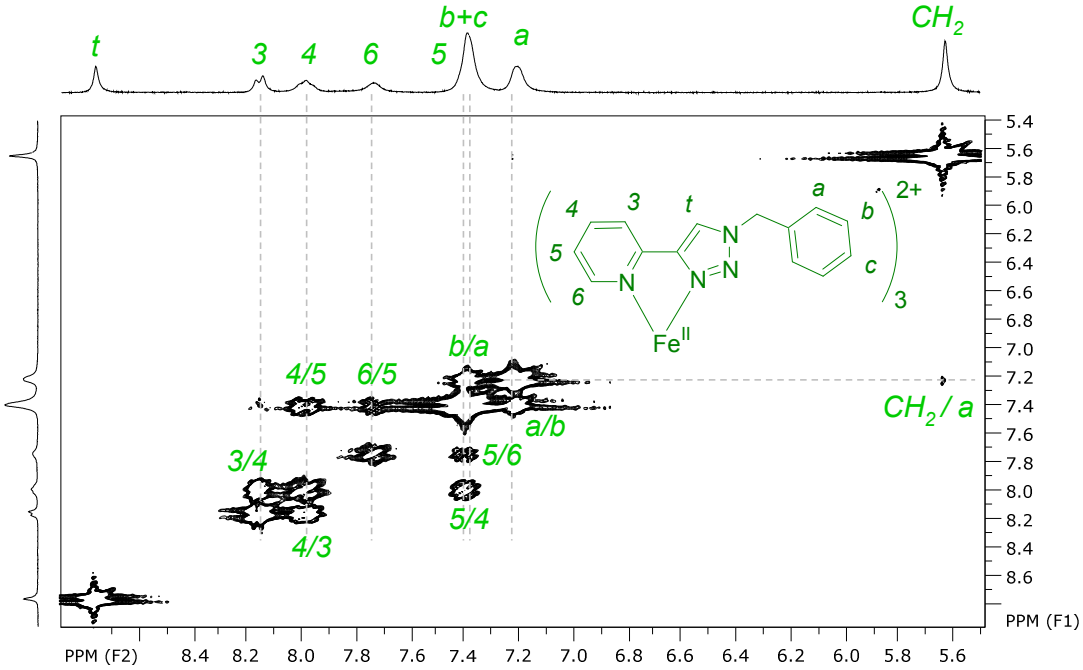

Figure S20: ^{1}H-^{1}H COSY NMR spectrum of Fe(**L1**)$_3^{2+}$ CD_3CN (25ºC, 300 MHz, ~ 2 10^{-3} M).

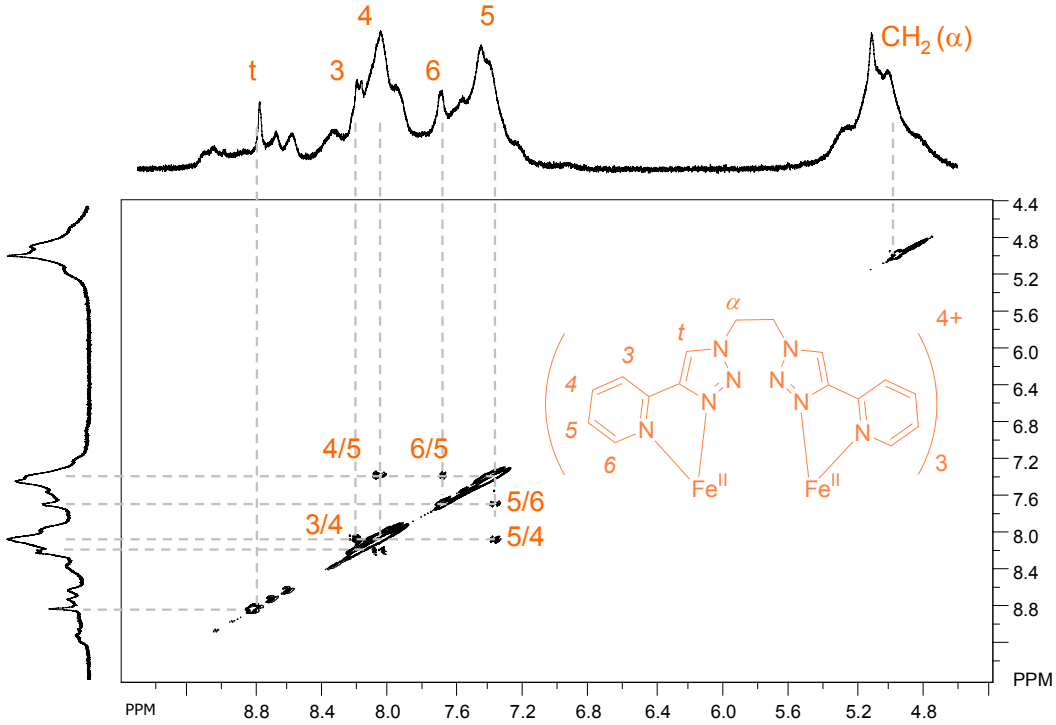

Figure S21: ^{1}H-^{1}H COSY NMR spectrum of Fe_2(**L2a**)$_3^{4+}$ CD_3CN (25ºC, 300 MHz, ~ 1 10^{-3} M).

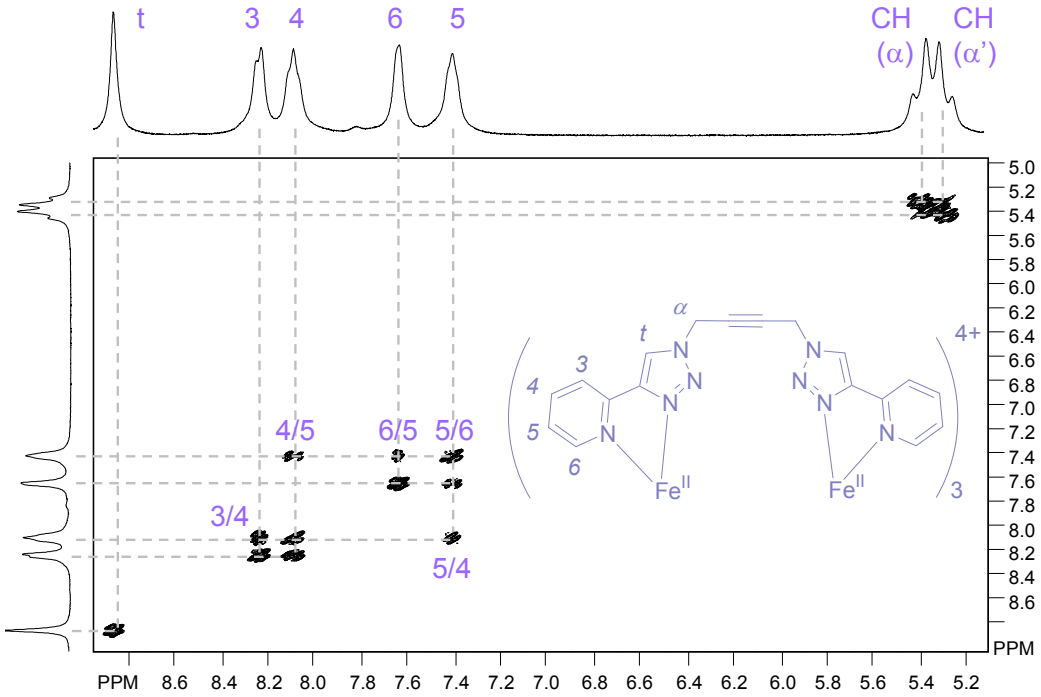

Figure S22: ^{1}H-^{1}H COSY NMR spectrum of Fe_2(**L2b**)$_3^{4+}$ CD_3CN (25ºC, 300 MHz, ~ 15 10^{-3} M).

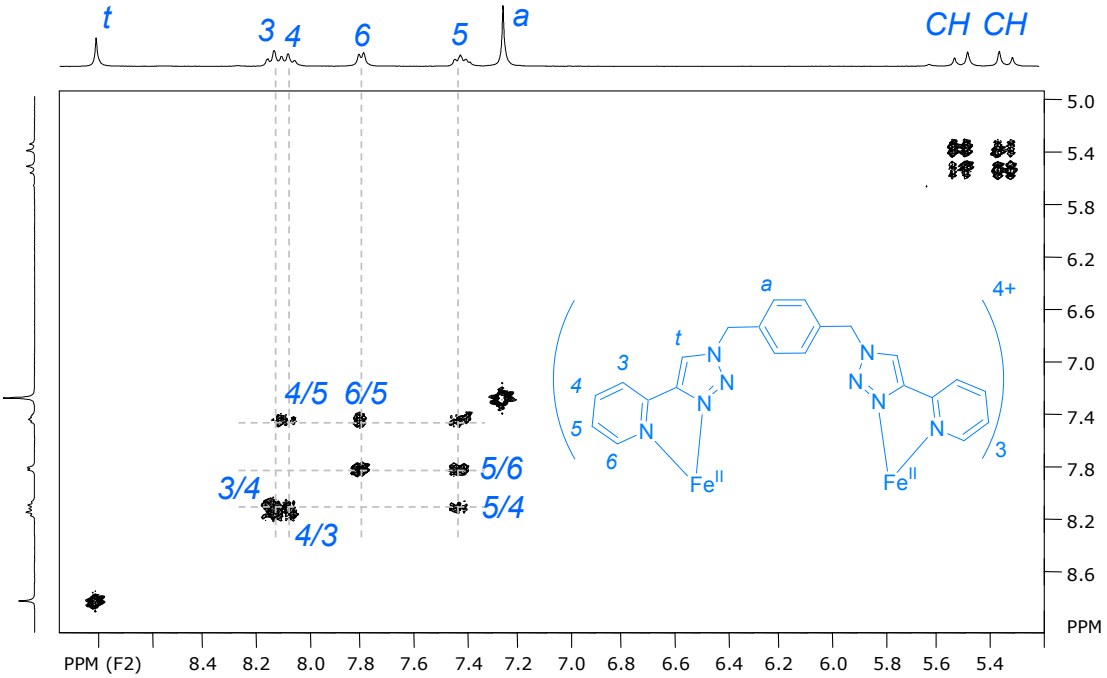

Figure S23: ^{1}H-^{1}H COSY NMR spectrum of Fe_2(**L2c**)$_3^{4+}$ CD_3CN (25ºC, 300 MHz, ~ 9 10^{-3} M).

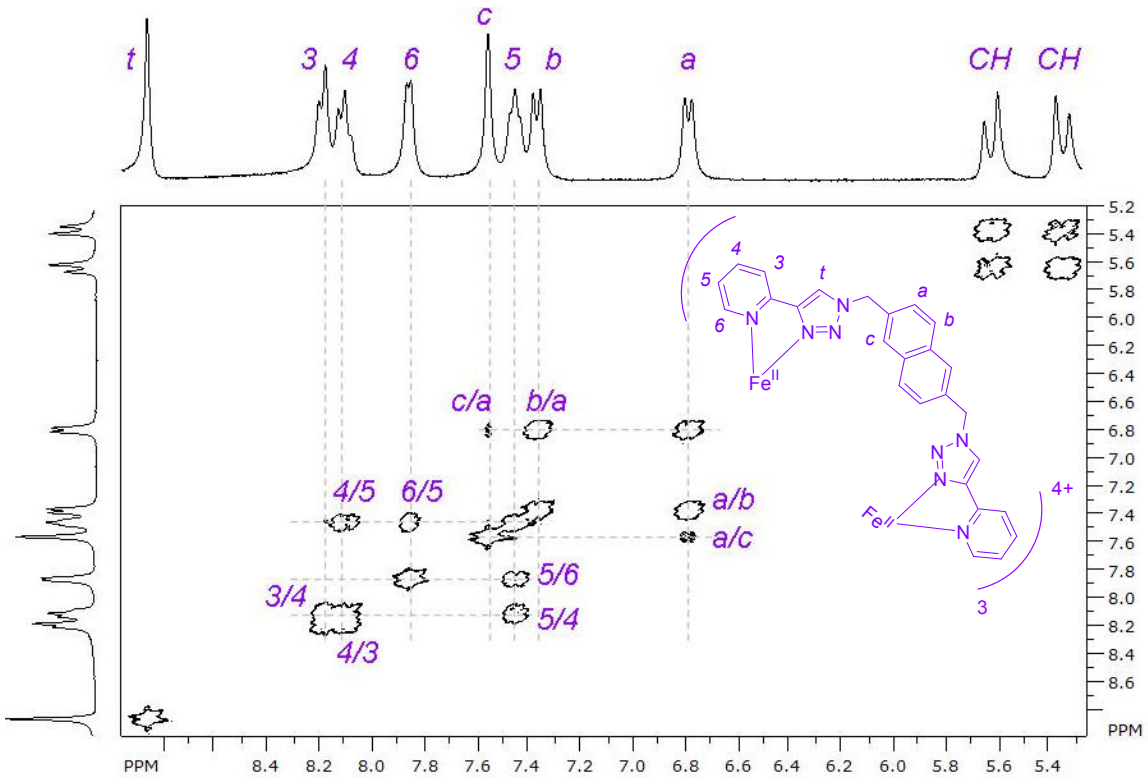

Figure S24: ^{1}H-^{1}H COSY NMR spectrum of Fe_2(**L2d**)$_3^{4+}$ CD_3CN (25ºC, 300 MHz, ~ 9 10^{-3} M).

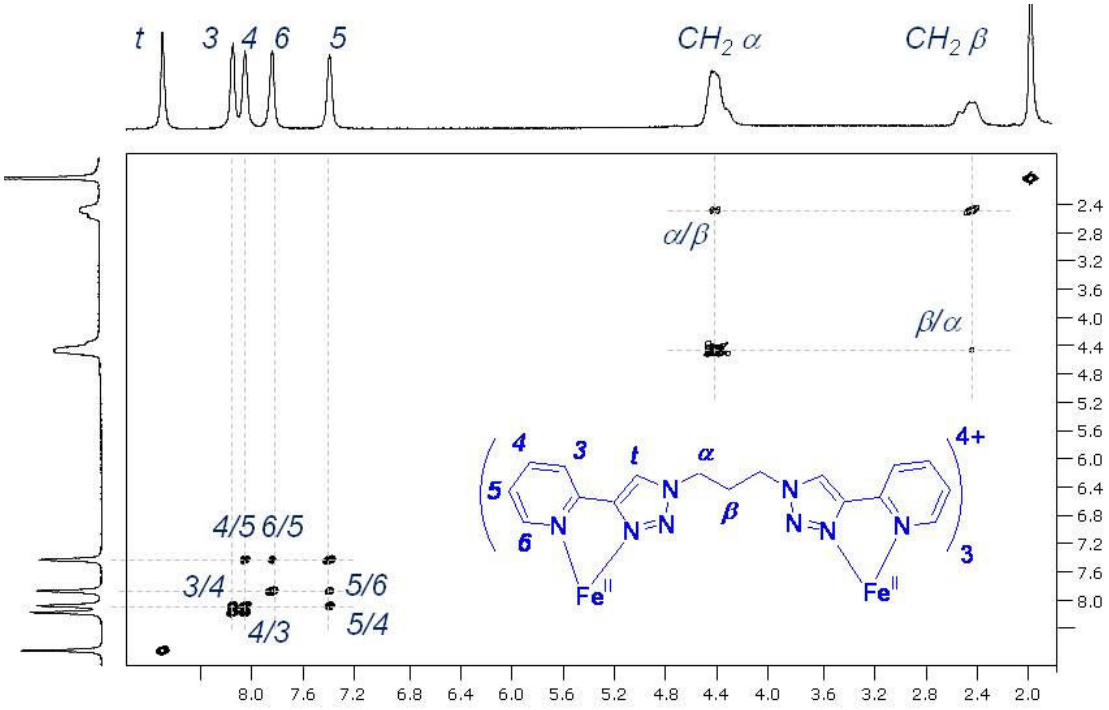

Figure S25: ^{1}H-^{1}H COSY NMR spectrum of Fe_2(**L3**)$_3^{4+}$ CD_3CN (25ºC, 500 MHz, ~ 10 10^{-3} M).

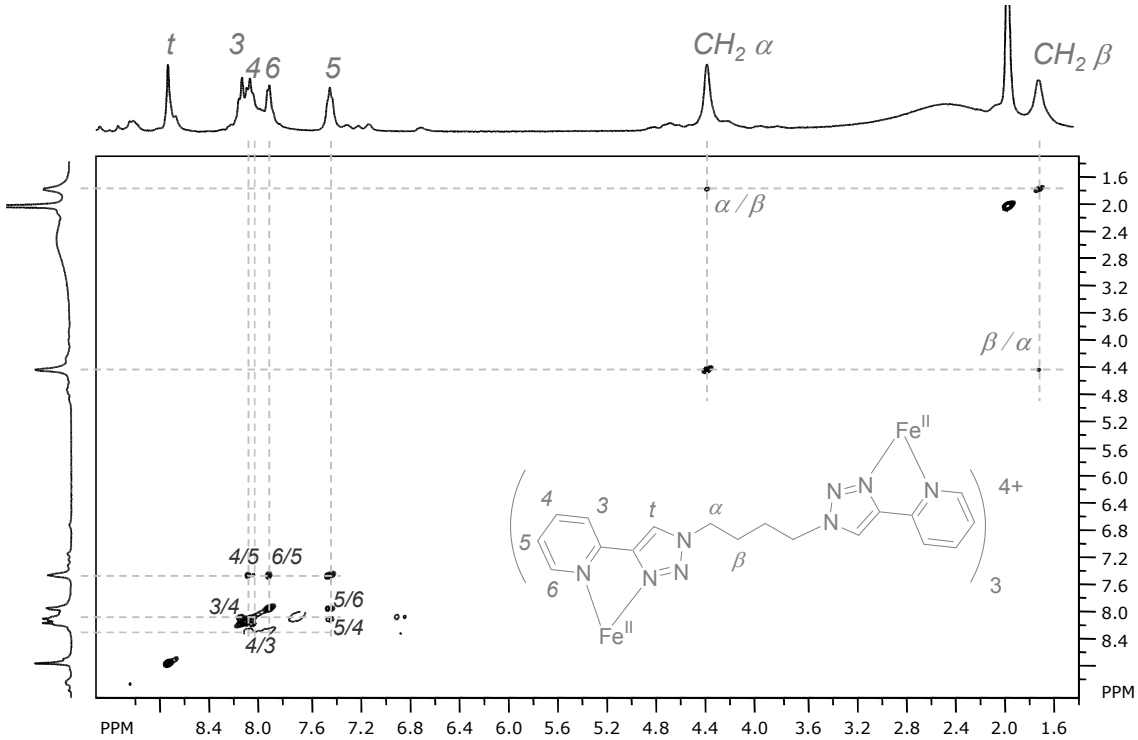

Figure S26: ^{1}H-^{1}H COSY NMR spectrum of $Fe_2(\mathbf{L4})_3^{4+}$ CD_3CN (25ºC, 300 MHz, ~ 10×10^{-3} M).

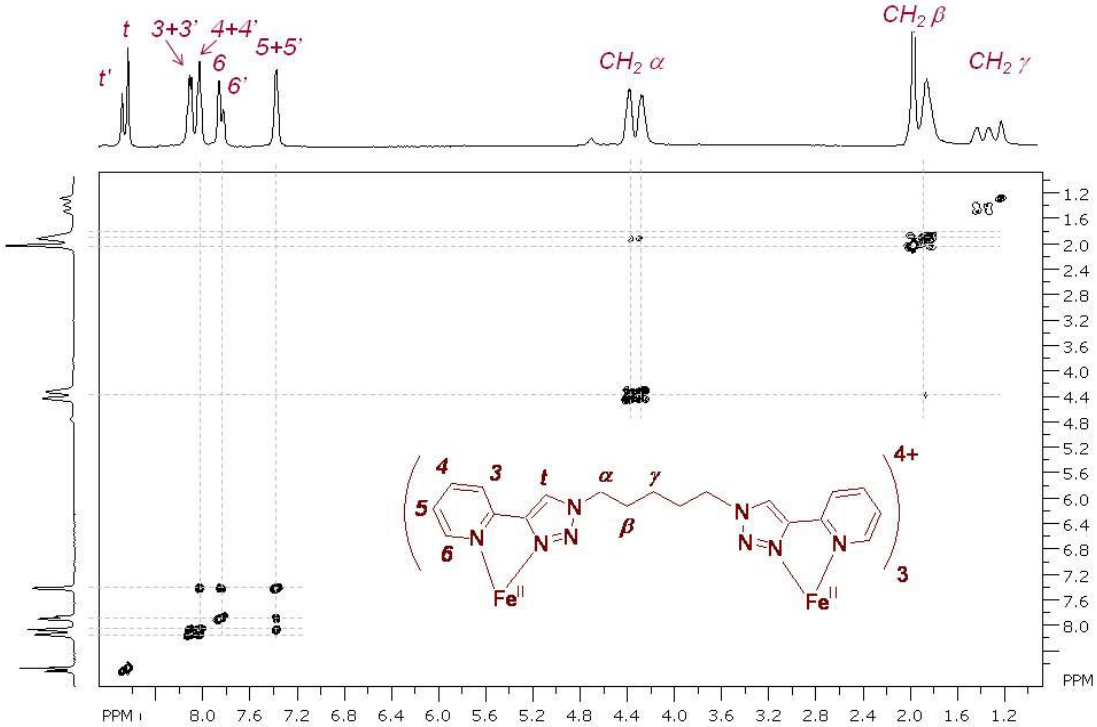

Figure S27: ^{1}H-^{1}H COSY NMR full spectrum of $Fe_2(\mathbf{L5})_3^{4+}$ CD_3CN (25ºC, 500 MHz, 10 m M).

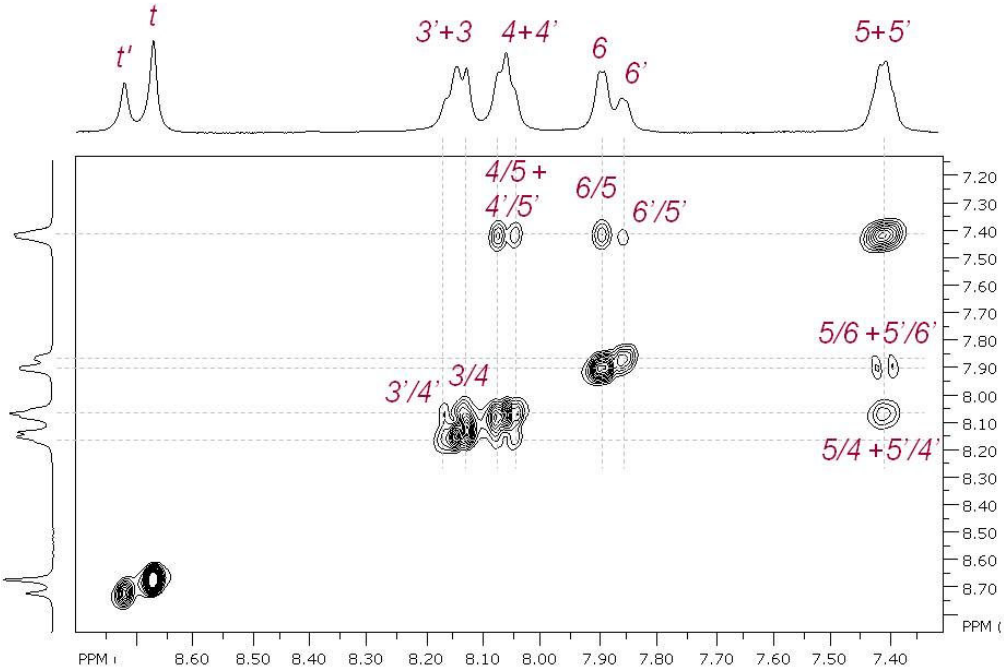

Figure S28: ^{1}H-^{1}H COSY spectrum, Fe_2(**L5**)$_3^{4+}$ CD_3CN (25ºC, 500 MHz, 10 m M), aromatic region.

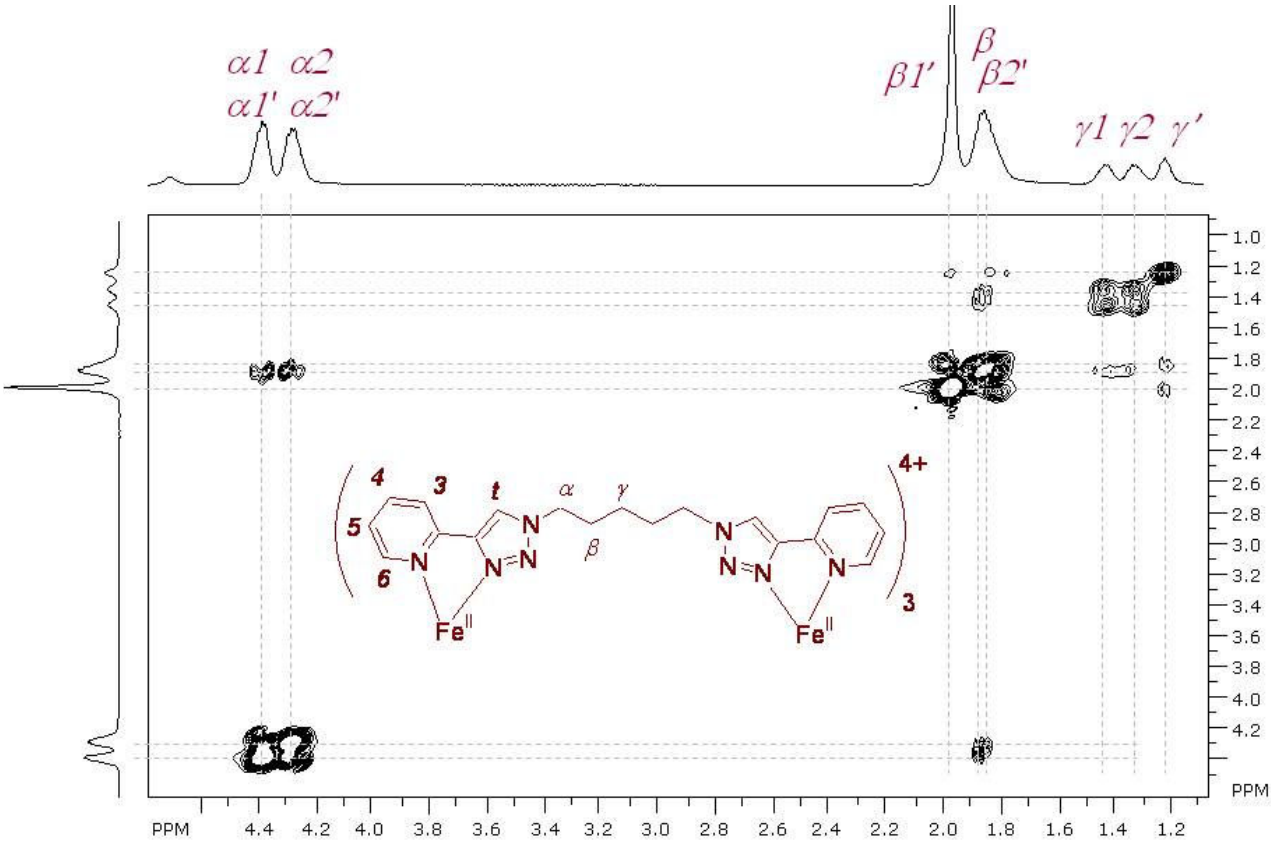

Figure S29: ^{1}H-^{1}H COSY spectrum, Fe_2(**L5**)$_3^{4+}$ CD_3CN (25ºC, 500 MHz, 10 m M), aliphatic region.

3) ^{1}H NMR spectra of the iron complexes of **L1M**, **L3M** and **L4M** (CD_3CN)

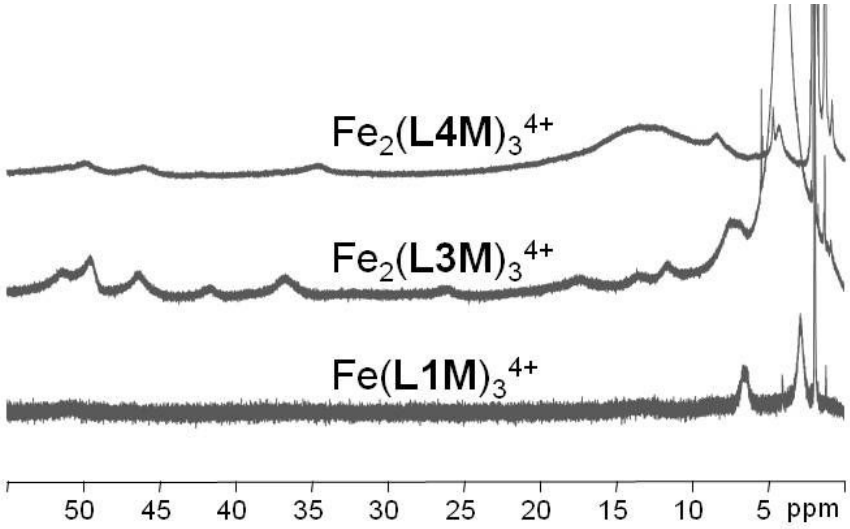

Figure S30: Stacked ^{1}H NMR spectra of iron(II) complexes of **L1M**, **L3M** and **L4M** (300 MHz, 25 °C).

4) Iron and zinc complexes: comparison of mono- and di-nuclear complexes

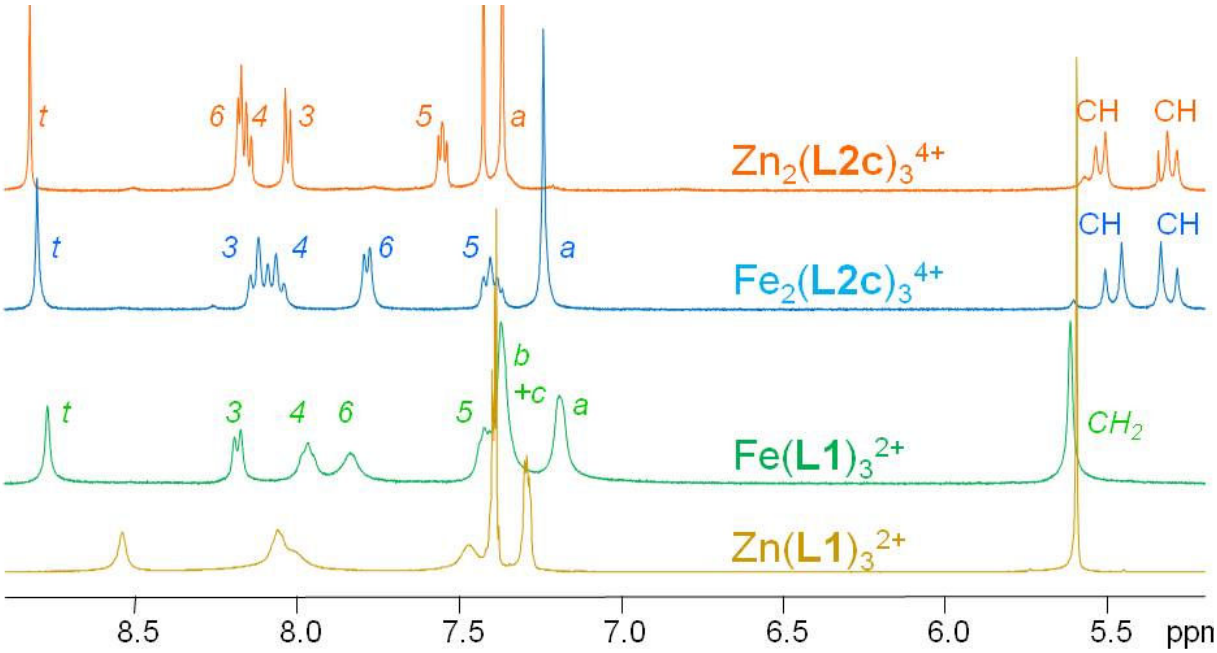

Figure S31: Stacked ^{1}H NMR spectra of zinc(II) and iron(II) complexes of **L1** (Zn^{2+}: 500 MHz, Fe^{2+}: 400 MHz), and of **L2c** (Fe^{2+}: 300 MHz, Zn^{2+}: 500 MHz), 25ºC, in CD_3CN except of Zn_2(**L2c**)$_3^{4+}$ which was prepared in 5:3 $CDCl_3$*/CD_3CN (c ~ 1-10 mM). Complexes were prepared *in situ* by mixing $[Fe(H_2O)_6](BF_4)_2$ or $Zn(OTf)_2$ and the corresponding ligand in 1/3 ratio for **L1** and 2/3 ratio for **L2c**.

5) Zinc complexes: COSY for the **L2a** and **L2c** double stranded complexes

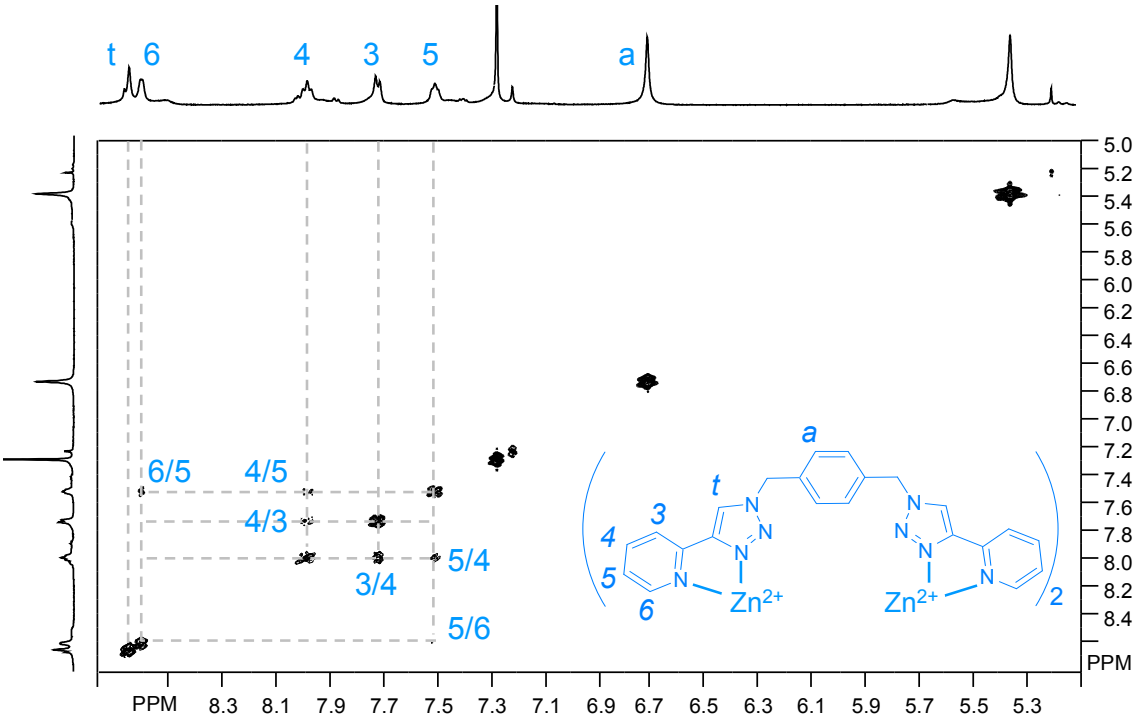

Figure S32: ^{1}H-^{1}H COSY NMR full spectrum of **L2c** + 1.3 equivalent of $Zn(OTf)_2$ (5:3 $CDCl_3/CD_3CN$, 25ºC, 500 MHz, 10 m M).

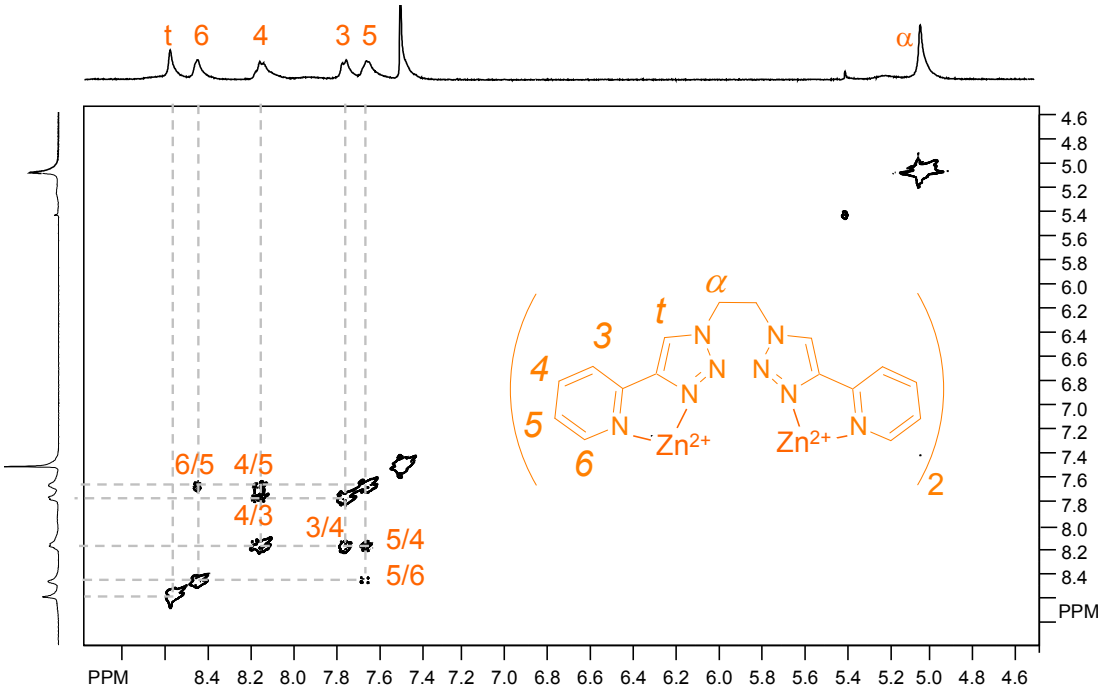

Figure S33: ^{1}H-^{1}H COSY NMR full spectrum of **L2a** + 1.1 equivalent of $Zn(OTf)_2$ (1:1 $CDCl_3/CD_3CN$, 25ºC, 400 MHz, 10 m M).

5) Ageing effect on the iron complex of **L3**: ^{1}H NNMR

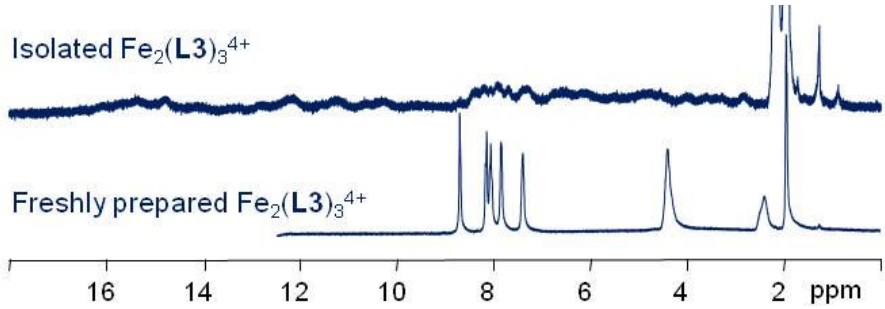

Figure S34: ^{1}H-NMR spectrum of freshly prepared (~10 mM) *vs* isolated $Fe_2(\mathbf{L3})_3^{4+}$ (~2 mM) (25ºC, 300 MHz).

6) Assessment of fluoride content in $Fe_2(\mathbf{L3})_3$ cation

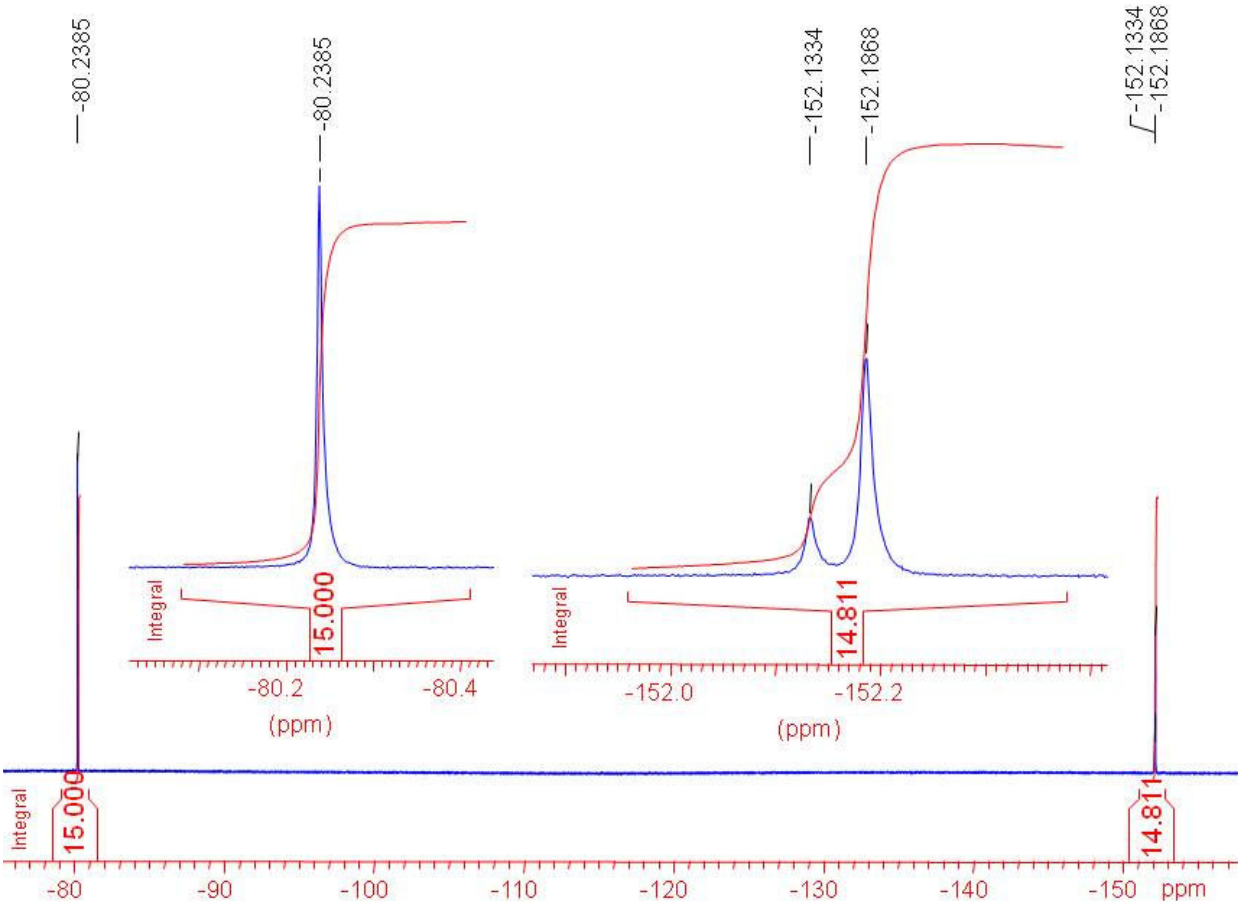

Figure S35: ^{19}F-NMR spectrum of isolated crystalline $Fe_2(\mathbf{L3})_3$ cations (2.1 mg) (25ºC, 400 MHz) mixed with 7.1 × 10^{-6} mol of N(*n*Bu)$_4$OTf as internal standard. The ratio of integrals (0.74) gives n(BF_4^-) = 5.3 × 10^{-6} mol. Calculated from the molecular weight determined for the crystal [$Fe_2(\mathbf{L3})_3$] $(BF_4)_4$•3 CH_3CN•H_2O (1597.26 g/mol), n(BF_4^-) = 5.26 × 10^{-6} mol. This figure shows that each $Fe_2(\mathbf{L3})_3$ cation comes with four BF_4^- anions, which confirms the Fe^{2+} state of each irion center. ^{19}F NMR fails to reveal any free F^- in the solid (from BF_4^- hydrolysis).

D. UV-vis spectroscopy

1) Ageing effect on the iron complex of **L3**: UV-vis

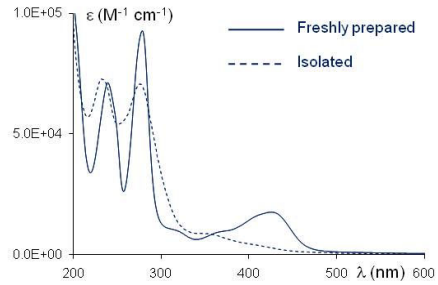

Figure S36: UV-vis spectrum of $Fe_2(\mathbf{L3})_3^{4+}$ freshly prepared (*via* titration) *vs* isolated after crystallization (25ºC, CH_3CN, ~ 8×10^{-6} M).

2) UV-vis titrations and Job plots

General methods: Titrations were conducted by adding aliquots of a concentrated solution of metal salt to a ligand solution in the same solvent. Ligand concentration was chosen so that absorbance does not exceed 1.5 in the course of the titration (2.4 to 3.5 × 10^{-5} M). Job plots were conducted at concentrations which yielded measurable, reproducible, ab-sorbances at a wavelength where free ligands have little absorbance, and metal complexes do absorb (iron(II) complexes: MLCT ~ 420 nm; nickel(II) complexes: shoulder ~ 300 nm). In both cases, ligand stock solution at 1.3 × 10^{-4} M were used in Job plot studies.

2.a) ***L1*** *ligand:* Fe^{II} *complex*

a

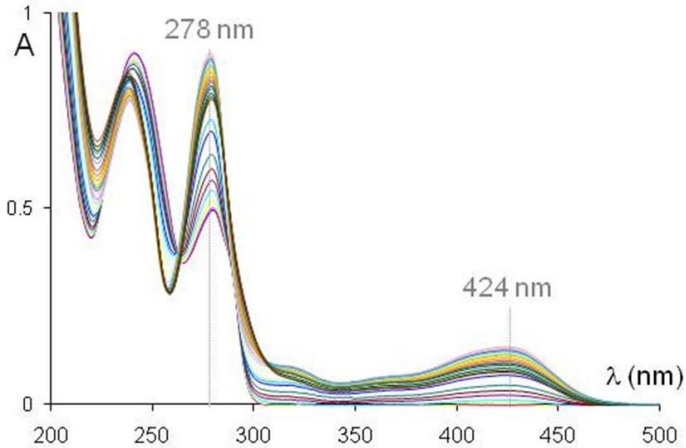

Figure S37: Titration of $[Fe(H_2O)_6](BF_4)_2$ to **L1** in CH_3CN;
a) full spectral curves
b) zoom between 230 and 300 nm
c) Absorbance as a function of n_{Fe} to n_{L1} ratio at 278 and 424 nm (lines have been added to guide the eye).

b

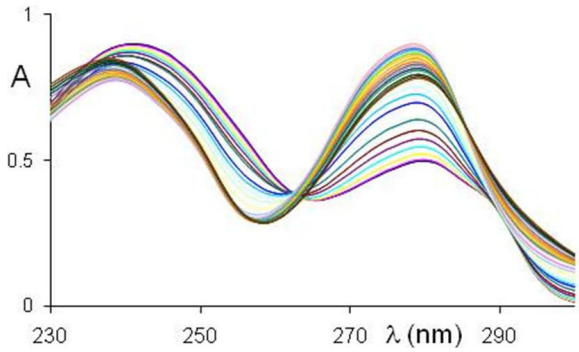

c

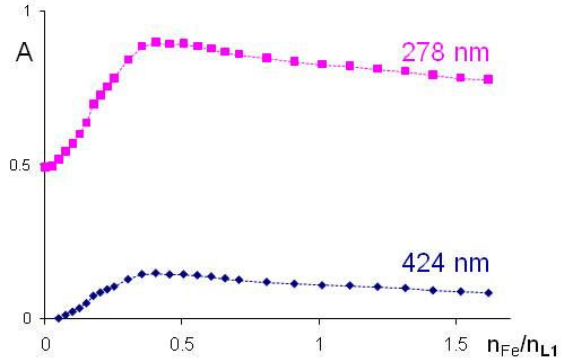

2.b) ***L2a*** *ligand*

Iron(II) complex

Figure S38: Titration data of $[Fe(H_2O)_6](BF_4)_2$ to **L2a** in CH_3CN; a) Spectral curves;

b) Absorbance as a function of n_{Fe} to $n_{\mathbf{L2a}}$ ratio at 425 nm;

c) Job plot (lines have been added to guide the eye).

a

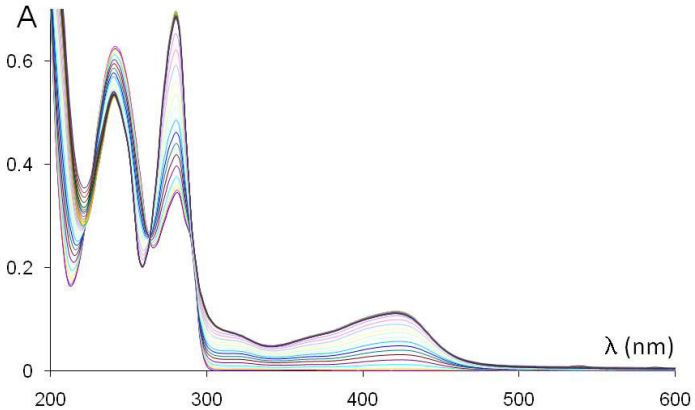

b

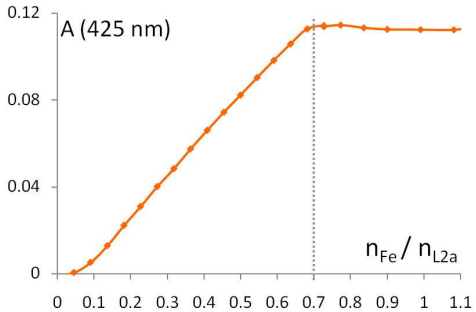

c

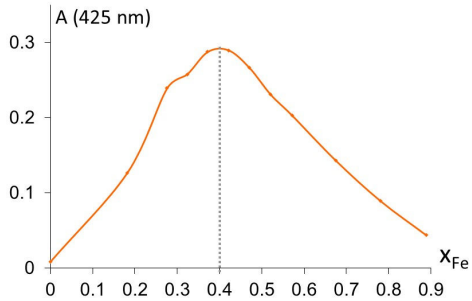

Nickel(II) complex

Figure S39: Titration data of $[Ni(H_2O)_6](BF_4)_2$ to **L2a** in CH_3CN;

a) Spectral curves;

b) Absorbance as a function of n_{Ni} to $n_{\mathbf{L2a}}$ ratio at 295 nm;

c) Job plot (lines have been added to guide the eye).

a

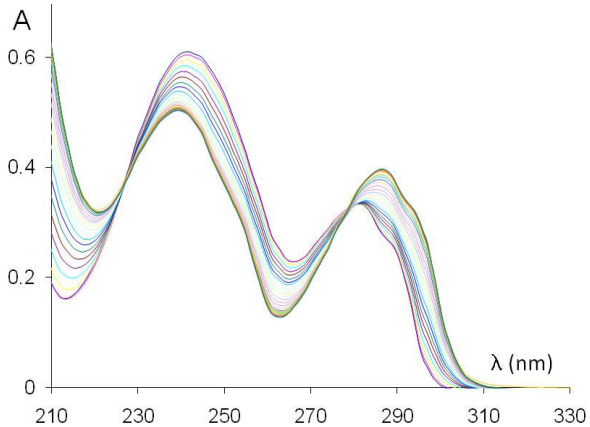

b

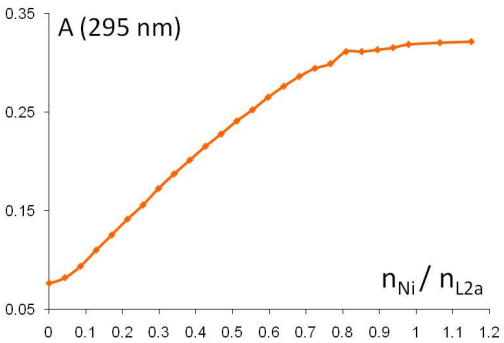

c

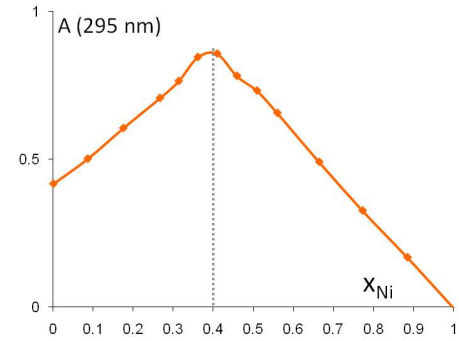

2.c) ***L2b*** *ligand*

Iron(II) complex

Figure S40: Titration data of $[Fe(H_2O)_6](BF_4)_2$ to **L2b** in CH_3CN;
a) Spectral curves;
b) Absorbance as a function of n_{Fe} to n_{L2b} ratio at 420 nm;
c) Job plot (lines have been added to guide the eye).

a

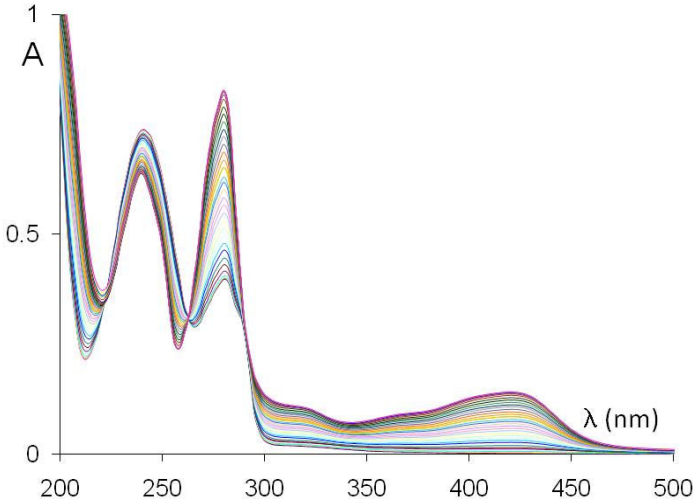

b

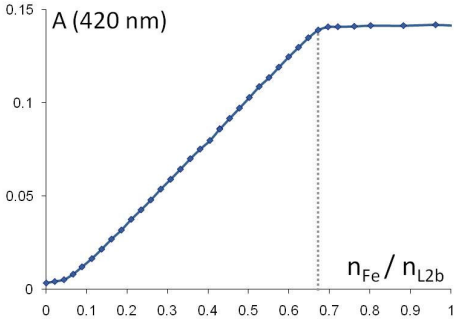

c

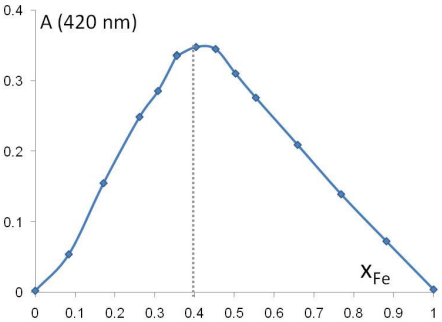

Nickel(II) complex

Figure S41: Titration data of $[Ni(H_2O)_6](BF_4)_2$ to **L2b** in CH_3CN.
a) Spectral curves;
b) Absorbance as a function of n_{Ni} to n_{L2b} ratio at 300 nm;
c) Job plot (lines have been added to guide the eye).

a

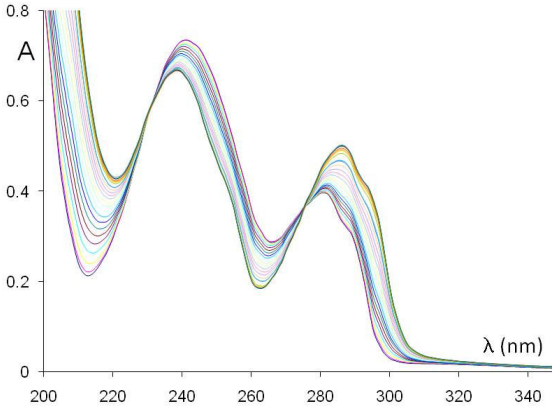

b

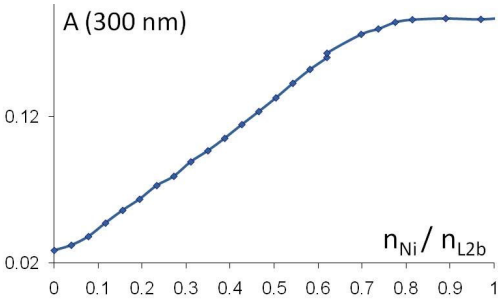

c

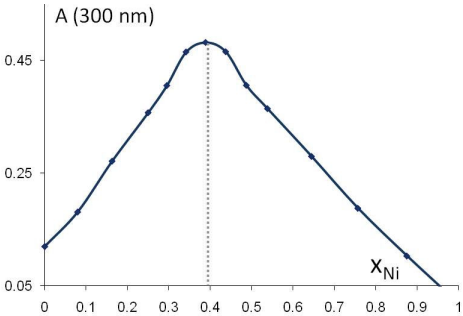

2.d) ***L2c*** *ligand*

Iron(II) complex

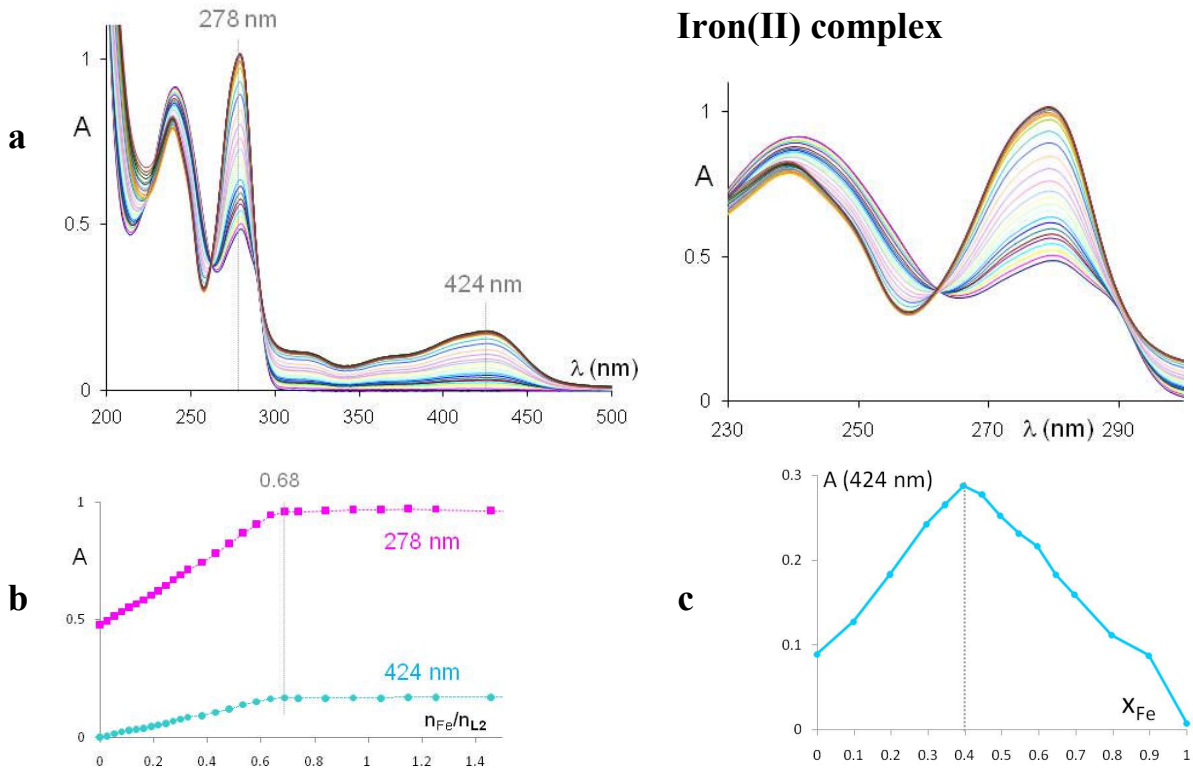

Figure S42: Titration data of $[Fe(H_2O)_6](BF_4)_2$ to **L2c** in CH_3CN; a) Spectral curves (full spectrum and zoom between 230 and 300 nm showing the isosbestic point); b) Absorbance as a function of n_{Fe} to n_{L2c} ratio at 278 and 424 nm; c) Job plot (lines have been added to guide the eye).

Nickel(II) complex

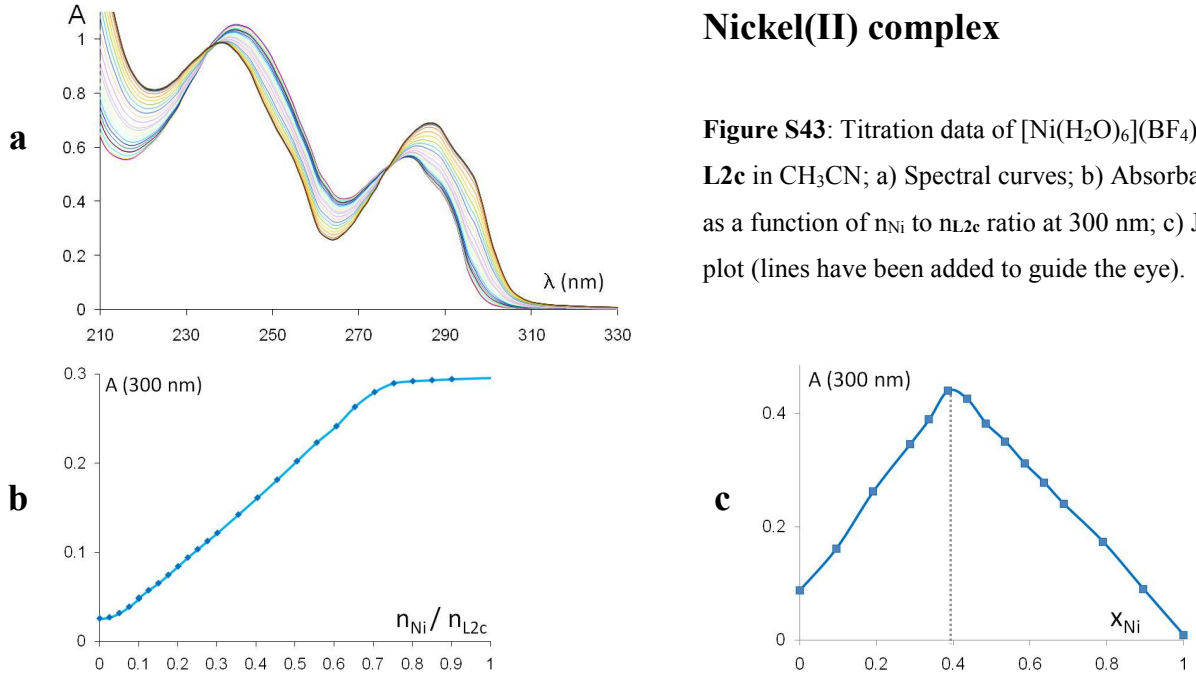

Figure S43: Titration data of $[Ni(H_2O)_6](BF_4)_2$ to **L2c** in CH_3CN; a) Spectral curves; b) Absorbance as a function of n_{Ni} to n_{L2c} ratio at 300 nm; c) Job plot (lines have been added to guide the eye).

2.e) ***L2d*** *ligand*

Iron(II) complex

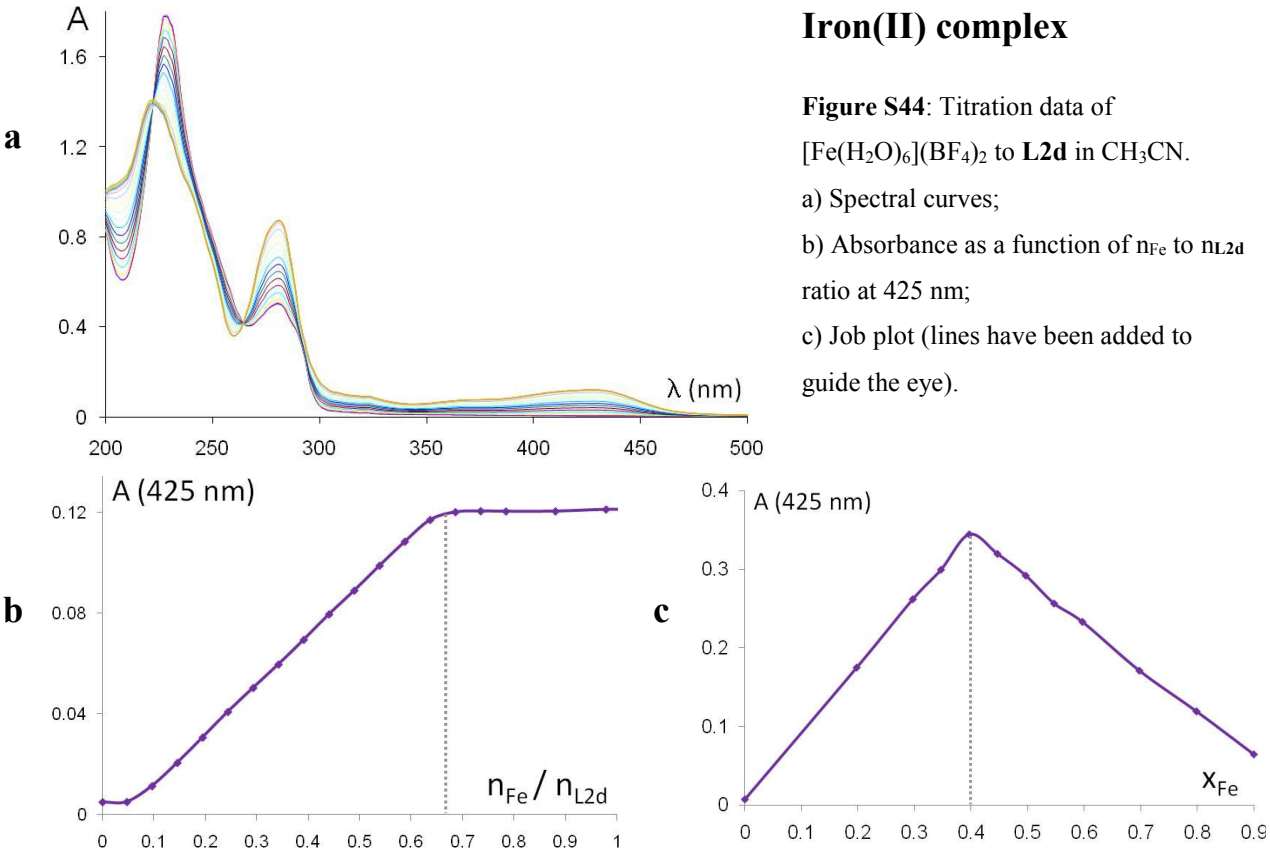

Figure S44: Titration data of $[Fe(H_2O)_6](BF_4)_2$ to **L2d** in CH_3CN.
a) Spectral curves;
b) Absorbance as a function of n_{Fe} to $n_{\mathbf{L2d}}$ ratio at 425 nm;
c) Job plot (lines have been added to guide the eye).

Nickel(II) complex

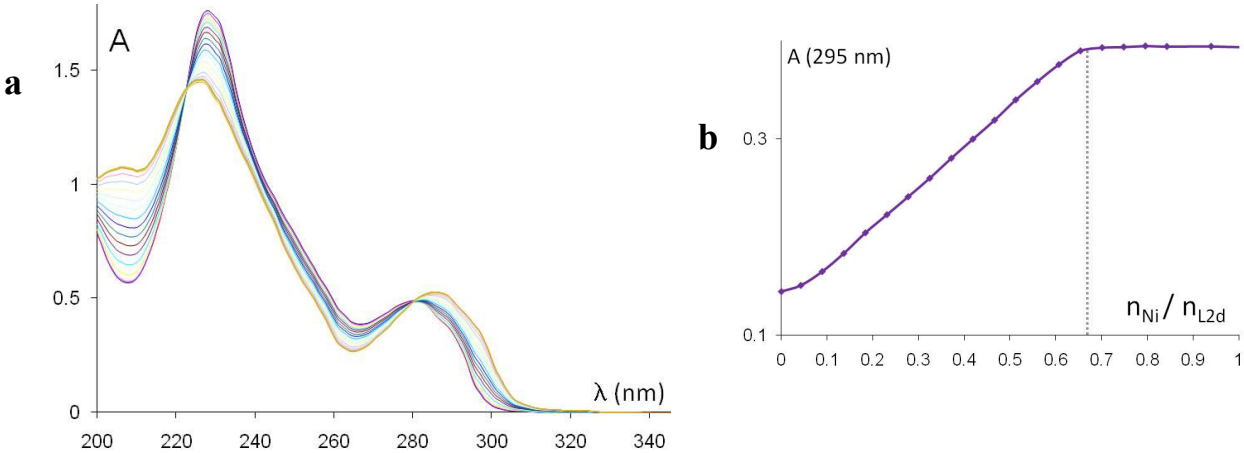

Figure S45: Titration data of $[Ni(H_2O)_6](BF_4)_2$ to **L2d** in CH_3CN; a) Spectral curves; b) Absorbance as a function of n_{Ni} to $n_{\mathbf{L2d}}$ ratio at 295 nm (lines have been added to guide the eye).

*2.f) **L3** ligand*

Iron(II) complex: **Figure S46**: Titration data of $[Fe(H_2O)_6](BF_4)_2$ to **L3** in CH_3CN; a) Spectral curves (full spectrum and zoom between 230 and 300 nm showing the isosbestic point); b) Absorbance as a function of n_{Fe} to n_{L3} ratio at 278 and 424 nm (lines have been added to guide the eye); c) Job plot at 420 nm.

a

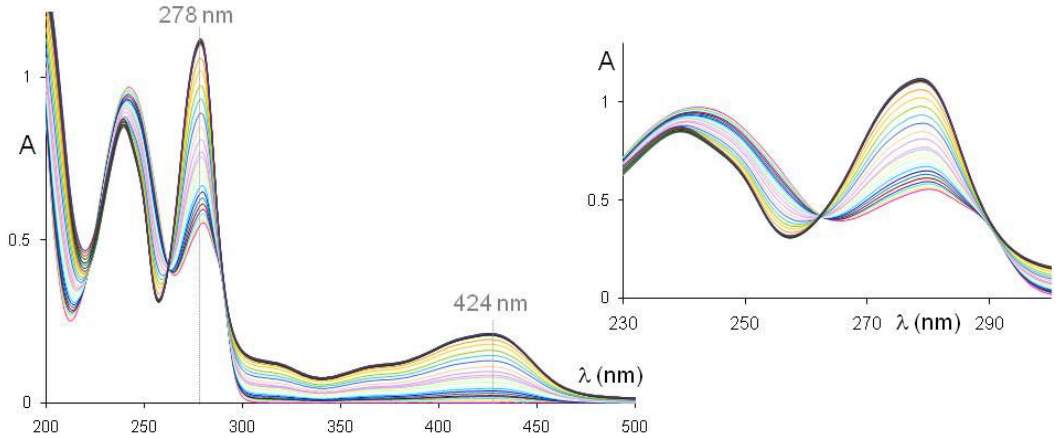

b

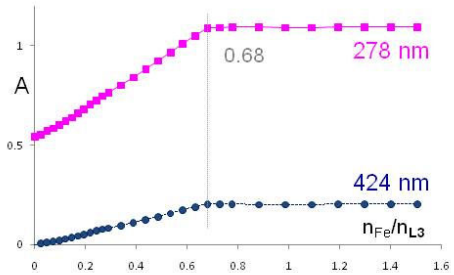

c

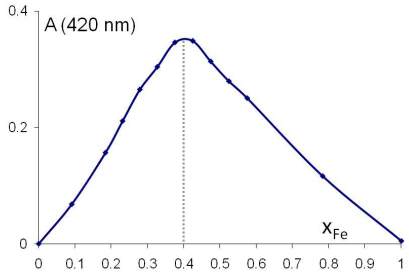

Nickel(II) complex

Figure S47: Titration data of $[Ni(H_2O)_6](BF_4)_2$ to **L3** in CH_3CN.

a) Spectral curves; b) Absorbance as a function of n_{Ni} to n_{L3} ratio at 300 nm; c) Job plot (lines have been added to guide the eye).

a

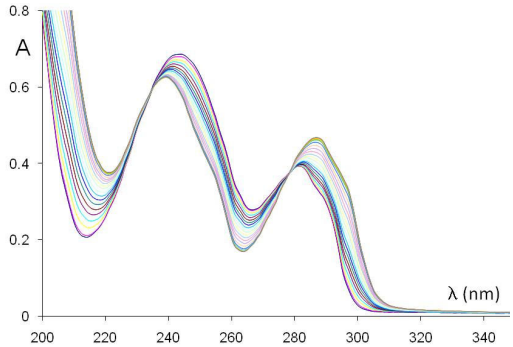

b

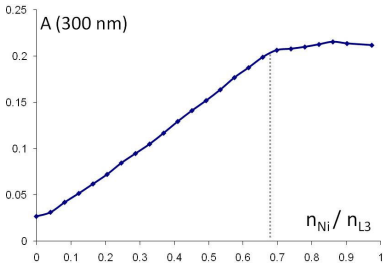

c

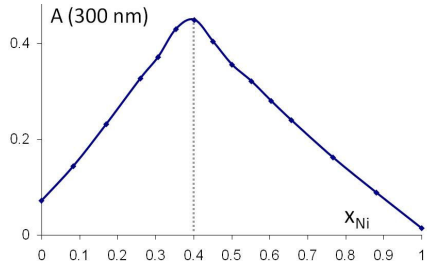

*2.g) **L4** ligand*

Iron(II) complex

Figure S48: Titration data of $[Fe(H_2O)_6](BF_4)_2$ to **L4** in CH_3CN.

a) Spectral curves;

b) Absorbance as a function of n_{Fe} to n_{L4} ratio at 425 nm;

c) Job plot (lines have been added to guide the eye).

a

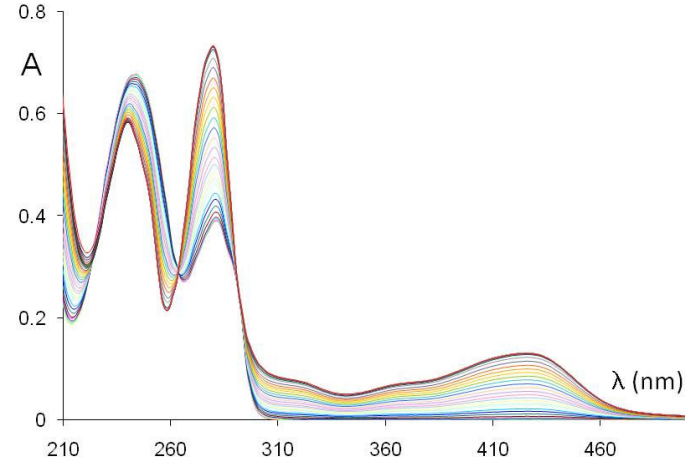

b

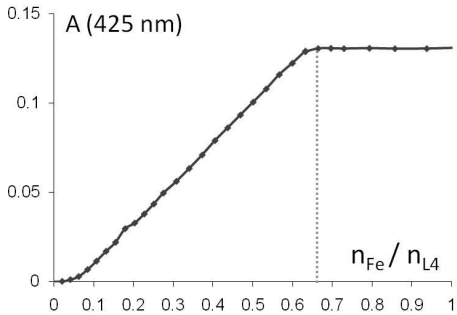

c

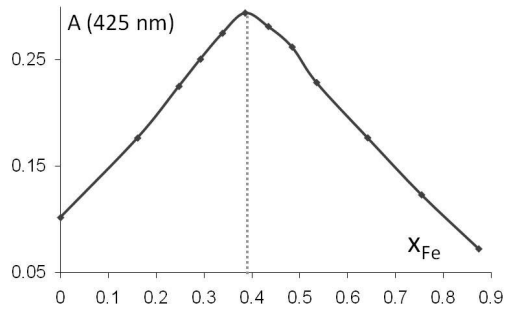

Nickel(II) complex

Figure S49: Titration data of $[Ni(H_2O)_6](BF_4)_2$ to **L4** in CH_3CN.

a) Spectral curves;

b) Absorbance as a function of n_{Ni} to n_{L4} ratio at 300 nm;

c) Job plot (lines have been added to guide the eye).

a

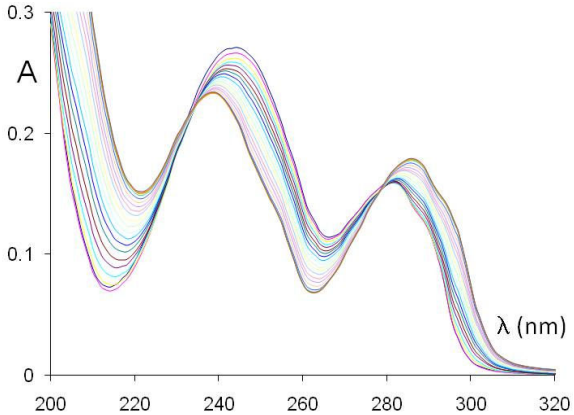

b

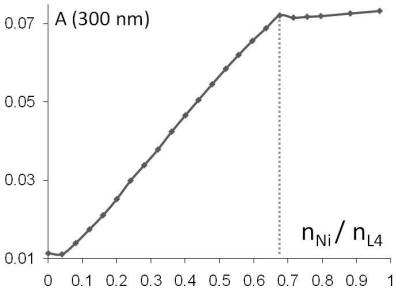

c

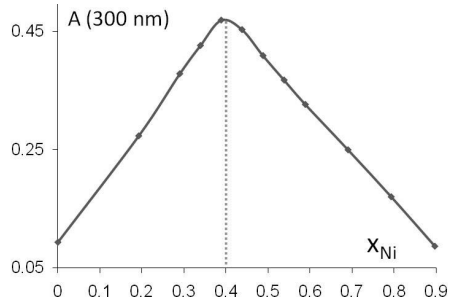

*2.h) **L5** ligand*

Iron(II) complex

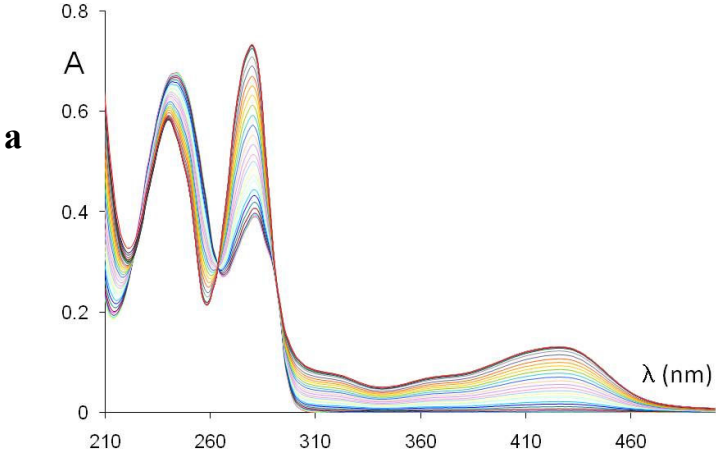

Figure S50: Titration data of $[Fe(H_2O)_6](BF_4)_2$ to **L5** in CH_3CN.

a) Spectral curves;

b) Absorbance as a function of n_{Fe} to n_{L5} ratio at 425 nm;

c) Job plot (lines have been added to guide the eye).

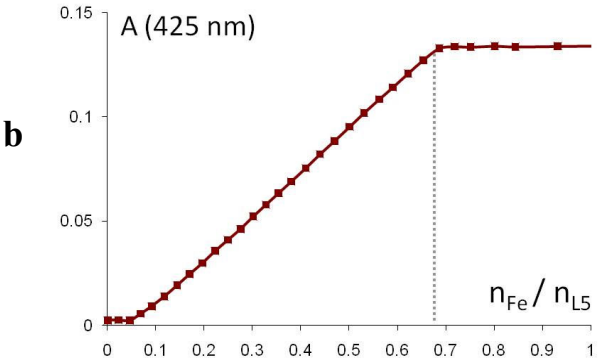

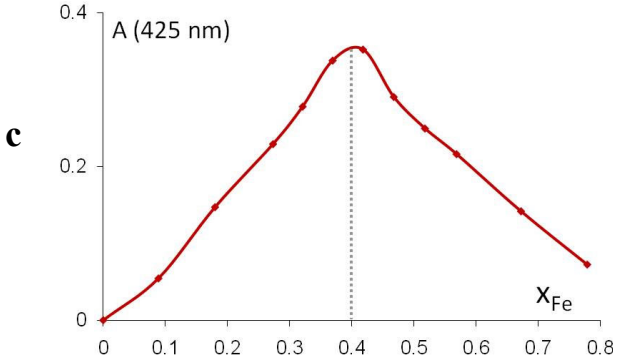

Nickel(II) complex

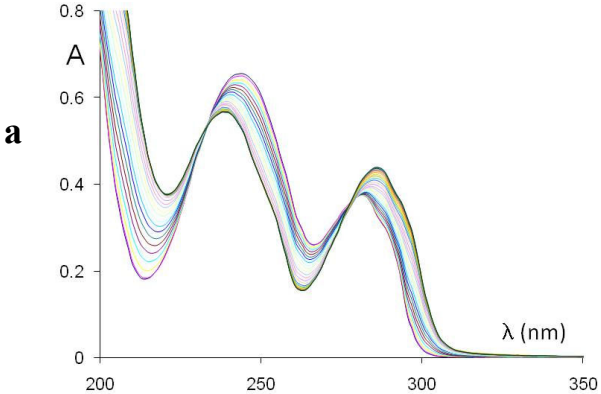

Figure S51: Titration data of $[Ni(H_2O)_6](BF_4)_2$ to **L5** in CH_3CN.

a) Spectral curves;

b) Absorbance as a function of n_{Ni} to n_{L5} ratio at 295 nm;

c) Job plot (lines have been added to guide the eye).

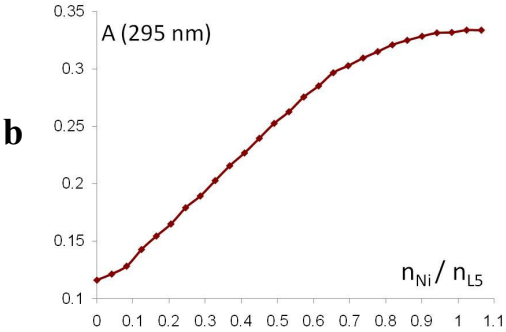

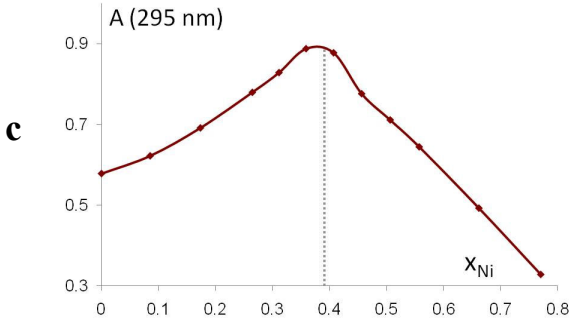

*2.i) **L6** ligand*

Iron(II) complex

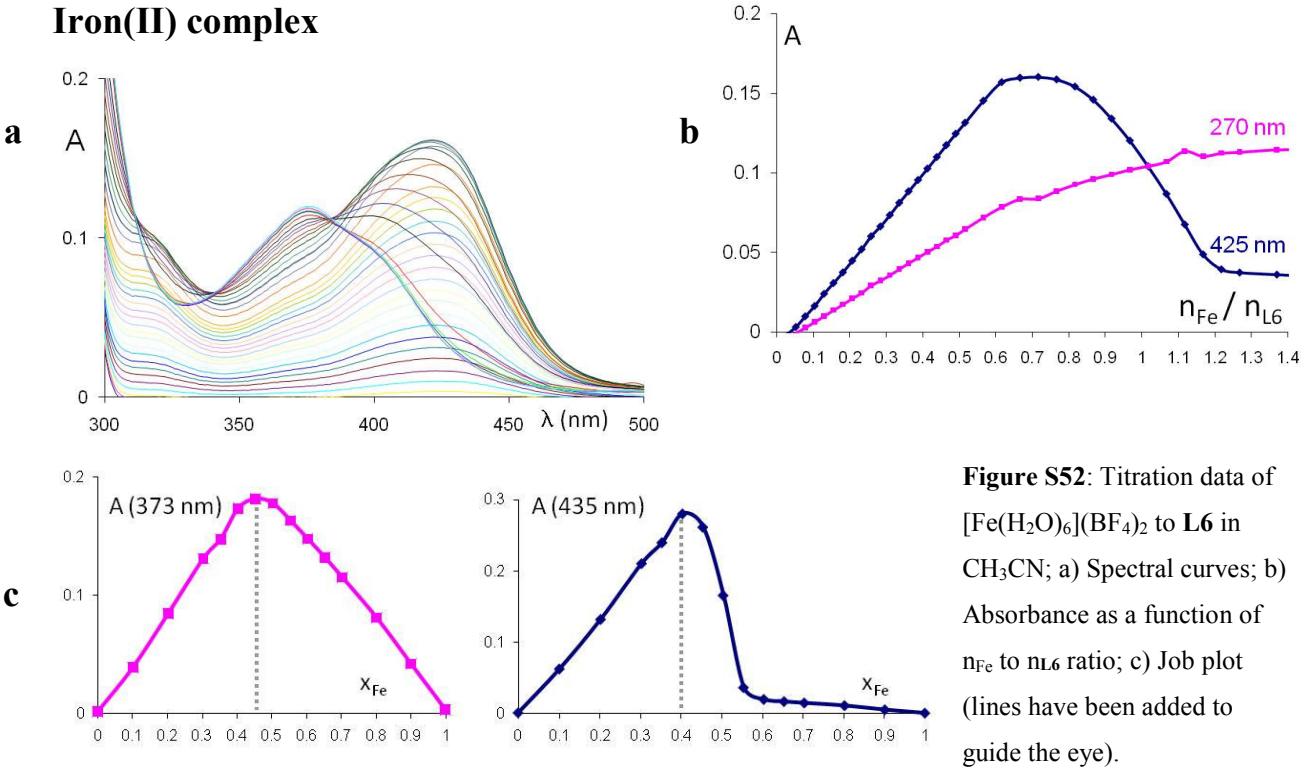

Figure S52: Titration data of $[Fe(H_2O)_6](BF_4)_2$ to **L6** in CH_3CN; a) Spectral curves; b) Absorbance as a function of n_{Fe} to n_{L6} ratio; c) Job plot (lines have been added to guide the eye).

Nickel(II) complex

Figure S53: Titration data of $[Ni(H_2O)_6](BF_4)_2$ to **L6** in CH_3CN.

a) Spectral curves;

b) Absorbance as a function of n_{Ni} to n_{L6} ratio at 240 and 285 nm;

c) Job plot (lines have been added to guide the eye).

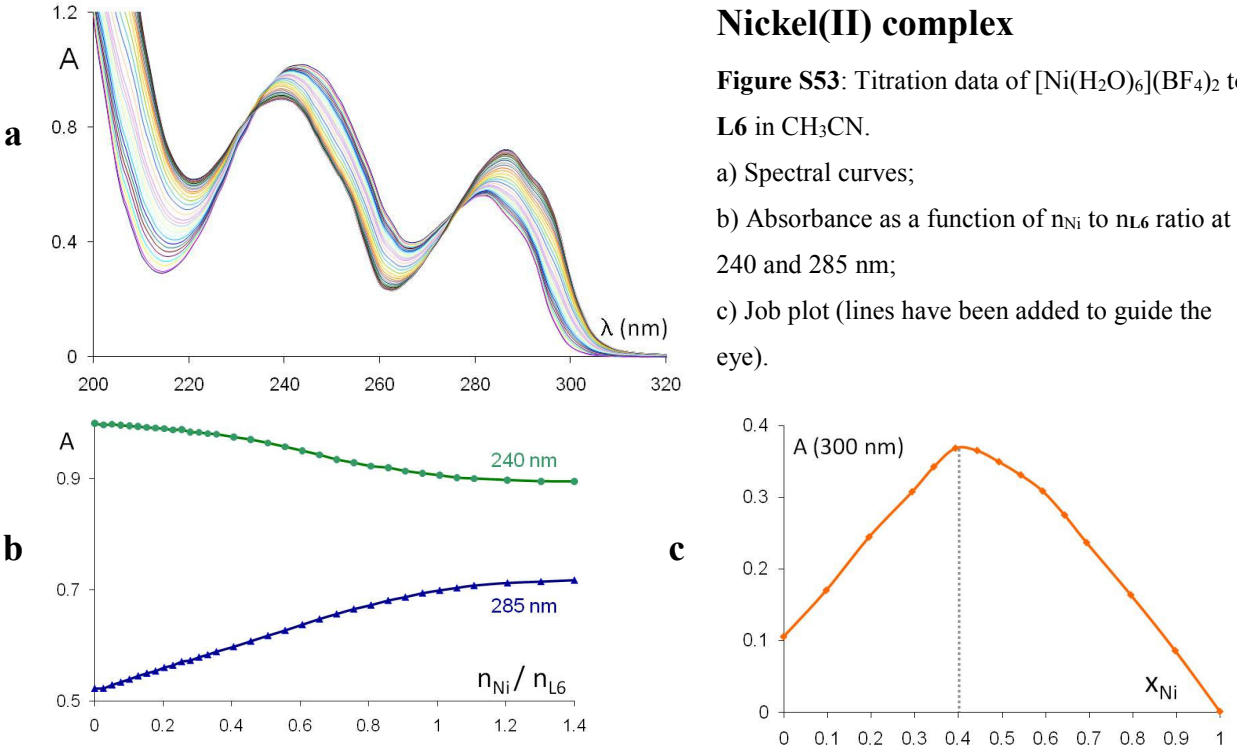

Zinc(II) complex:

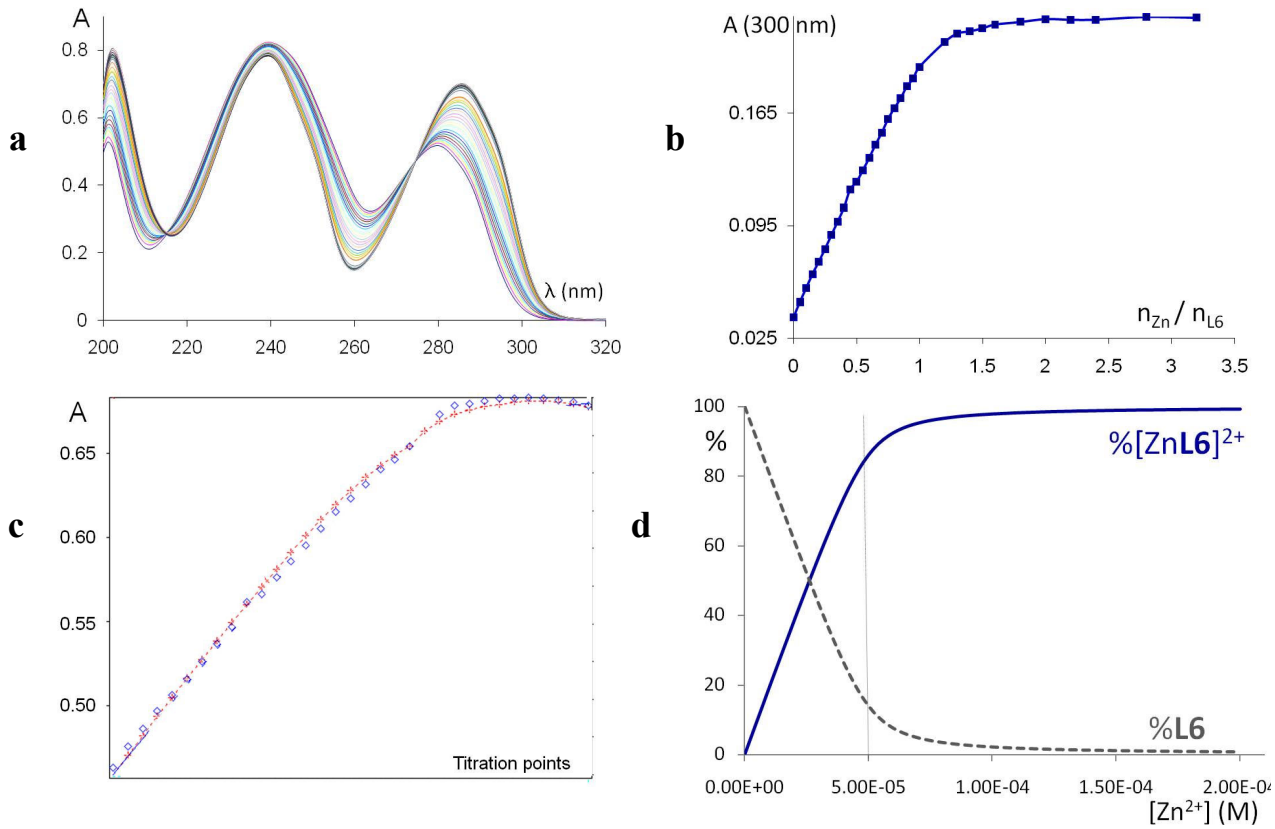

Figure S54: Titration data of $Zn(OTf)_2$ to **L6** in CH_3OH; a) Spectral curves; b) Absorbance as a function of n_{Zn} to n_{L6} ratio at 300 nm; c) Fit at 285 nm giving $\log\beta_{11} = 5.95 \pm 0.02$ (blue diamonds: data; red dotted lines: fit; Hyperquad2006); d) species distribution based on $\log\beta_{11} = 5.95$ (in blue, %[Zn **L6**]$^{2+}$, in dotted grey lines %**L6**; conditions for the simulations are $[\mathbf{L6}]_{initial} = 5.0 \times 10^{-5}$ M, $[Zn^{2+}]_{total}$ varies from 0 to 2.0×10^{-4} M; faint line signifies $[Zn^{2+}]_{total} = [\mathbf{L6}]_{initial} = 5.0 \times 10^{-5}$ M). Fitting equations and algorithms are described in P. Gans, A. Sabatini, A. Vacca, *Talanta* 1996, **43**, 1739-1753.

*2.j) **L2cM** ligand*

Nickel(II) complex

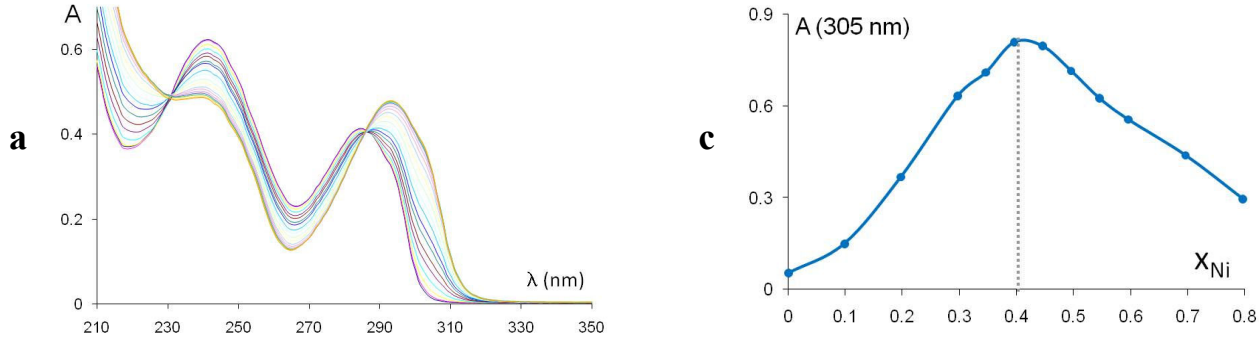

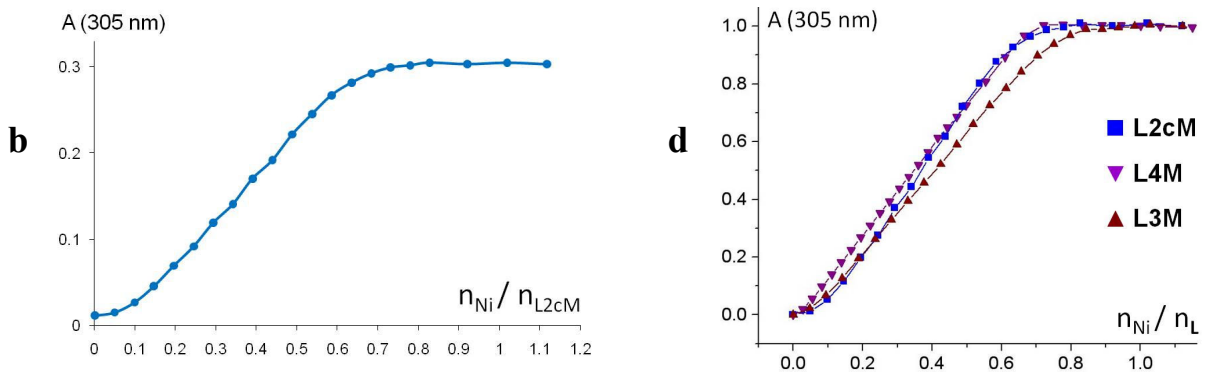

Figure S55: Titration data of $[Ni(H_2O)_6](BF_4)_2$ to **L2cM** in CH_3CN; a) Spectral curves; b) Absorbance as a function of n_{Ni} to n_{L2cM} ratio at 305 nm; c) Job plot (lines have been added to guide the eye); d) compared absorption profiles for the **L2cM**, **L3M** and **L4M** ligands at 305 nm.

Iron(II) complex

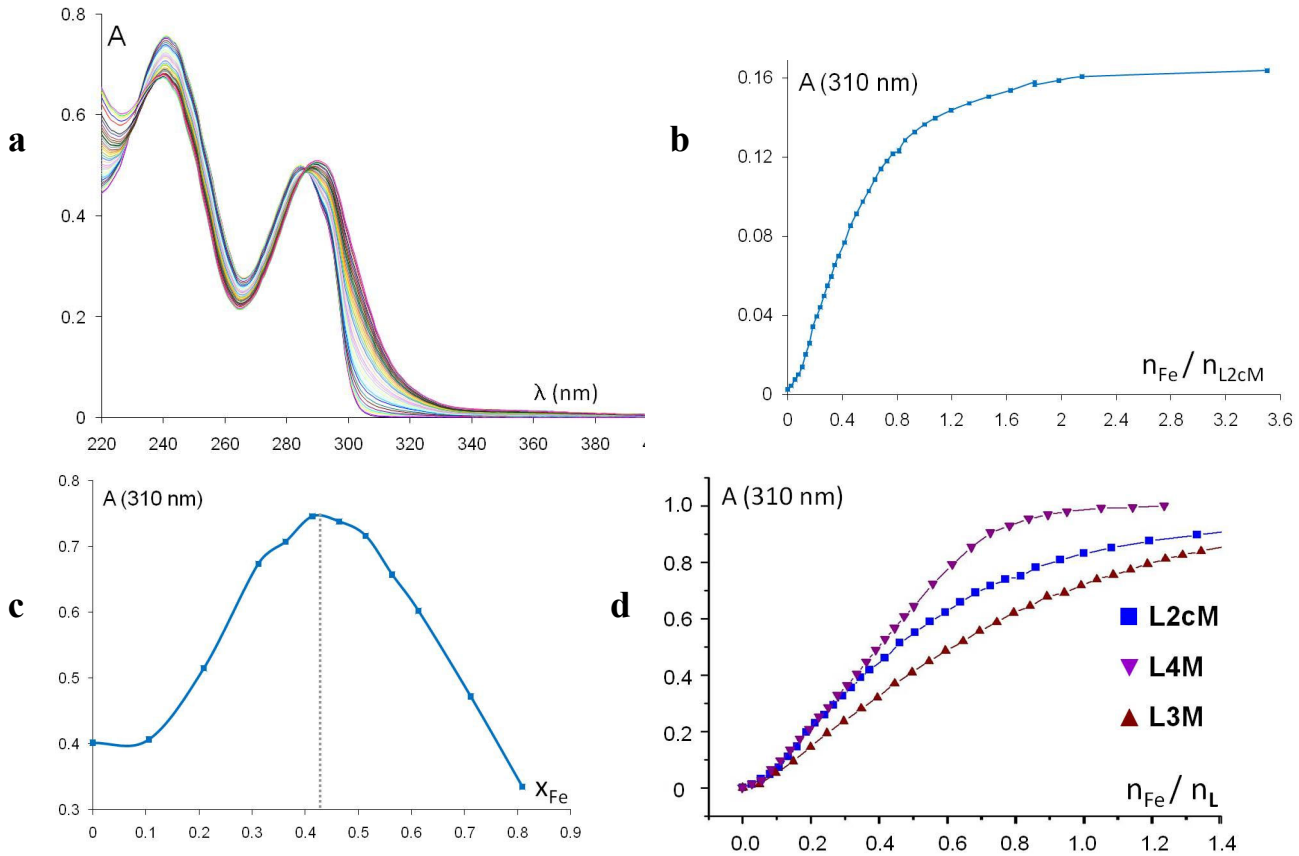

Figure S56: Titration data of $[Fe(H_2O)_6](BF_4)_2$ to **L2cM** in CH_3CN; a) Spectral curves; b) Absorbance as a function of n_{Fe} to n_{L2cM} ratio at 310 nm; c) Job plot (lines have been added to guide the eye); d) compared absorption profiles for the **L2cM**, **L3M** and **L4M** ligands at 310 nm (each curve has been normalized to 1.0 at full saturation of the signal).

2.k) ***L3M*** *ligand*

Iron(II) complex

Figure S57: Titration data of $[Fe(H_2O)_6](BF_4)_2$ to **L3M** in CH_3CN.

a) Spectral curves;

b) Absorbance as a function of n_{Fe} to n_{L3M} ratio at 305 nm;

c) Job plot (lines have been added to guide the eye).

a

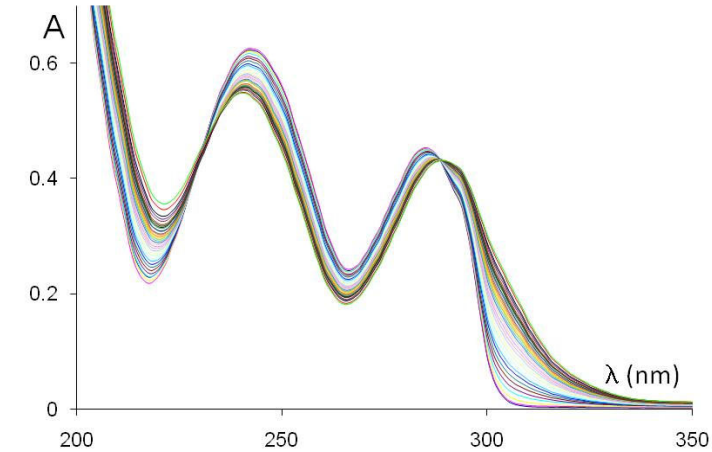

b

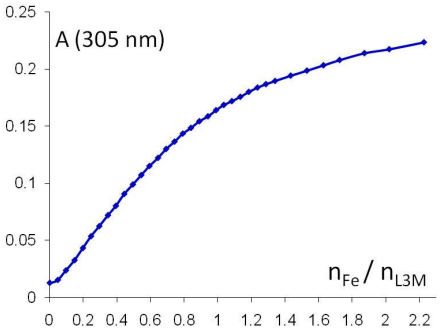

c

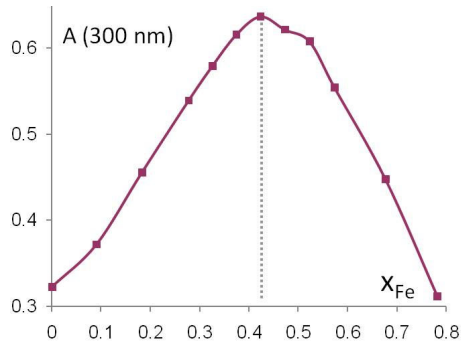

Nickel(II) complex

Figure S58: Titration data of $[Ni(H_2O)_6](BF_4)_2$ to **L3M** in CH_3CN.

a) Spectral curves;

b) Absorbance as a function of n_{Ni} to n_{L3M} ratio at 300 nm;

c) Job plot (lines have been added to guide the eye).

a

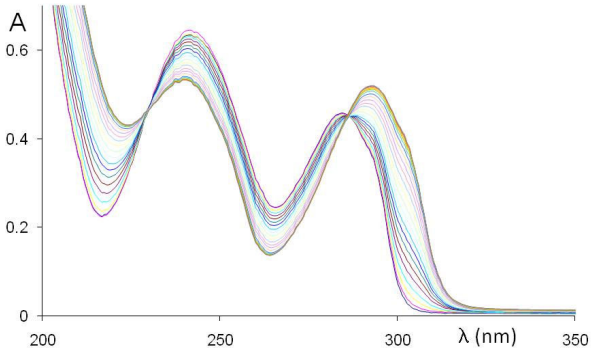

b

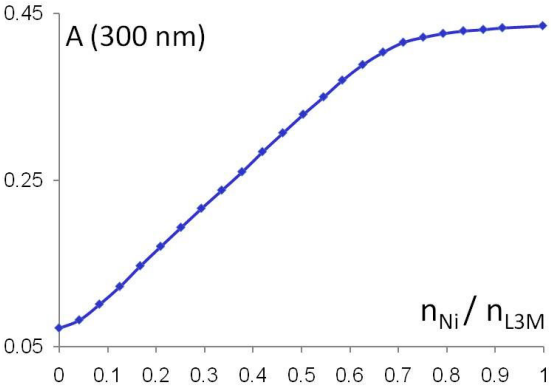

c

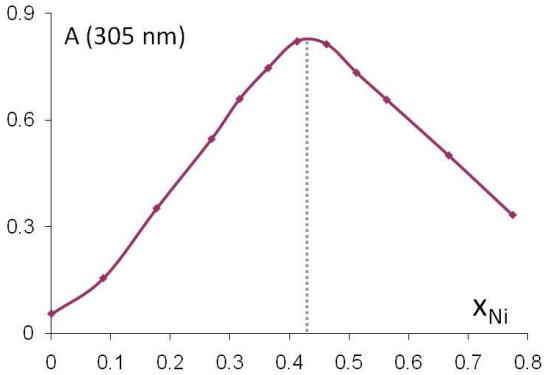

2.l) ***L4M*** *ligand*

Iron(II) complex

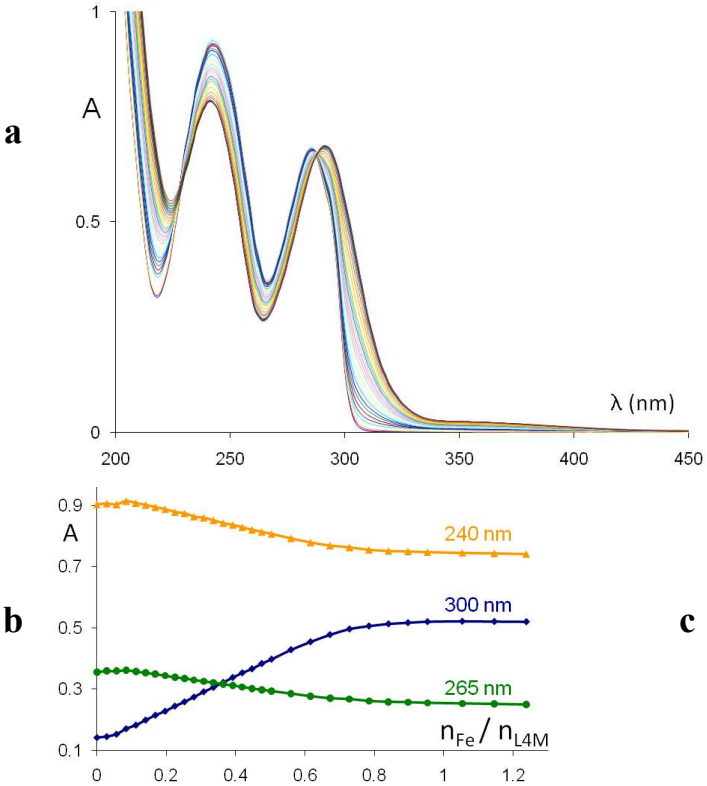

Figure S59: Titration data of $[Fe(H_2O)_6](BF_4)_2$ to **L4M** in CH_3CN.

a) Spectral curves;

b) Absorbance as a function of n_{Fe} to n_{L4M} ratio;

c) Job plot (lines have been added to guide the eye).

Nickel (II) complex

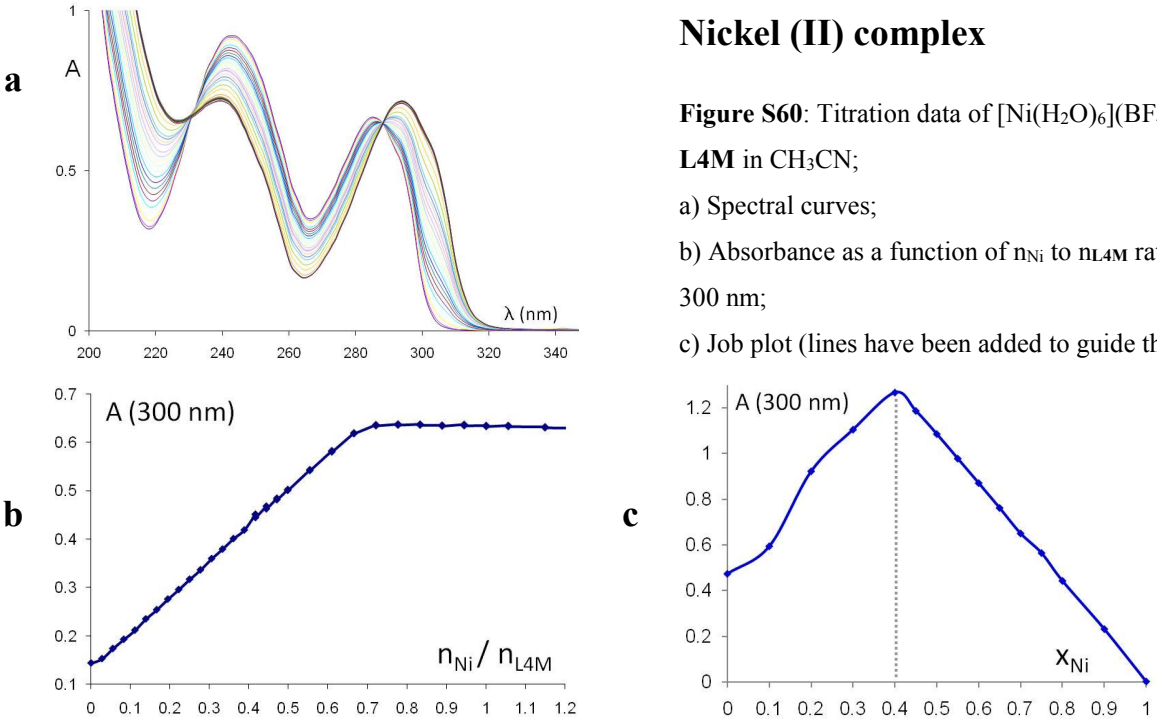

Figure S60: Titration data of $[Ni(H_2O)_6](BF_4)_2$ to **L4M** in CH_3CN;

a) Spectral curves;

b) Absorbance as a function of n_{Ni} to n_{L4M} ratio at 300 nm;

c) Job plot (lines have been added to guide the eye).

E. DFT for $[Fe(L1)_3]^{2+}$

DFT calculations were completed for $[Fe(\mathbf{L1'})_3]^{2+}$ and $[Fe(\mathbf{L1M'})_3]^{2+}$ only. The Fe^{2+} centers are distant enough in the dinuclear complexes that no dominant electronic effect is expected to be induced by the second Fe^{2+}, since crystal data showed no major local effects from dinuclear to mononuclear species.

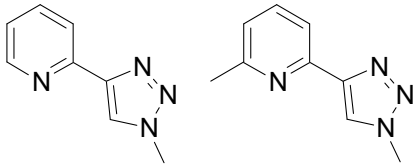

L1' **L1M'**

Methods: UV/Vis spectra of selected model compounds were performed using time-dependent density functional theory (TD-DFT) at the B3LYP*/TZVP level of theory.[1,2] The B3LYP* functional has been shown to accurately reproduce the ground states of several Fe(II) complexes[1,3] and yielded properties that were in good agreement with experiment for the complexes considered in this study. The geometries of the calculated structures were first optimized on the ground state and characterized as local minima *via* frequency calculations. TD-DFT calculations were then performed on these structures to evaluate the 160 lowest energy electronic transitions, which were used to construct simulated UV/Vis spectra. All calculations were performed with the Gaussian09 software package.[4]

[1] M. Reiher, O. Salomon, B.A. Hess "Reparameterization of hybrid functionals based on energy differences of states of different multiplicity" *Theor. Chem. Acc.*, **107**, (2001) 48-55.

[2] A. Schaefer, C. Huber, R. Ahlrichs, "Fully optimized contracted Gaussian basis sets of triple zeta valence quality for atoms Li to Kr" *J. Chem. Phys.*, **100** (1994) 5829-5835.

[3] O. Salomon, M. Reiher, B.A. Hess "Assertion and validation of the performance of the B3LYP* functional for the first transition metal row and the G2 test set" *J. Chem. Phys.*, **117**, (2002) 4729-4737.

[4] M. J. Frisch, G. W. Trucks, H. B. Schlegel, G. E. Scuseria, M. A. Robb, J. R. Cheeseman, G. Scalmani, V. Barone, B. Mennucci, G. A. Petersson, H. Nakatsuji, M. Caricato, X. Li, H. P. Hratchian, A. F. Izmaylov, J. Bloino, G. Zheng, J. L. Sonnenberg, M. Hada, M. Ehara, K. Toyota, R. Fukuda, J. Hasegawa, M. Ishida, T. Nakajima, Y. Honda, O. Kitao, H. Nakai, T. Vreven, J. A. Montgomery, Jr., J. E. Peralta, F. Ogliaro, M. Bearpark, J. J. Heyd, E. Brothers, K. N. Kudin, V. N. Staroverov, T. Keith, R. Kobayashi, J. Normand, K. Raghavachari, A. Rendell, J. C. Burant, S. S. Iyengar, J. Tomasi, M. Cossi, N. Rega, J. M. Millam, M. Klene, J. E. Knox, J. B. Cross, V. Bakken, C. Adamo, J. Jaramillo, R. Gomperts, R. E. Stratmann, O. Yazyev, A. J. Austin, R. Cammi, C. Pomelli, J. W. Ochterski, R. L. Martin, K. Morokuma, V. G. Zakrzewski, G. A. Voth, P. Salvador, J. J. Dannenberg, S. Dapprich, A. D. Daniels, O. Farkas, J. B. Foresman, J. V. Ortiz, J. Cioslowski, and D. J. Fox, *Gaussian 09, Revision C.01;* Gaussian, Inc., Wallingford CT., 2010.

Optimized geometries (mono-nuclear complexes)

	Low spin, *fac*	Low spin, *mer*
$[Fe(\mathbf{L1'})_3]^{2+}$	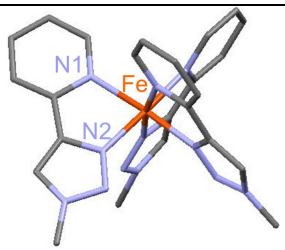 Fe-N1: 2.074 Å, Fe-N2: 1.989 Å.	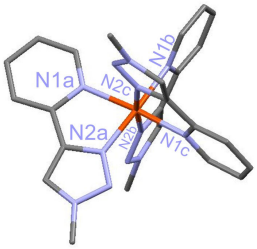 Fe-N1a: 2.069 Å, Fe-N1b: 2.074 Å, Fe-N1c: 2.066 Å, Fe-N2a: 1.990 Å, Fe-N2b: 1.998 Å, Fe-N2c: 1.998 Å.
	High spin, *fac*	High spin, *mer*
$[Fe(\mathbf{L1M'})_3]^{2+}$	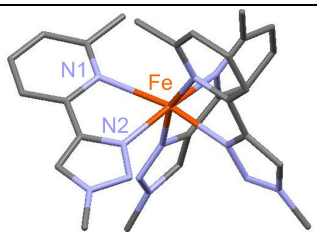 Fe-N1 (Me-Py): 2.358-2.454 Å, Fe-N2 (triazole): 2.171-2.223 Å.	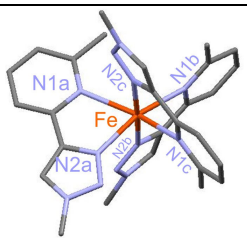 Fe-N1a: 2.378 Å, Fe-N1b: 2.446 Å, Fe-N1c: 2.360 Å, Fe-N2a: 2.192 Å, Fe-N2b: 2.205 Å, Fe-N2c: 2.190 Å.

Energy levels for mono-nuclear complexes in low spin and high-spin states of **L1'** and **L1M'** iron complexes, in *fac* and *mer* conformations (energies in kcal/mol, relative to the low spin *fac* species)

	fac		*mer*	
	Low spin	High spin	Low spin	High spin
$[Fe(\mathbf{L1'})_3]^{2+}$	0	8.09	-0.10	7.25
$[Fe(\mathbf{L1M'})_3]^{2+}$	0	-0.29	-0.83	-3.56

Calculated spectra, orbital coefficient and charge density changes: Experimental and calculated electronic spectra (low spin) are displayed on Fig. S11a. In the visible region, bands at ~305-330 nm and 405 nm are associated with charge transfer transitions 28, 29, 31, 32 and 10, 11 respectively.

a

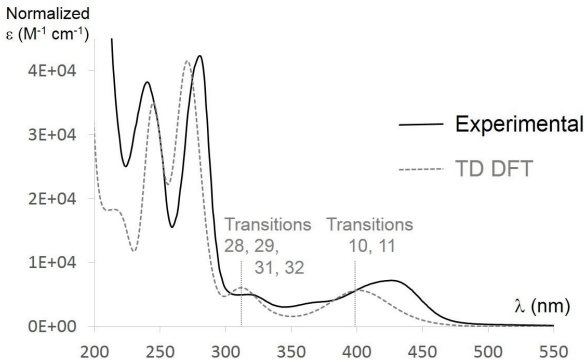

Figure S61: a) Electronic spectra and b) charge density differences for low spin *fac* Fe(**L1'**)$_3^{2+}$
[ρ(excited) – ρ(ground)]: 0.003 au change in density.
Increase = purple; decrease = orange
Details of the orbitals contributing to each transition are given below.

b

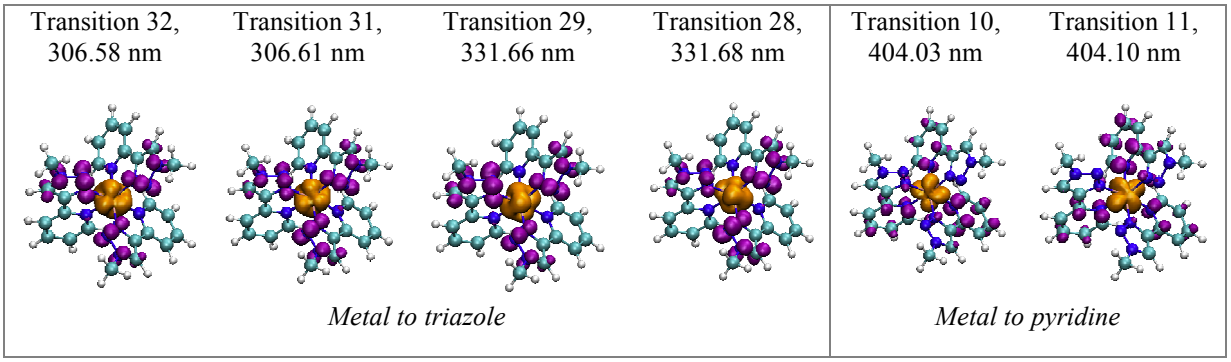

<u>Details on molecular orbitals involved in the electronic transitions</u> (molecular orbitals on the right, unoccupied on the left; 0.05 au isosurface; positive phase in purple, negative phase in orange; numbers above the arrows represent the contribution of transition between orbitals to each excitation):

Transition 10

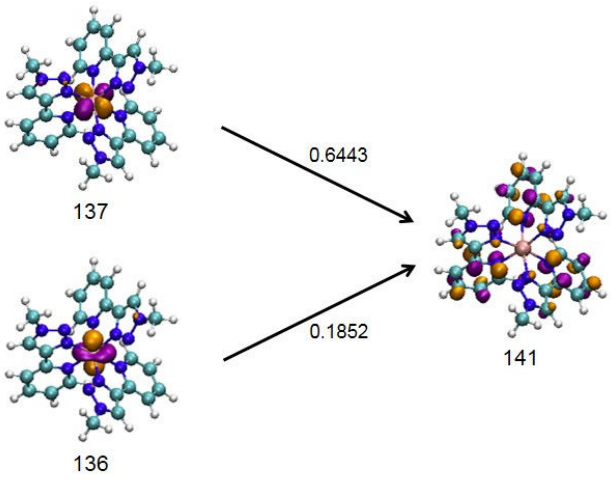

Transition 11

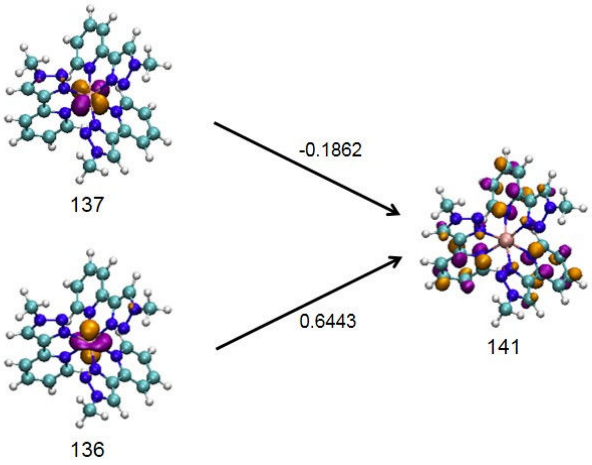

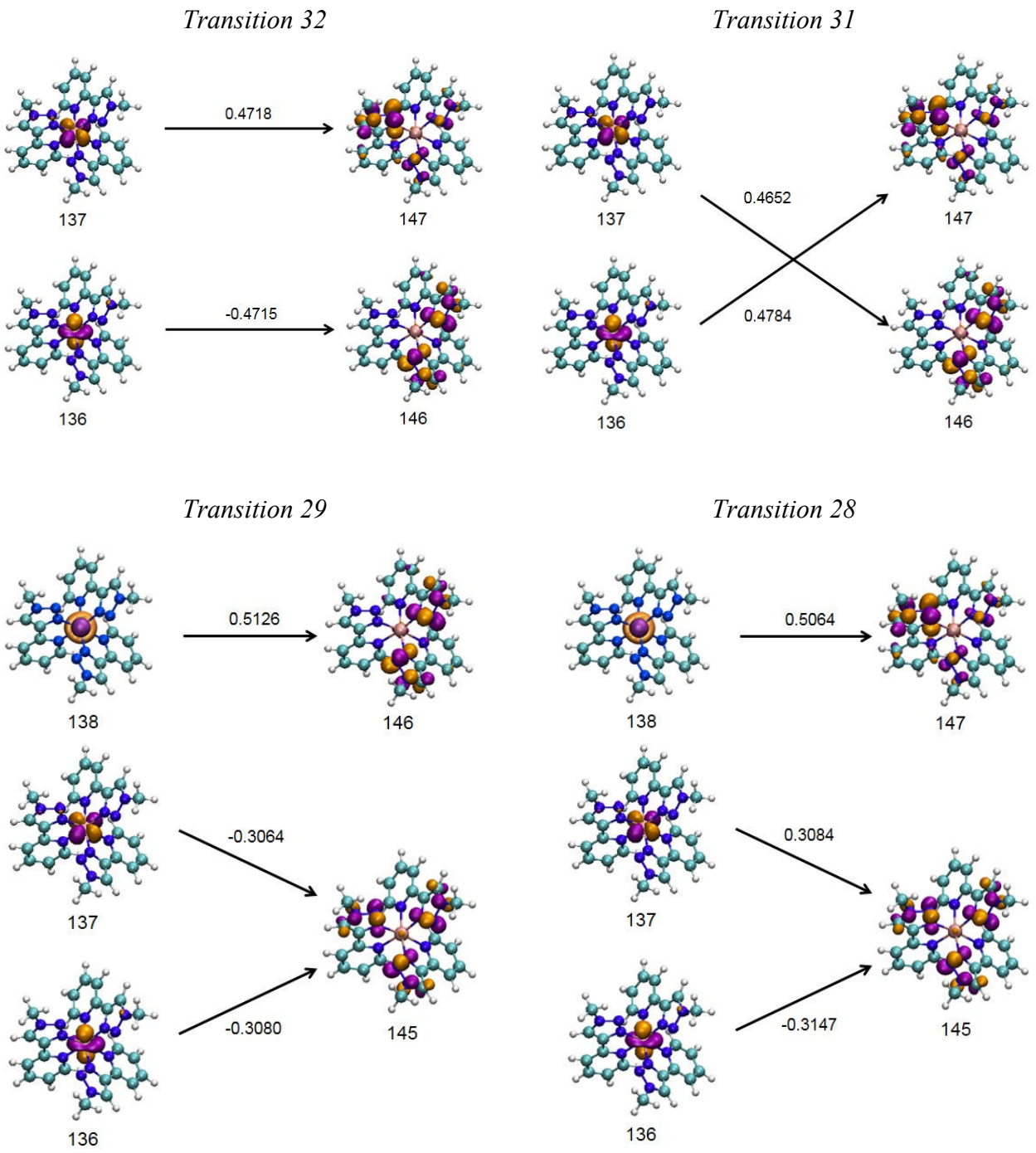

Figure S62: Orbital involved in transitions associated with charge transfer in the visible region.

F. Mass spectrometry analysis

1) General methods:

Solutions were prepared by solubilizing a mixture of ligands and $[Fe(H_2O)_6](BF_4)_2$ in 3:2 ratio in acetonitrile, evaporating the mixture to dryness and redissolving the salts in acetonitrile at the desired concentration (10^{-6} M, 10^{-5} M and 10^{-4} M; only the more concentrated solutions showed significant complex formation). ESI-MS experiments were performed in the positive ion mode on a Bruker Daltonics microTOF spectrometer (Bruker Daltonik GmgH, Bremen, Germany) equipped with an orthogonal electrospray (ESI) interface. Calibration was performed using Tuning mix (Agilent Technologies). Prior to analyses, samples were diluted at 10^{-4} M in CH_3CN. Sample solutions were introduced into the spectrometer source with a syringe pump (Harvard type 55 1111: Harvard Apparatus Inc., South Natick, MA, USA) with a flow rate of 5 $\mu L.min^{-1}$. In order to preserve non-covalent interactions during the ionization/desorption process, instrumental settings were carefully tuned. For that, the capillary exit voltage was adjusted with a particular attention (between 100 V and 150 V). Interpretations were obtained with the help of DataAnalysis v4.0 software.

2) Zoomed spectra in the area of triple-stranded iron(II) complexes with **L2c**, **L2a**, **L3** and **L4**

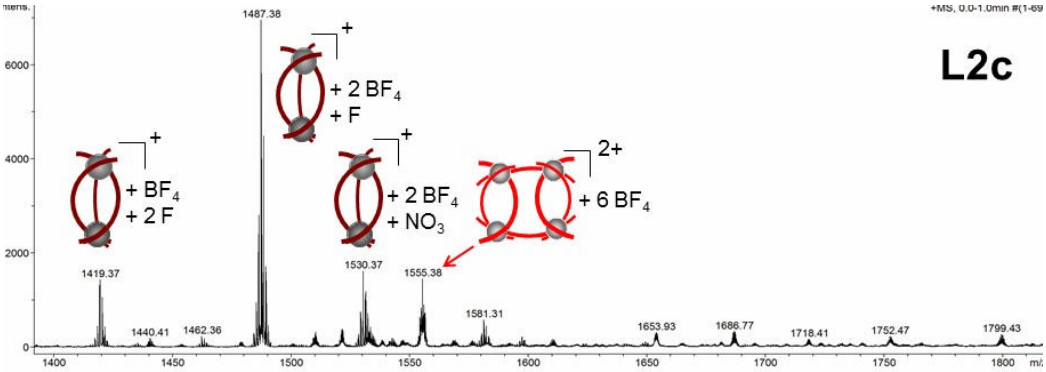

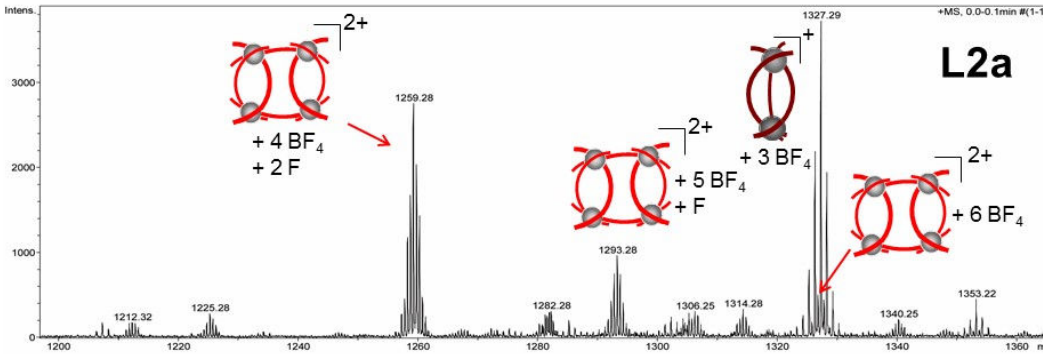

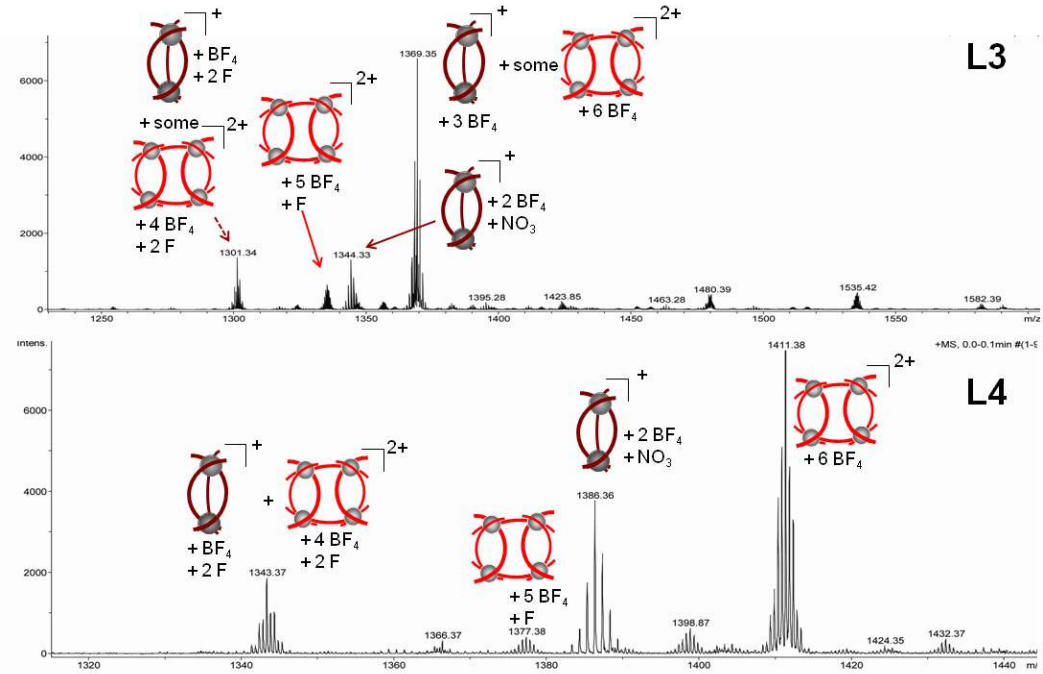

Figure S63: ESI MSfor m/z regions where triple-stranded (1+) and hexa-stranded complexes (2+) would appear.

3) Full mass spectra for methylpyridine-based ligands **L2cM**, **L3M** and **L4M**

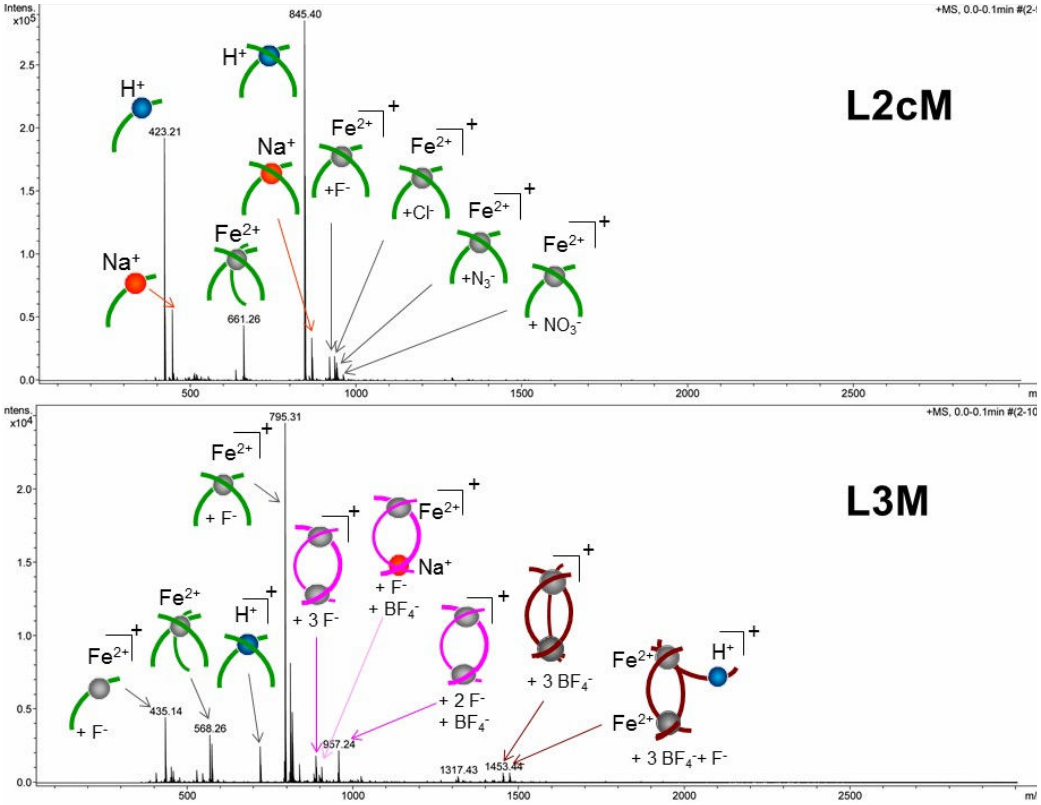

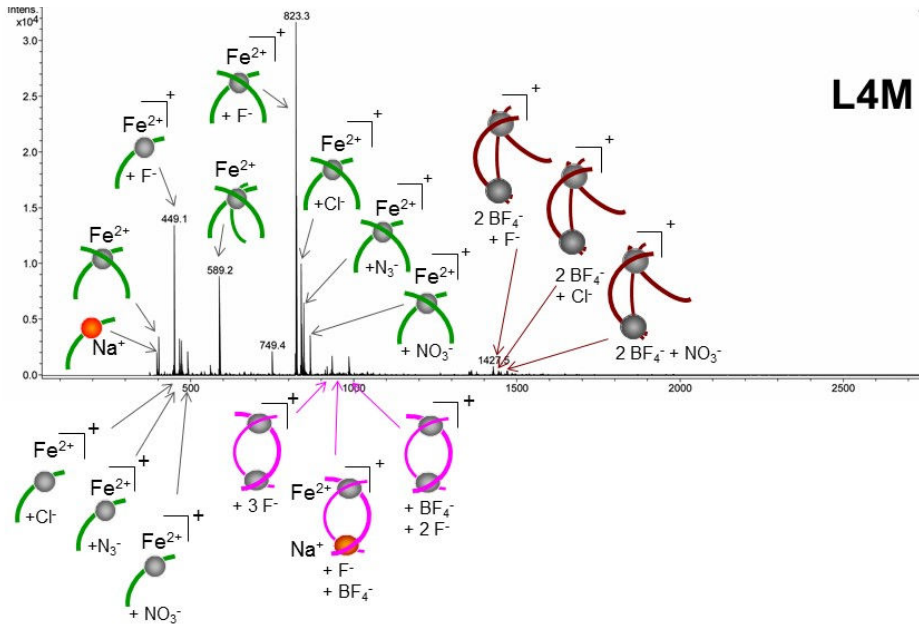

Figure S64: ESI mass spectra for iron complexes of methylated ligands **L2cM**, **L3M** and **L4M**.

G. Vapour pressure osmometry

Vapour pressure osmometry experiments were conducted on a Knauer K-7000 Vapor Pressure Osmometer according to the manufacturer's instructions. Concentrated stock solutions of ligand and $[Fe(H_2O)_6](BF_4)_2$ in 3:2 molar ratio in acetonitrile were prepared at 15-20 g/kg, and diluted to produce solutions down to 2 g/kg. No supporting electrolyte was used to shield the charges, as only relative response was sought. Each point was measured in triplicate at 38 °C.

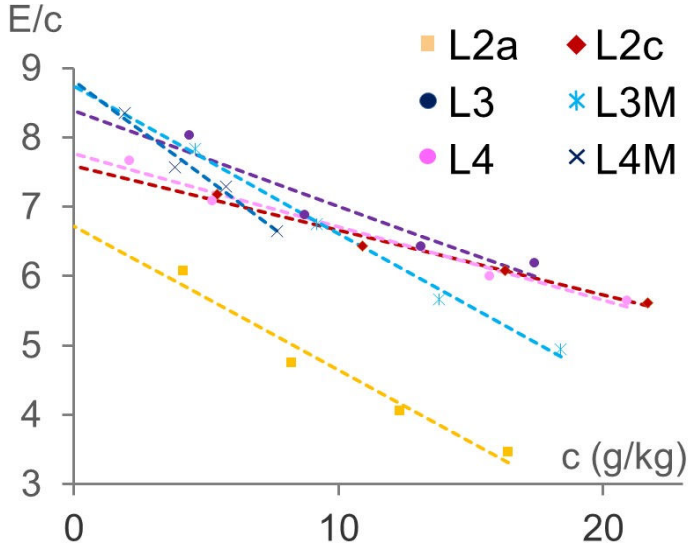

Figure S65: VPO analysis of iron complexes of **L2a**, **L2c**, **L3**, **L4**, **L3M** and **L4M**. The ratio of the change in electrical imbalance to the concentration (g/kg) is given on the y axis (the change in voltage reflects the ΔT at the thermistors). Markers indicate measured values. Dotted lines are linear regressions of the marked measured values.

H. Magnetic studies

Magnetic susceptibility measurements were obtained using a Quantum Design MPMS-XL7 SQUID magnetometer at the University of Ottawa. Direct current (dc) magnetic measurements were performed on a 21.7 mg polycrystalline sample of $[Fe_2(\mathbf{L3})_3](BF_4)_4$ in a polyethylene wrap in the temperature range of 2.5-300 K and under applied fields of -7 to 7 T. Measurements were performed on powder samples of 15.5, 21.1 and 16.8 mg for $[Fe_2(\mathbf{L3M})_3](BF_4)_4$, $[Fe_2(\mathbf{L4M})_3](BF_4)_4$ and $[Fe(\mathbf{L1M})_3](BF_4)_2$, respectively. The absence of ferromagnetic impurities was confirmed for all samples by an *M vs*. *H* measurement which was performed at 100 K. Experimental data were corrected for the sample holder and the diamagnetic contributions of the sample. Alternating current (ac) susceptibility measurements were carried out under an oscillating ac field of 3 Oe and ac frequencies ranging from 10 to 1500 Hz.

I. Models for L4-, L5-, L6- and L2a-derived architectures

1) Methods: simple models were created using the Cache software, with either the MM3 or stand methods ('stand' was used to minimize small fragments). The goal of such models is to create a visual analysis of the accessibility of helicate, mesocate and looped structures for the larger alkyl spacers. These do not presume of the absolute minima in the conformational energy profiles.

2) Models for **L4**-helicate, and **L5**-derived Fe(II) helicates and mesocates

***L4**-derived helicate (a)* ***L5**-derived helicate (b) and mesocate (c)*

a)

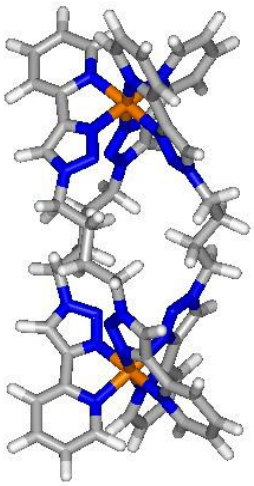

(Λ, Λ) enantiomer

b)

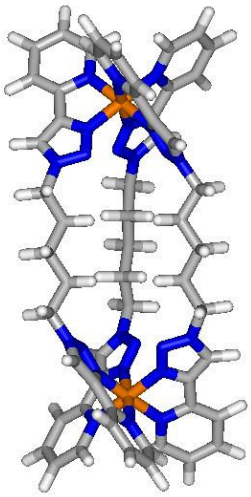

(Λ, Λ) enantiomer

c)

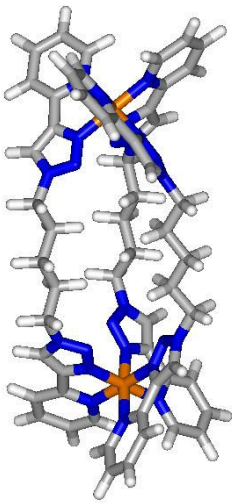

(Λ, Δ) enantiomer

3) Models for looped structures (**L6**):

a) 1:1 Fe/**L6** complex with axial water ligands.

b) 2:3 Fe/**L6** complex, with two equivalent 'capping' **L6** ligands and one bridging **L6** ligand.

a)

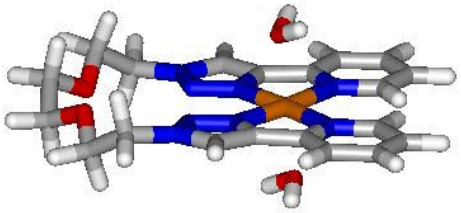

b)

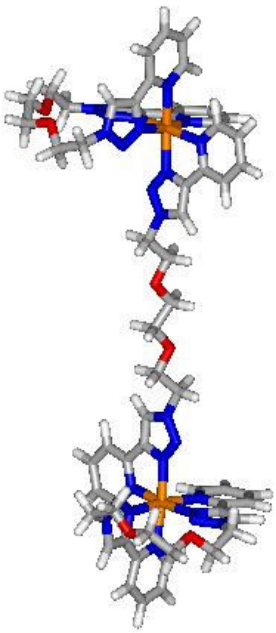

4) A model for **L2a**-based hexamer: Although there are many possible ligand and metal combinations to form a tetranuclear hexameric architecture considering the diversity in metal-based chirality, and *fac vs mer* isomerism, below is one possible hexameric structure (only *fac*, all Λ isomers) , where the relief of the nitrogen lone pair for the bridging ligand is visible a) stick and b) CPK representations).

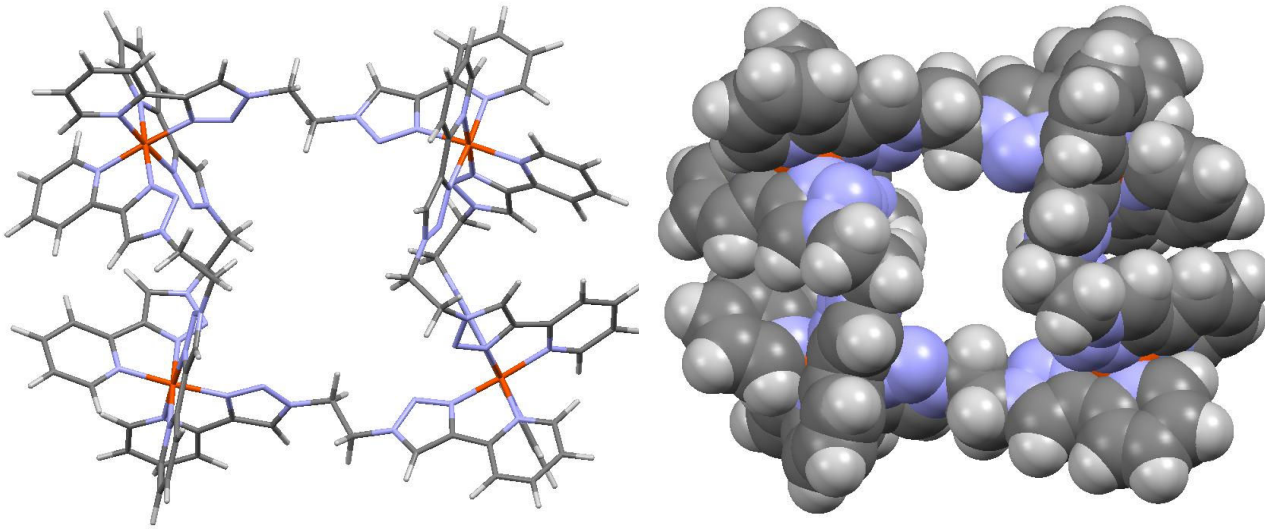

J. Crystallographic data $[Fe_2(\mathbf{L3})_3](BF_4)_4$ crystal structure [CCDC: 1057879]

Data collection: A crystal of the compound (red, block-shaped, size 0.10 × 0.25 × 0.25 mm) was mounted on a glass fiber with grease and cooled to -93 °C in a stream of nitrogen gas controlled with Cryostream Controller 700. Data collection was performed on a Bruker SMART APEX II X-ray diffractometer with graphite-monochromated Mo K_α radiation (λ = 0.71073 Å), operating at 50 kV and 30 mA over 2θ ranges of 2.56 ~ 52.00º. No significant decay was observed during the data collection. The collected frames were integrated with the Bruker SAINTsoftware[2] package using a narrow-frame algorithm. The integration of the data using a triclinic unit cell yielded a total of 58459 reflections to a maximum θ angle of 27.07° (0.78 Å resolution). The final cell constants are based upon the refinement of the XYZ-centroids of 9934 reflections above 20 σ(I) with 4.599° < 2θ < 53.18°:

a = 13.8603(5) Å	α = 109.535(2)°
b = 17.9020(7) Å	β = 101.234(3)°
c = 17.9413(7) Å	γ = 103.518(2)°
Volume	3894.0(3) Å^3

The space group was determined to be: $P\bar{1}$ [2].

Data reduction: was performed with the Bruker SAINT software,[2] which corrects for beam inhomogeneity, possible crystal decay, Lorentz and polarisation effects. The linear absorption coefficient, μ, is 0.157 mm^{-1}. A multi-scan absorption correction was applied (Bruker SADABS,[3]). The value for $wR_2(int)$ was 0.0581 before and 0.0478 after correction. The ratio of minimum to maximum transmission is 0.9195. The resulting mean value $<E^2-1>$ for all data is 0.933 [expected 0.968 for centrosymmetric and 0.736 for non-centrosymmetric structures, respectively],[1] which corresponds to a centrosymmetric structure. Using the program XPREP[4] an intensity statistics, showing the resolution dependence of *R(sigma)* and *R(int)*, was created for the reflection file:

INTENSITY STATISTICS FOR DATASET # 1 ap28_0m.hkl

Resolution	#Data	#Theory	%Complete	Redundancy	Mean I	Mean I/s	Rmerge	Rsigma
Inf - 3.19	254	255	99.6	3.94	118.83	61.92	0.0162	0.0129
3.19 - 2.12	607	610	99.5	4.77	39.26	56.54	0.0195	0.0136
2.12 - 1.68	853	857	99.5	4.93	26.57	46.39	0.0221	0.0153
1.68 - 1.47	841	841	100.0	4.75	16.91	36.27	0.0271	0.0190
1.47 - 1.34	844	846	99.8	4.41	12.71	28.09	0.0328	0.0234

[1] E: normalized structure factor.

1.34 - 1.24	877	877	100.0	4.11	11.55	25.57	0.0378	0.0271
1.24 - 1.16	943	945	99.8	3.88	8.76	20.95	0.0439	0.0341
1.16 - 1.11	728	728	100.0	3.70	6.96	17.26	0.0501	0.0413
1.11 - 1.06	883	883	100.0	3.53	6.54	15.31	0.0554	0.0456
1.06 - 1.02	864	864	100.0	3.42	4.95	12.46	0.0663	0.0575
1.02 - 0.98	961	961	100.0	3.26	4.61	11.12	0.0716	0.0639
0.98 - 0.95	837	837	100.0	3.14	4.66	11.03	0.0736	0.0674
0.95 - 0.92	976	976	100.0	3.07	3.93	9.40	0.0828	0.0777
0.92 - 0.90	708	710	99.7	2.97	3.57	8.50	0.0914	0.0869
0.90 - 0.88	780	784	99.5	2.86	3.23	7.74	0.0941	0.0967
0.88 - 0.86	824	832	99.0	2.82	2.99	7.12	0.1044	0.1061
0.86 - 0.84	955	964	99.1	2.72	2.43	5.91	0.1144	0.1276
0.84 - 0.82	999	1016	98.3	2.66	2.01	5.08	0.1380	0.1523
0.82 - 0.81	549	558	98.4	2.56	1.71	4.31	0.1563	0.1784
0.81 - 0.79	1182	1213	97.4	2.50	1.72	4.28	0.1657	0.1850
0.79 - 0.78	475	610	77.9	1.56	1.39	3.07	0.1826	0.2658
0.88 - 0.78	4984	5193	96.0	2.52	2.09	5.11	0.1328	0.1518
Inf - 0.78	16940	17167	98.7	3.38	9.61	17.09	0.0360	0.0353

Merged [A], lowest resolution = 16.14 Angstroms

Dataset # 2 created containing 55626 data (resolution cutoff at 0.8 Å)

INTENSITY STATISTICS FOR DATASET # 2 ap28_0m.hkl

Resolution	#Data	#Theory	%Complete	Redundancy	Mean I	Mean I/s	Rmerge	Rsigma
Inf - 3.23	239	240	99.6	3.91	124.05	62.55	0.0161	0.0129
3.23 - 2.17	563	566	99.5	4.74	40.36	56.88	0.0194	0.0135
2.17 - 1.72	787	790	99.6	4.92	26.68	46.93	0.0219	0.0152
1.72 - 1.50	818	819	99.9	4.80	18.49	38.03	0.0261	0.0181
1.50 - 1.36	825	826	99.9	4.50	13.54	29.42	0.0313	0.0223
1.36 - 1.26	820	821	99.9	4.17	12.11	26.70	0.0357	0.0260
1.26 - 1.19	779	780	99.9	3.95	9.24	21.97	0.0432	0.0320
1.19 - 1.13	810	811	99.9	3.76	7.87	19.00	0.0469	0.0377
1.13 - 1.08	825	825	100.0	3.61	6.49	15.79	0.0547	0.0448
1.08 - 1.04	771	771	100.0	3.43	5.87	13.98	0.0590	0.0506
1.04 - 1.00	892	892	100.0	3.38	4.61	11.45	0.0700	0.0608
1.00 - 0.97	795	795	100.0	3.22	4.64	11.13	0.0720	0.0653
0.97 - 0.94	879	879	100.0	3.13	4.59	10.88	0.0765	0.0686
0.94 - 0.92	665	665	100.0	3.01	3.66	8.79	0.0856	0.0832
0.92 - 0.90	708	710	99.7	2.97	3.57	8.50	0.0914	0.0869
0.90 - 0.88	780	784	99.5	2.86	3.23	7.74	0.0941	0.0967
0.88 - 0.86	824	832	99.0	2.82	2.99	7.12	0.1044	0.1061
0.86 - 0.84	955	964	99.1	2.72	2.43	5.91	0.1144	0.1276
0.84 - 0.82	999	1016	98.3	2.66	2.01	5.08	0.1380	0.1523
0.82 - 0.81	549	558	98.4	2.56	1.71	4.31	0.1563	0.1784
0.81 - 0.80	584	598	97.7	2.55	1.81	4.53	0.1593	0.1734
0.90 - 0.80	4691	4752	98.7	2.71	2.41	5.89	0.1187	0.1289
Inf - 0.80	15867	15942	99.5	3.49	10.16	18.00	0.0352	0.0334

Merged [A], lowest resolution = 16.14 Angstroms

***Note**:* The R_{int} column gives a measure of whether symmetry equivalents have the same intensity. In the higher resolution shells (lower down the table), the R_{int} values get larger. The mean intensity and mean *I/sigma* tend to get smaller at higher resolution, while the R_{sigma} get larger. These variations with resolution happen because diffraction intensities tend to be weaker and more susceptible to noise at higher resolution. As a general rule, the data are usable so long as mean I/σ for a shell is ≥ 2 and the $R_{sigma} \leq 0.25$. Shells with mean $I/\sigma \leq 2$ contain very weak reflections.

This listing provides an indication of the resolution cutoff to be applied to the data. A resolution cutoff at 0.8 Å was applied. Of the 55626 reflections 29 reflections were rejected (SHELXL-2013 [6]).[2] The remaining data (55597 reflections) were merged (all symmetry equivalents and Friedel opposites; R_{int} = 0.0355)[3] to provide 15859 data, of which all were unique (R_{sigma} = 0.0365) and 12812 observed ($I > 2\sigma(I)$) reflections (SHELXL-2013 [6]). The ranges of indices were $-17 \leq h \leq 17$, $-22 \leq k \leq 22$, $-21 \leq l \leq 22$ corresponding to a θ-range of 1.275 to 26.371°.[4]

Structure solution and refinement: The structure was solved using direct methods in the space group $P\bar{1}$ [2] (SHELXT-2014[5]) and refined by full-matrix least-squares method on F^2 with

SHELXL-2013[6] using ShelXle[8] as the graphical user interface (*GUI*).

The non-hydrogen atoms were refined anisotropically. Hydrogen atoms of the phenyl-, CH_2- and CH_3-groups were included at geometrically idealized positions (C-H bond distances: 0.95 / 0.99 / 0.98 Å) and were not refined. The isotropic thermal parameters of these hydrogen atoms were fixed at 1.2 (phenyl- and CH_2-groups) or 1.5 (CH_3-groups) times that of the preceding carbon or nitrogen atom, respectively.

The fluorine atoms [labelled as F(13A) to F(16A) and F(13B) to F(16B)] of one of the BF_4^- anions were disordered over two positions each. In order to model the disorder satisfactory restraints on bond lengths and angles (SADI) as well as on atomic displacement parameters (SIMU, DELU) were applied. The site occupancy factors were refined to 0.696(7) and 0.304(7), respectively. The remaining three BF_4^- anions also showed possible disorder, but modelling the disorders using the *atom split model* was unsuccessful.

The carbon atom of Me-group [labelled as C(63A) and C(63B)] in one of the acetonitrile molecules showed rotational disorder around the CN triple bond. The anisotropic displacement

---

2 Of the 29 rejected reflections 0 were presumably systematic absences and the remaining reflections were omitted because their F^2_o values were negative or their $\Delta F^2/esd$ were very high.

3 $R_{int} = [\Sigma|F_o^2-F_o^2(\text{mean})|]/[\Sigma|F_o^2|]$.

4 The scattering angle θ defines the sphere in the reciprocal space outside of which data are not measured. With Mo radiation, this should be at least 25° and should not be less than 22°, the corresponding minimum lattice plane spacing, referred to as the "resolution" of the data, is 0.84 [10]. According to the guidelines given by the International Union of Crystallography, the diffractometer should be set so that a θ_{max} of 25° for Mo radiation is reached. If the crystal diffracts *sufficiently well*, it is strongly recommended, that θ_{max} is set to an even higher value.

parameters of the disordered carbon atoms were constraint to be identical (EADP). The site occupancy factors were refined to 0.603(10) and 0.397(10), respectively.

The site occupancy factors for the oxygen atoms [labelled as O(1W) and C(2W)] of the water molecules were allowed to refine at first and then set to 0.5. The tool HADD in OLEX [13] was used to place the protons for the water molecule in geometrically sensible positions, since they could be located in the Fourier difference map.

Approximately 14% of the unit cell comprises a region of disordered solvent molecules and their atoms could not be modeled as discrete atomic sites (solvent accessible volume: 560.2 Å^3). Attempts to refine the peaks of the residual electron density as 0.5 Et_2O and two molecules of MeCN within the asymmetric unit were unsuccessful. The program PLATON/SQUEEZE was used to calculate the contribution from the solvent region to the diffraction. The data were corrected for the disordered electron density using the SQUEEZE routine as implemented in PLATON[11] leading to set of solvent-free diffraction intensities. A total electron count of 127 electrons was found in the total solvent accessible void volume within the unit cell. The electron densities identified in the solvent accessible are as follows:

# of void	Centre of Void			Volume [Å^3]	Volume [%] based on the total solvent accessible volume	Electron count/Void
	x_{av}	y_{av}	z_{av}			
1	0.000	0.500	0.500	191	4.9	41
2	0.000	0.500	1.000	161	4.1	46
3	0.750	0.333	0.000	190	4.9	40

Expected molar volume / electron count for Et_2O: 104.8 Å^3 [12] / 42 e$^-$. Expected molar volume / electron count for MeCN: 82 Å^3 [12] / 22 e$^-$. With this in mind, this accounts for additional four molecules of MeCN plus two 0.5(Et_2O) within the unit cell and two molecules of MeCN plus one 0.5(Et_2O) within the asymmetric unit (total electron count of 130 electrons within the unit cell). This result is supported by the observations in the electron difference map.

The modified data improved the *R*-factors (before SQUEEZE: R_1 = 0.0933, wR_2 = 0.2561; largest peak and hole, 2.248 and -0.832 e$^-$/Å^3; after SQUEEZE: R_1 = 0.0588, wR_2 = 0.1641; largest peak and hole, 1.429 and -0.778 e$^-$/Å^3). Derived values (formula weight, density, absorption coefficient) do not contain the contribution of the disordered solvent.

The final cycle of full-matrix least squares refinement using F^2 (SHELXL-2013,[5]) was based on 15859 reflections, 210 restraints, 1024 variable parameters and converged (largest parameter shift was 0.000 times its esd) with an unweighted factor of R_1 = 0.0588 for $I > 2\sigma(I)$. The standard deviation of an observation of unit weight (*goodness-of-fit*)[7] was 1.025. The maximum and minimum peaks in the final difference Fourier map corresponded to 1.429 and -0.778 $e^-/Å^3$, respectively. Neutral atom scattering factors for non-hydrogen atoms and anomalous dispersion coefficients are contained in the SHELXTL[4] program library. The plots for the crystal structure were generated using the program XP (part of the SHELXTL 6.14[4] program library) and then imported into CorelDRAW™ X6.[9] If not otherwise stated, the thermal ellipsoids in the molecular plots are shown at the 30% probability level.

The obtained crystal data suggest that the Fe^{2+} ion is in the low spin state based on the *Bond Valence* model. [14]

References:

[1] *APEX2 software package v2013.10-0*, Bruker AXS Inc.: Madison, WI, 2013.

[2] *Bruker SAINT v8.30A*: Part of the *APEX2 software package v2013.10-0*, Bruker AXS Inc.: Madison, WI, 2013.

[3] *Bruker SADABS v2012/1*: Part of the *APEX2 software package v2013.10-0*, Bruker AXS Inc.: Madison, WI, 2013.

[4] *SHELXTL (Version 6.14), XPREP (Version 2013/3), Program Library for Structure Solution and Molecular Graphics*; Bruker AXS, Inc.: Madison, WI, 2000-2013.

[5] G. M. Sheldrick, *SHELXT-2013, Program for the Solution of Crystal Structures;* University of Göttingen, Göttingen, Germany 2013.

[6] G. M. Sheldrick, *SHELXL-2014, Program for the Solution and Refining of Crystal Structures;* University of Göttingen, Göttingen, Germany 2014. G. M. Sheldrick, *Acta Cryst.* **2008**, *A64*, 112–122.

Function minimized: $\Sigma w(|F_o|^2-|kF_c|^2)^2$; k: overall scale factor.

Refinement on F_o^2 for all reflections (all of these having $F_o^2 \geq -3\sigma(F_o^2)$). Weighted R-factors wR_2 and the values for *GooF* are based on F_o^2; conventional R-factors R_1 are based on F_o, with F_o set to zero for negative F_o^2. The observed criterion of $F_o^2 > 2\sigma(F_o^2)$ is used only for calculating R_1, and is not relevant to the choice of reflections for refinement. R-factors based on F_o^2 are statistically about twice as large as those based on F_o, and R-factors based on ALL data will be even larger.

[7] Standard deviation of an observation of unit weight (*goodness-of-fit* on F^2):

$$GooF = \{\Sigma[w(F_o^2-F_c^2)^2]/(n - p)\}^{1/2}$$

n: number of reflections, p: number of parameters

[8] *ShelXle v4.8.0 (2013)*: *A Qt graphical user interface for SHELXL.* C. B. Hübschle, G. M. Sheldrick and B. Dittrich, *J. Appl. Crystallogr.* **2011**, *44*, 1281-1284.

[9] *CorelDRAW™ X6 v16.0.0.707*: Corel Corporation, Ottawa, Ontario, Canada, 2012.

[10] W. Massa, *Crystal Structure Determination*, Springer Verlag, Berlin, 2000.

[11] Spek, A. L., Single-crystal structure validation with the program *PLATON. J. Appl. Crystallogr.* **2003**, *36*, 7-13.

[12] At 298.15 K (25 °C). *Hansen Solubility Parameters*: *A User's Handbook, 2nd Edition*, Charles M. Hansen, CRC Press, Boca Raton, FL, 2007.
[13] Dolomanov, O.V.; Bourhis, L.J.; Gildea, R.J.; Howard, J.A.K.; Puschmann, H., OLEX2: A complete structure solution, refinement and analysis program. *J. Appl. Cryst*., **2009** 42, 339-341.
[14] Brown, I. D., *Chem. Rev.* **2009,** *109,* 6858–6919.

Figure S66. Molecular ellipsoid plot of the cation, anions and solvent (CH_3CN).

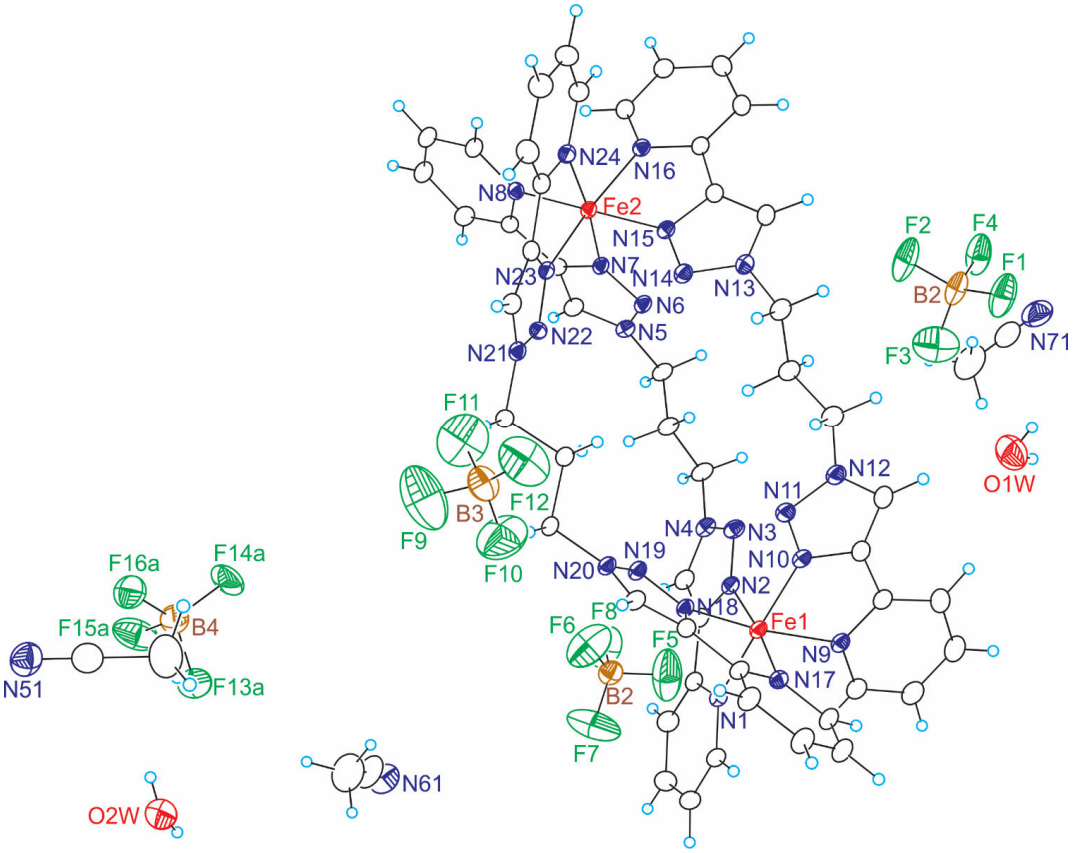

Table S1. Crystal data and structure refinement for *ap28_sq*

A. Crystal data

Identification code	*ap28_sq*
Empirical formula	$C_{114}H_{118}B_8F_{32}Fe_4N_{54}O_2$
Formula weight	3194.50
Crystal Color, Habit	red, block-like
Crystal dimensions (mm)	0.250 × 0.250 × 0.100

Crystal system	triclinic
Space group	$P\bar{1}$ [2]
Unit cell parameters[a]	
a (Å)	13.8603(5)
b (Å)	17.9020(7)
c (Å)	17.9413(7)
α (°)	109.535(2)
β (°)	101.234(3)
γ (°)	103.518(2)
V (Å^3)	3894.0(3)
Z[b]	2
F(000)	1628
Density (ρ_{calcd})	1.362 Mg/m^3
Absorption coefficient (μ)	0.467 mm^{-1}

B. Data collection and refinement conditions

Diffractometer	Bruker-AXS Smart Apex II diffractometer[c]
Radiation	monochromated Mo K$_\alpha$
Wavelength (Mo K$_\alpha$)	0.71073 Å
Temperature	-93(2) °C [180(2) K]
Scan type	ω-scans (0.5º/frame, 10 s exposure/frame, 7 sets)
Theta range for data collection	1.275 to 26.371°
Completeness to theta = 25.242°	99.6%
Reflections collected[d]	55597
Index ranges	$-17 \le h \le 17$, $-22 \le k \le 22$, $-21 \le l \le 22$
Independent reflections [$F_o^2 \ge -3\sigma(F_o^2)$][e]	15859 [R_{int} = 0.0355][f]
Observed reflections [$F_o^2 > 2\sigma(F_o^2)$][g]	12812
Absorption correction method	multi-scan [SADABS][k]
Anomalous Dispersion	For all non-hydrogen atoms
Structure solution method	Direct methods (SHELXT-2014)[h]
Refinement method	Full-matrix least-squares on F^2 (SHELXL-2013)[i]
Function Minimized	$\Sigma w(\lvert F_o\rvert^2-\lvert kF_c\rvert^2)^2$ (k: overall scale factor)
Weighing scheme, w $w = [\sigma(F_o^2) + (a\,P)^2 + (b\,P)]^{-1}$	$w = [\sigma(F_o^2) + (0.0804\,P)^2 + (5.9446\,P)]^{-1}$

P-factor	$[\mathrm{Max}(F_o^2,0) + 2\,F_c^2]/3$
Data / restraints / parameters	15859 $[F_o^2 \geq -3\sigma(F_o^2)]$ / 210 / 1024
Reflection (observed)/parameter ratio	12:1
Reflection (data)/parameter ratio	15:1
Goodness-of-fit[j] on F^2	1.025
$GooF = \{\Sigma[w(F_o^2-F_c^2)^2]/(n - p)\}^{1/2}$ n: number of reflections, p: number of parameters	
Final R indices	
$R_1 = [\Sigma\|\|F_o\|-\|F_c\|\|]/[\Sigma\|F_o\|]$ for $[F_o^2 > 2\sigma(F_o^2)]$[i]	0.0588
$wR_2 = \{[\Sigma w(F_o^2-F_c^2)^2]/[\Sigma w(F_o^2)^2]\}^{1/2}$ [all data]	0.1641
Max. Shift/Error in Final Cycle	0.000
Largest difference peak and hole	1.429 and -0.778 $e^-/Å^3$
Transmission factor (min)	0.6855 [SADABS][k]
Transmission factor (max)	0.7455 [SADABS][k]

---

[a] Obtained from least-squares refinement of 9934 centered reflections with 2.23º < θ < 26.59º (mosaicity: 0.35°).

[b] Z is the number of formula units per unit cell. Comparison of Z with the multiplicity of the general position n_a of the space group will then require that the asymmetric unit is Z/n_a times the formula unit. The asymmetric unit is the minimum group of atoms whose positions, together with those generated by the symmetry operations of the space group generate the complete contents of the unit cell.

[c] Bruker-AXS Smart Apex II: 3-circle diffractometer; sealed Mo X-ray tube; Apex II: type of detector.

[d] Number of reflections after truncation or rejection (before merging).

[e] The criterion for the independent or unique reflections $[F_o^2 \geq -3\sigma(F_o^2)]$ was taken from:
G. M. Sheldrick, *SHELXL-2013, Program for the Solution of Crystal Structures;* University of Göttingen: Göttingen, Germany 2013.

[f] $R_{int} = [\Sigma|F_o^2-F_o^2(\mathrm{mean})|]/[\Sigma|F_o^2|]$

[g] The criterion for the observed reflections $[F_o^2 > 2\sigma(F_o^2)]$ is equivalent to $[I > 2\sigma(I)]$: I is proportional to F_o^2.

[h] G. M. Sheldrick, *SHELXT-2013, Program for the Solution of Crystal Structures;* University of Göttingen, Göttingen, Germany 2013..

[i] G. M. Sheldrick, *SHELXL-2013, Program for the Solution of Crystal Structures;* University of Göttingen, Göttingen, Germany 2013. G. M. Sheldrick, *Acta Cryst.* 2008, **A64**, 112–122.

Function minimized: $\Sigma w(|F_o|^2-|kF_c|^2)^2$; k: overall scale factor.

Refinement on F_o^2 for all reflections (all of these having $F_o^2 \geq -3\sigma(F_o^2)$). Weighted R-factors wR_2 and the values for $GooF$ are based on F_o^2; conventional R-factors R_1 are based on F_o, with F_o set to zero for negative F_o^2. The observed criterion of $F_o^2 > 2\sigma(F_o^2)$ is used only for calculating R_1, and is not relevant to the choice of reflections for refinement. R-factors based on F_o^2 are statistically about twice as large as those based on F_o, and R-factors based on ALL data will be even larger.

[j] Standard deviation of an observation of unit weight (*goodness-of-fit* on F^2):

$GooF = \{\Sigma[w(F_o^2-F_c^2)^2]/(n - p)\}^{1/2}$
n: number of reflections, p: number of parameters

[k] *Bruker SADABS v2012/1*: Part of the *APEX2 software package v2013.10-0*, Bruker AXS Inc.: Madison, WI, 2013.

Table S2. Atomic coordinates (× 10^4), equivalent isotropic displacement parameters (Å^2 (× 10^3) and site occupancy factors for *ap28_sq*

U(eq) is defined as one third of the trace of the orthogonalized U^{ij} tensor.

Atom	x	y	z	U(eq)	s.o.f.
Fe(1)	2637(1)	1245(1)		3586(1)	25(1)
Fe(2)	5102(1)	6536(1)		8564(1)	22(1)
N(1)	3464(2)	950(2)		2802(2)	27(1)
N(2)	4010(2)	1680(1)		4374(2)	27(1)
N(3)	4356(2)	2067(2)		5184(2)	31(1)
N(4)	5392(2)	2237(2)		5375(2)	30(1)
N(5)	6598(2)	4864(2)		7841(2)	27(1)
N(6)	5705(2)	4995(1)		7932(2)	27(1)
N(7)	5919(2)	5813(1)		8251(1)	24(1)
N(8)	6485(2)	7405(1)		8905(1)	24(1)
N(9)	2365(2)	153(2)		3726(2)	29(1)
N(10)	1954(2)	1486(2)		4436(2)	28(1)
N(11)	1705(2)	2142(2)		4826(2)	31(1)
N(12)	1274(2)	1949(2)		5372(2)	33(1)
N(13)	2453(2)	4615(2)		7776(2)	28(1)
N(14)	3110(2)	5149(2)		7588(2)	28(1)
N(15)	3854(2)	5622(1)		8284(2)	24(1)
N(16)	5274(2)	6451(1)		9666(2)	25(1)
N(17)	1281(2)	884(2)		2721(2)	27(1)
N(18)	2693(2)	2321(1)		3528(2)	25(1)
N(19)	3346(2)	3089(2)		3936(2)	28(1)
N(20)	2850(2)	3584(1)		3720(2)	26(1)
N(21)	4097(2)	6245(1)		6188(2)	26(1)
N(22)	4758(2)	6110(2)		6749(1)	26(1)
N(23)	4665(2)	6539(1)		7469(2)	24(1)
N(24)	4293(2)	7335(2)		8803(2)	26(1)
C(1)	3094(2)	532(2)		1970(2)	30(1)
C(2)	3726(3)	326(2)		1482(2)	35(1)
C(3)	4782(3)	560(2)		1849(2)	38(1)
C(4)	5178(3)	983(2)		2700(2)	37(1)

C(5)	4506(2)	1168(2)	3152(2)	28(1)
C(6)	4801(2)	1601(2)	4049(2)	28(1)
C(7)	5704(2)	1962(2)	4701(2)	32(1)
C(8)	6017(3)	2670(2)	6244(2)	34(1)
C(9)	5923(3)	3539(2)	6619(2)	32(1)
C(10)	6622(3)	4004(2)	7506(2)	31(1)
C(11)	7379(2)	5591(2)	8099(2)	30(1)
C(12)	6937(2)	6200(2)	8364(2)	26(1)
C(13)	7276(2)	7111(2)	8750(2)	27(1)
C(14)	8285(2)	7633(2)	8961(2)	35(1)
C(15)	8497(3)	8489(2)	9357(2)	38(1)
C(16)	7704(3)	8795(2)	9520(2)	34(1)
C(17)	6712(2)	8237(2)	9282(2)	31(1)
C(18)	2581(2)	-530(2)	3300(2)	33(1)
C(19)	2366(3)	-1252(2)	3449(2)	41(1)
C(20)	1919(3)	-1277(2)	4067(2)	45(1)
C(21)	1695(3)	-581(2)	4517(2)	40(1)
C(22)	1917(2)	116(2)	4322(2)	31(1)
C(23)	1689(2)	881(2)	4727(2)	31(1)
C(24)	1256(3)	1179(2)	5336(2)	37(1)
C(25)	941(2)	2571(2)	5927(2)	36(1)
C(26)	1883(2)	3287(2)	6568(2)	34(1)
C(27)	1547(2)	3968(2)	7108(2)	33(1)
C(28)	2768(2)	4742(2)	8582(2)	30(1)
C(29)	3679(2)	5399(2)	8911(2)	26(1)
C(30)	4478(2)	5874(2)	9707(2)	26(1)
C(31)	4459(3)	5749(2)	10423(2)	34(1)
C(32)	5295(3)	6229(2)	11130(2)	36(1)
C(33)	6112(3)	6807(2)	11094(2)	34(1)
C(34)	6084(2)	6898(2)	10357(2)	30(1)
C(35)	604(2)	103(2)	2301(2)	33(1)
C(36)	-345(3)	-69(2)	1754(2)	39(1)
C(37)	-635(3)	575(2)	1631(2)	41(1)
C(38)	43(2)	1385(2)	2055(2)	36(1)

C(39)	994(2)	1514(2)	2586(2)	28(1)	
C(40)	1797(2)	2324(2)	3060(2)	27(1)	
C(41)	1890(2)	3141(2)	3182(2)	30(1)	
C(42)	3358(2)	4493(2)	4069(2)	29(1)	
C(43)	3522(3)	4887(2)	4994(2)	32(1)	
C(44)	3981(2)	5833(2)	5306(2)	28(1)	
C(45)	3598(2)	6757(2)	6544(2)	28(1)	
C(46)	3964(2)	6946(2)	7375(2)	26(1)	
C(47)	3759(2)	7411(2)	8125(2)	28(1)	
C(48)	3087(3)	7879(2)	8166(2)	37(1)	
C(49)	2961(3)	8283(2)	8923(2)	42(1)	
C(50)	3500(3)	8214(2)	9616(2)	39(1)	
C(51)	4155(2)	7737(2)	9533(2)	32(1)	
F(1)	-41(2)	1780(2)	7842(2)	92(1)	
F(2)	1214(3)	2987(2)	8221(2)	100(1)	
F(3)	1445(4)	1829(3)	7484(3)	133(2)	
F(4)	1463(2)	2091(2)	8788(2)	88(1)	
B(1)	996(4)	2167(3)	8079(4)	59(1)	
F(5)	7407(3)	937(3)	3840(4)	167(2)	
F(6)	7775(3)	2180(3)	3945(3)	145(2)	
F(7)	8119(5)	1292(4)	3007(3)	174(2)	
F(8)	9059(2)	1710(2)	4330(3)	117(1)	
B(2)	8170(4)	1559(3)	3791(3)	54(1)	
F(9)	1291(4)	6382(5)	3275(4)	178(2)	
F(10)	1555(4)	5206(3)	3235(4)	157(2)	
F(11)	2189(3)	6326(3)	4328(3)	151(2)	
F(12)	462(3)	5725(3)	3851(3)	132(2)	
B(3)	1344(4)	5865(4)	3691(4)	65(1)	
F(13A)	2824(5)	7139(4)	742(3)	85(2)	0.696(7)
F(14A)	3354(6)	7560(4)	2117(3)	87(2)	0.696(7)
F(15A)	4440(3)	7991(4)	1408(3)	98(2)	0.696(7)
F(16A)	3117(4)	8468(3)	1563(3)	75(1)	0.696(7)
F(13B)	3352(12)	7226(9)	796(8)	99(4)	0.304(7)
F(14B)	2858(9)	7472(10)	1946(9)	83(4)	0.304(7)

F(15B)	4491(7)	7706(7)	2027(7)	89(4)	0.304(7)
F(16B)	3733(13)	8580(7)	1752(10)	117(5)	0.304(7)
B(4)	3511(4)	7783(3)	1519(3)	67(2)	
N(51)	1303(3)	9067(2)	111(2)	63(1)	
C(52)	1091(3)	8519(3)	285(3)	54(1)	
C(53)	800(5)	7811(4)	508(4)	101(2)	
N(61)	9954(3)	3214(3)	1761(3)	71(1)	
C(62)	9409(4)	3553(3)	1684(4)	71(1)	
C(63A)	8621(11)	3938(9)	1427(15)	89(4)	0.65(3)
C(63B)	8820(20)	4117(19)	1920(20)	89(4)	0.35(3)
N(71)	3547(4)	298(3)	9247(4)	91(2)	
C(72)	3396(4)	536(3)	8749(4)	66(1)	
C(73)	3202(5)	824(4)	8113(5)	108(2)	
O(1W)	723(8)	93(6)	6332(6)	93(2)	0.5
O(2W)	7789(7)	5916(5)	30(5)	88(2)	0.5

Table S3a. Interatomic distances [Å] for *ap28_sq*

Fe(1)-N(10)	1.929(3)	C(9)-C(10)	1.517(4)
Fe(1)-N(2)	1.936(2)	C(11)-C(12)	1.366(4)
Fe(1)-N(18)	1.946(2)	C(12)-C(13)	1.457(4)
Fe(1)-N(17)	1.995(2)	C(13)-C(14)	1.385(4)
Fe(1)-N(1)	1.996(3)	C(14)-C(15)	1.385(5)
Fe(1)-N(9)	2.012(2)	C(15)-C(16)	1.376(5)
Fe(2)-N(15)	1.925(2)	C(16)-C(17)	1.384(4)
Fe(2)-N(7)	1.927(2)	C(18)-C(19)	1.383(5)
Fe(2)-N(23)	1.942(2)	C(19)-C(20)	1.380(5)
Fe(2)-N(8)	1.996(2)	C(20)-C(21)	1.380(5)
Fe(2)-N(24)	2.004(2)	C(21)-C(22)	1.389(4)
Fe(2)-N(16)	2.004(2)	C(22)-C(23)	1.459(4)
N(1)-C(1)	1.352(4)	C(23)-C(24)	1.362(5)
N(1)-C(5)	1.361(4)	C(25)-C(26)	1.522(4)
N(2)-N(3)	1.313(3)	C(26)-C(27)	1.515(4)
N(2)-C(6)	1.352(4)	C(28)-C(29)	1.369(4)
N(3)-N(4)	1.343(4)	C(29)-C(30)	1.456(4)

N(4)-C(7)	1.342(4)	C(30)-C(31)	1.379(4)		
N(4)-C(8)	1.461(4)	C(31)-C(32)	1.386(5)		
N(5)-N(6)	1.342(3)	C(32)-C(33)	1.372(5)		
N(5)-C(11)	1.351(4)	C(33)-C(34)	1.380(4)		
N(5)-C(10)	1.464(4)	C(35)-C(36)	1.375(4)		
N(6)-N(7)	1.316(3)	C(36)-C(37)	1.375(5)		
N(7)-C(12)	1.359(4)	C(37)-C(38)	1.382(4)		
N(8)-C(17)	1.341(4)	C(38)-C(39)	1.385(4)		
N(8)-C(13)	1.358(4)	C(39)-C(40)	1.456(4)		
N(9)-C(18)	1.343(4)	C(40)-C(41)	1.374(4)		
N(9)-C(22)	1.349(4)	C(42)-C(43)	1.517(4)		
N(10)-N(11)	1.313(4)	C(43)-C(44)	1.520(4)		
N(10)-C(23)	1.360(4)	C(45)-C(46)	1.372(4)		
N(11)-N(12)	1.339(4)	C(46)-C(47)	1.449(4)		
N(12)-C(24)	1.353(4)	C(47)-C(48)	1.386(4)		
N(12)-C(25)	1.457(4)	C(48)-C(49)	1.375(5)		
N(13)-N(14)	1.336(3)	C(49)-C(50)	1.381(5)		
N(13)-C(28)	1.351(4)	C(50)-C(51)	1.380(5)		
N(13)-C(27)	1.469(4)	F(1)-B(1)	1.352(6)		
N(14)-N(15)	1.312(3)	F(2)-B(1)	1.350(5)		
N(15)-C(29)	1.360(4)	F(3)-B(1)	1.376(7)		
N(16)-C(34)	1.347(4)	F(4)-B(1)	1.377(6)		
N(16)-C(30)	1.358(4)	F(5)-B(2)	1.384(6)		
N(17)-C(35)	1.345(4)	F(6)-B(2)	1.324(6)		
N(17)-C(39)	1.358(4)	F(7)-B(2)	1.306(6)		
N(18)-N(19)	1.317(3)	F(8)-B(2)	1.316(5)		
N(18)-C(40)	1.360(4)	F(9)-B(3)	1.376(7)		
N(19)-N(20)	1.348(3)	F(10)-B(3)	1.327(7)		
N(20)-C(41)	1.351(4)	F(11)-B(3)	1.324(7)		
N(20)-C(42)	1.466(3)	F(12)-B(3)	1.295(6)		
N(21)-C(45)	1.343(4)	F(13A)-B(4)	1.440(7)	F(13B)-B(4)	1.283(12)
N(21)-N(22)	1.350(3)	F(14A)-B(4)	1.303(7)	F(14B)-B(4)	1.427(12)
N(21)-C(44)	1.464(4)	F(15A)-B(4)	1.327(6)	F(15B)-B(4)	1.545(10)
N(22)-N(23)	1.313(3)	F(16A)-B(4)	1.439(7)	F(16B)-B(4)	1.284(11)

N(23)-C(46)	1.361(4)	N(51)-C(52)	1.118(6)		
N(24)-C(51)	1.342(4)	C(52)-C(53)	1.449(7)		
N(24)-C(47)	1.363(4)	N(61)-C(62)	1.089(5)		
C(1)-C(2)	1.379(5)	C(62)-C(63A)	1.500(13)	C(62)-C(63B)	1.45(3)
C(2)-C(3)	1.380(5)	N(71)-C(72)	1.118(8)		
C(3)-C(4)	1.382(5)	C(72)-C(73)	1.405(10)		
C(4)-C(5)	1.377(5)				
C(5)-C(6)	1.456(4)				
C(6)-C(7)	1.377(4)				
C(8)-C(9)	1.522(4)				

NOTE: All e.s.d.'s (except the e.s.d. in the dihedral angle between two l.s. planes) are estimated using the full covariance matrix. The cell e.s.d.'s are taken into account individually in the estimation of e.s.d.'s in distances, angles and torsion angles; correlations between e.s.d.'s in cell parameters are only used when they are defined by crystal symmetry. An approximate (isotropic) treatment of cell e.s.d.'s is used for estimating e.s.d.'s involving l.s. planes.

Table S3b. Interatomic angles [°] for *ap28_sq*

N(10)-Fe(1)-N(2)	93.59(11)	N(3)-N(2)-C(6)	110.9(2)
N(10)-Fe(1)-N(18)	89.87(10)	N(3)-N(2)-Fe(1)	133.0(2)
N(2)-Fe(1)-N(18)	93.62(10)	C(6)-N(2)-Fe(1)	116.1(2)
N(10)-Fe(1)-N(17)	89.91(10)	N(2)-N(3)-N(4)	105.3(2)
N(2)-Fe(1)-N(17)	173.85(10)	C(7)-N(4)-N(3)	112.2(2)
N(18)-Fe(1)-N(17)	81.32(10)	C(7)-N(4)-C(8)	128.8(3)
N(10)-Fe(1)-N(1)	172.46(10)	N(3)-N(4)-C(8)	119.0(3)
N(2)-Fe(1)-N(1)	80.63(10)	N(6)-N(5)-C(11)	111.8(2)
N(18)-Fe(1)-N(1)	95.29(10)	N(6)-N(5)-C(10)	119.3(2)
N(17)-Fe(1)-N(1)	96.28(10)	C(11)-N(5)-C(10)	128.9(3)
N(10)-Fe(1)-N(9)	80.79(10)	N(7)-N(6)-N(5)	105.8(2)
N(2)-Fe(1)-N(9)	91.08(10)	N(6)-N(7)-C(12)	110.2(2)
N(18)-Fe(1)-N(9)	169.80(10)	N(6)-N(7)-Fe(2)	133.60(19)
N(17)-Fe(1)-N(9)	94.47(10)	C(12)-N(7)-Fe(2)	116.24(19)
N(1)-Fe(1)-N(9)	94.40(10)	C(17)-N(8)-C(13)	117.4(3)
N(15)-Fe(2)-N(7)	93.94(10)	C(17)-N(8)-Fe(2)	126.9(2)
N(15)-Fe(2)-N(23)	89.94(10)	C(13)-N(8)-Fe(2)	115.64(19)
N(7)-Fe(2)-N(23)	93.92(10)	C(18)-N(9)-C(22)	117.2(3)
N(15)-Fe(2)-N(8)	173.31(10)	C(18)-N(9)-Fe(1)	127.6(2)
N(7)-Fe(2)-N(8)	80.84(10)	C(22)-N(9)-Fe(1)	115.2(2)
N(23)-Fe(2)-N(8)	94.58(10)	N(11)-N(10)-C(23)	110.7(3)
N(15)-Fe(2)-N(24)	89.34(10)	N(11)-N(10)-Fe(1)	133.0(2)
N(7)-Fe(2)-N(24)	173.93(10)	C(23)-N(10)-Fe(1)	116.2(2)

N(23)-Fe(2)-N(24)	80.97(10)	N(10)-N(11)-N(12)	105.4(2)
N(8)-Fe(2)-N(24)	96.23(10)	N(11)-N(12)-C(24)	111.9(3)
N(15)-Fe(2)-N(16)	80.84(10)	N(11)-N(12)-C(25)	118.8(3)
N(7)-Fe(2)-N(16)	91.76(10)	C(24)-N(12)-C(25)	129.3(3)
N(23)-Fe(2)-N(16)	169.49(10)	N(14)-N(13)-C(28)	112.3(2)
N(8)-Fe(2)-N(16)	95.06(10)	N(14)-N(13)-C(27)	118.5(2)
N(24)-Fe(2)-N(16)	93.80(10)	C(28)-N(13)-C(27)	129.2(3)
C(1)-N(1)-C(5)	117.0(3)	N(15)-N(14)-N(13)	105.2(2)
C(1)-N(1)-Fe(1)	127.0(2)	N(14)-N(15)-C(29)	111.1(2)
C(5)-N(1)-Fe(1)	115.9(2)	N(14)-N(15)-Fe(2)	132.7(2)
C(29)-N(15)-Fe(2)	116.22(19)	C(7)-C(6)-C(5)	137.1(3)
C(34)-N(16)-C(30)	117.2(3)	N(4)-C(7)-C(6)	104.4(3)
C(34)-N(16)-Fe(2)	127.3(2)	N(4)-C(8)-C(9)	110.8(2)
C(30)-N(16)-Fe(2)	115.43(19)	C(10)-C(9)-C(8)	110.6(2)
C(35)-N(17)-C(39)	117.2(3)	N(5)-C(10)-C(9)	110.4(2)
C(35)-N(17)-Fe(1)	127.5(2)	N(5)-C(11)-C(12)	104.6(3)
C(39)-N(17)-Fe(1)	115.17(19)	N(7)-C(12)-C(11)	107.7(3)
N(19)-N(18)-C(40)	110.3(2)	N(7)-C(12)-C(13)	115.1(3)
N(19)-N(18)-Fe(1)	134.46(19)	C(11)-C(12)-C(13)	137.2(3)
C(40)-N(18)-Fe(1)	114.33(18)	N(8)-C(13)-C(14)	122.7(3)
N(18)-N(19)-N(20)	105.5(2)	N(8)-C(13)-C(12)	112.1(3)
N(19)-N(20)-C(41)	112.2(2)	C(14)-C(13)-C(12)	125.1(3)
N(19)-N(20)-C(42)	120.2(2)	C(15)-C(14)-C(13)	118.5(3)
C(41)-N(20)-C(42)	127.6(3)	C(16)-C(15)-C(14)	119.4(3)
C(45)-N(21)-N(22)	112.2(2)	C(15)-C(16)-C(17)	119.0(3)
C(45)-N(21)-C(44)	128.1(2)	N(8)-C(17)-C(16)	123.0(3)
N(22)-N(21)-C(44)	119.7(2)	N(9)-C(18)-C(19)	123.0(3)
N(23)-N(22)-N(21)	105.2(2)	C(20)-C(19)-C(18)	119.1(3)
N(22)-N(23)-C(46)	110.7(2)	C(19)-C(20)-C(21)	119.0(3)
N(22)-N(23)-Fe(2)	133.07(19)	C(20)-C(21)-C(22)	118.6(3)
C(46)-N(23)-Fe(2)	115.03(19)	N(9)-C(22)-C(21)	123.0(3)
C(51)-N(24)-C(47)	117.5(3)	N(9)-C(22)-C(23)	112.6(3)
C(51)-N(24)-Fe(2)	127.3(2)	C(21)-C(22)-C(23)	124.3(3)
C(47)-N(24)-Fe(2)	114.86(19)	N(10)-C(23)-C(24)	107.2(3)

N(1)-C(1)-C(2)	122.7(3)	N(10)-C(23)-C(22)	115.1(3)		
C(1)-C(2)-C(3)	119.3(3)	C(24)-C(23)-C(22)	137.7(3)		
C(2)-C(3)-C(4)	119.1(3)	N(12)-C(24)-C(23)	104.7(3)		
C(5)-C(4)-C(3)	118.8(3)	N(12)-C(25)-C(26)	110.1(3)		
N(1)-C(5)-C(4)	123.1(3)	C(27)-C(26)-C(25)	110.6(3)		
N(1)-C(5)-C(6)	111.6(3)	N(13)-C(27)-C(26)	110.1(2)		
C(4)-C(5)-C(6)	125.3(3)	N(13)-C(28)-C(29)	104.6(3)		
N(2)-C(6)-C(7)	107.2(3)	N(15)-C(29)-C(28)	106.9(3)		
N(2)-C(6)-C(5)	115.7(3)	N(15)-C(29)-C(30)	115.3(3)		
C(28)-C(29)-C(30)	137.8(3)	F(2)-B(1)-F(1)	111.0(4)		
N(16)-C(30)-C(31)	122.9(3)	F(2)-B(1)-F(3)	106.7(5)		
N(16)-C(30)-C(29)	112.1(2)	F(1)-B(1)-F(3)	112.3(5)		
C(31)-C(30)-C(29)	124.9(3)	F(2)-B(1)-F(4)	109.3(4)		
C(30)-C(31)-C(32)	118.6(3)	F(1)-B(1)-F(4)	109.8(4)		
C(33)-C(32)-C(31)	119.1(3)	F(3)-B(1)-F(4)	107.6(4)		
C(32)-C(33)-C(34)	119.4(3)	F(7)-B(2)-F(8)	117.8(5)		
N(16)-C(34)-C(33)	122.7(3)	F(7)-B(2)-F(6)	106.9(5)		
N(17)-C(35)-C(36)	122.6(3)	F(8)-B(2)-F(6)	115.2(5)		
C(37)-C(36)-C(35)	119.7(3)	F(7)-B(2)-F(5)	104.5(5)		
C(36)-C(37)-C(38)	119.0(3)	F(8)-B(2)-F(5)	109.2(4)		
C(37)-C(38)-C(39)	118.4(3)	F(6)-B(2)-F(5)	101.5(5)		
N(17)-C(39)-C(38)	123.1(3)	F(12)-B(3)-F(11)	117.2(6)		
N(17)-C(39)-C(40)	112.1(2)	F(12)-B(3)-F(10)	117.1(6)		
C(38)-C(39)-C(40)	124.8(3)	F(11)-B(3)-F(10)	106.5(5)		
N(18)-C(40)-C(41)	107.9(2)	F(12)-B(3)-F(9)	103.7(5)		
N(18)-C(40)-C(39)	116.2(3)	F(11)-B(3)-F(9)	101.9(6)		
C(41)-C(40)-C(39)	135.9(3)	F(10)-B(3)-F(9)	109.1(6)		
N(20)-C(41)-C(40)	104.1(3)	F(14A)-B(4)-F(13A)	108.9(5)	F(15A)-B(4)-F(13A)	106.3(5)
N(20)-C(42)-C(43)	112.1(2)	F(16A)-B(4)-F(13A)	101.5(5)	F(13B)-B(4)-F(16B)	128.9(10)
C(42)-C(43)-C(44)	109.5(2)	F(14A)-B(4)-F(15A)	123.0(6)	F(14B)-B(4)-F(15B)	93.7(6)
N(21)-C(44)-C(43)	111.5(2)	F(14A)-B(4)-F(16A)	108.3(5)	F(16B)-B(4)-F(14B)	111.4(9)
N(21)-C(45)-C(46)	104.6(3)	F(15A)-B(4)-F(16A)	106.8(5)	F(16B)-B(4)-F(15B)	102.2(8)
N(23)-C(46)-C(45)	107.3(3)	F(13B)-B(4)-F(14B)	111.1(9)		
N(23)-C(46)-C(47)	115.8(3)	F(13B)-B(4)-F(15B)	101.8(8)		

C(45)-C(46)-C(47)	136.8(3)	N(51)-C(52)-C(53)	179.1(5)	N(61)-C(62)-C(63B)	158.4(16)
N(24)-C(47)-C(48)	122.5(3)	N(61)-C(62)-C(63A)	170.5(11)		
N(24)-C(47)-C(46)	112.5(2)	N(71)-C(72)-C(73)	179.1(6)		
C(48)-C(47)-C(46)	125.0(3)				
C(49)-C(48)-C(47)	118.6(3)				
C(48)-C(49)-C(50)	119.5(3)				
C(51)-C(50)-C(49)	119.0(3)				
N(24)-C(51)-C(50)	122.8(3)				

Note: All e.s.d.'s (except the e.s.d. in the dihedral angle between two l.s. planes) are estimated using the full covariance matrix. The cell e.s.d.'s are taken into account individually in the estimation of e.s.d.'s in distances, angles and torsion angles; correlations between e.s.d.'s in cell parameters are only used when they are defined by crystal symmetry. An approximate (isotropic) treatment of cell e.s.d.'s is used for estimating e.s.d.'s involving l.s. planes.

Table S4. Anisotropic displacement parameters ($Å^2 \times 10^3$) for *ap28_sq*

The anisotropic displacement factor exponent takes the form:

$$[-2\pi^2(h^2a^{*2}U_{11} + k^2b^{*2}U_{22} + l^2c^{*2}U_{33} + 2klb^*c^*U_{23} + 2hla^*c^*U_{13} + 2hka^*b^*U_{12})]$$

Atom	U_{11}	U_{22}	U_{33}	U_{23}	U_{13}	U_{12}
Fe(1)	24(1)	21(1)	24(1)	7(1)	2(1)	3(1)
Fe(2)	24(1)	19(1)	23(1)	9(1)	4(1)	6(1)
N(1)	27(1)	23(1)	28(1)	9(1)	5(1)	7(1)
N(2)	30(1)	21(1)	25(1)	8(1)	2(1)	6(1)
N(3)	31(1)	28(1)	27(1)	7(1)	-1(1)	9(1)
N(4)	29(1)	25(1)	30(1)	9(1)	-2(1)	9(1)
N(5)	29(1)	25(1)	24(1)	8(1)	2(1)	11(1)
N(6)	32(1)	21(1)	27(1)	10(1)	6(1)	9(1)
N(7)	27(1)	20(1)	22(1)	9(1)	3(1)	6(1)
N(8)	28(1)	23(1)	23(1)	11(1)	5(1)	7(1)
N(9)	27(1)	24(1)	29(1)	9(1)	1(1)	5(1)
N(10)	26(1)	23(1)	26(1)	6(1)	3(1)	4(1)
N(11)	28(1)	29(1)	28(1)	7(1)	6(1)	4(1)
N(12)	27(1)	29(1)	32(1)	6(1)	7(1)	2(1)
N(13)	25(1)	25(1)	31(1)	10(1)	6(1)	6(1)
N(14)	28(1)	24(1)	28(1)	9(1)	4(1)	5(1)
N(15)	24(1)	20(1)	26(1)	8(1)	4(1)	8(1)
N(16)	28(1)	22(1)	25(1)	9(1)	6(1)	10(1)
N(17)	26(1)	26(1)	25(1)	8(1)	3(1)	4(1)
N(18)	21(1)	22(1)	25(1)	7(1)	2(1)	2(1)
N(19)	26(1)	22(1)	28(1)	8(1)	1(1)	3(1)

N(20)	27(1)	21(1)	24(1)	7(1)	1(1)	3(1)
N(21)	31(1)	22(1)	25(1)	11(1)	4(1)	7(1)
N(22)	29(1)	24(1)	21(1)	10(1)	5(1)	7(1)
N(23)	26(1)	19(1)	26(1)	9(1)	7(1)	6(1)
N(24)	27(1)	23(1)	27(1)	10(1)	7(1)	7(1)
C(1)	31(2)	24(1)	28(2)	8(1)	2(1)	6(1)
C(2)	42(2)	29(2)	30(2)	9(1)	8(1)	13(1)
C(3)	42(2)	38(2)	38(2)	12(2)	19(2)	19(2)
C(4)	31(2)	38(2)	39(2)	12(2)	7(1)	12(1)
C(5)	27(1)	23(1)	30(2)	9(1)	3(1)	4(1)
C(6)	27(2)	23(1)	31(2)	11(1)	3(1)	7(1)
C(7)	27(2)	26(2)	36(2)	9(1)	2(1)	8(1)
C(8)	36(2)	26(2)	28(2)	5(1)	-5(1)	11(1)
C(9)	36(2)	26(2)	29(2)	8(1)	-1(1)	13(1)
C(10)	37(2)	23(1)	30(2)	7(1)	2(1)	14(1)
C(11)	27(2)	27(2)	30(2)	7(1)	3(1)	9(1)
C(12)	25(1)	27(1)	24(1)	9(1)	4(1)	7(1)
C(13)	30(2)	25(1)	23(1)	9(1)	6(1)	7(1)
C(14)	29(2)	33(2)	38(2)	9(1)	9(1)	7(1)
C(15)	30(2)	29(2)	40(2)	8(1)	6(1)	-3(1)
C(16)	37(2)	23(1)	33(2)	8(1)	3(1)	3(1)
C(17)	33(2)	24(1)	32(2)	11(1)	8(1)	6(1)
C(18)	33(2)	27(2)	36(2)	11(1)	5(1)	10(1)
C(19)	42(2)	30(2)	46(2)	14(2)	4(2)	13(1)
C(20)	46(2)	33(2)	55(2)	23(2)	7(2)	11(2)
C(21)	39(2)	36(2)	46(2)	21(2)	12(2)	10(1)
C(22)	29(2)	26(2)	31(2)	9(1)	3(1)	5(1)
C(23)	29(2)	28(2)	32(2)	11(1)	5(1)	4(1)
C(24)	33(2)	31(2)	39(2)	13(1)	8(1)	2(1)
C(25)	28(2)	34(2)	36(2)	6(1)	9(1)	4(1)
C(26)	26(2)	31(2)	34(2)	5(1)	6(1)	3(1)
C(27)	22(1)	31(2)	34(2)	7(1)	2(1)	3(1)
C(28)	29(2)	26(2)	36(2)	14(1)	11(1)	8(1)
C(29)	30(2)	24(1)	28(2)	13(1)	8(1)	11(1)

C(30)	27(1)	23(1)	27(2)	10(1)	6(1)	8(1)
C(31)	39(2)	31(2)	33(2)	16(1)	11(1)	7(1)
C(32)	43(2)	38(2)	28(2)	18(1)	8(1)	12(1)
C(33)	37(2)	32(2)	28(2)	11(1)	4(1)	9(1)
C(34)	29(2)	28(2)	28(2)	11(1)	3(1)	6(1)
C(35)	33(2)	23(1)	33(2)	10(1)	0(1)	2(1)
C(36)	33(2)	31(2)	36(2)	10(1)	-4(1)	-5(1)
C(37)	27(2)	37(2)	41(2)	13(2)	-7(1)	-1(1)
C(38)	31(2)	30(2)	37(2)	12(1)	-2(1)	6(1)
C(39)	26(1)	23(1)	25(2)	5(1)	2(1)	3(1)
C(40)	23(1)	27(1)	25(2)	9(1)	4(1)	4(1)
C(41)	28(2)	26(1)	27(2)	8(1)	-1(1)	6(1)
C(42)	34(2)	20(1)	26(2)	9(1)	3(1)	3(1)
C(43)	38(2)	25(2)	25(2)	9(1)	3(1)	2(1)
C(44)	36(2)	25(1)	21(1)	10(1)	4(1)	7(1)
C(45)	29(2)	28(1)	29(2)	14(1)	4(1)	10(1)
C(46)	27(1)	24(1)	29(2)	14(1)	7(1)	8(1)
C(47)	30(2)	24(1)	31(2)	14(1)	9(1)	9(1)
C(48)	41(2)	41(2)	42(2)	23(2)	15(2)	22(2)
C(49)	50(2)	39(2)	52(2)	22(2)	24(2)	29(2)
C(50)	49(2)	37(2)	39(2)	15(2)	21(2)	22(2)
C(51)	36(2)	30(2)	32(2)	12(1)	11(1)	12(1)
F(1)	52(2)	73(2)	125(3)	50(2)	-13(2)	-9(1)
F(2)	96(2)	48(2)	145(3)	54(2)	9(2)	4(2)
F(3)	134(4)	153(4)	107(3)	33(3)	35(3)	65(3)
F(4)	67(2)	81(2)	99(2)	58(2)	-14(2)	-9(2)
B(1)	48(3)	36(2)	82(4)	28(2)	1(3)	2(2)
F(5)	102(3)	178(5)	205(5)	137(4)	-19(3)	-17(3)
F(6)	106(3)	103(3)	200(5)	29(3)	7(3)	63(3)
F(7)	223(6)	264(7)	85(3)	67(4)	68(3)	155(5)
F(8)	58(2)	121(3)	144(3)	65(3)	-35(2)	12(2)
B(2)	51(3)	54(3)	49(3)	21(2)	0(2)	13(2)
F(9)	141(4)	273(7)	218(6)	186(6)	67(4)	98(5)
F(10)	145(4)	122(4)	191(5)	17(3)	81(4)	59(3)

F(11)	73(2)	181(5)	175(5)	67(4)	-6(3)	41(3)
F(12)	57(2)	215(5)	148(4)	82(3)	43(2)	61(3)
B(3)	43(3)	86(4)	80(4)	42(3)	28(3)	26(3)
F(13A)	102(4)	69(3)	66(3)	14(2)	30(3)	12(3)
F(14A)	160(6)	88(3)	55(3)	51(3)	46(4)	69(4)
F(15A)	66(3)	155(5)	66(3)	30(3)	27(2)	36(3)
F(16A)	102(4)	61(3)	74(3)	31(2)	25(3)	42(3)
F(13B)	141(9)	93(7)	82(7)	37(5)	61(7)	49(8)
F(14B)	91(7)	96(7)	73(7)	42(5)	15(6)	44(6)
F(15B)	71(6)	100(6)	110(7)	47(5)	25(5)	45(5)
F(16B)	144(10)	67(6)	134(8)	56(6)	15(8)	23(7)
B(4)	91(4)	51(3)	67(4)	22(3)	43(3)	27(3)
N(51)	55(2)	57(2)	62(2)	22(2)	3(2)	8(2)
C(52)	46(2)	57(3)	48(2)	17(2)	5(2)	10(2)
C(53)	108(5)	89(4)	95(5)	50(4)	11(4)	5(4)
N(61)	56(2)	67(2)	90(3)	25(2)	13(2)	35(2)
C(62)	48(2)	48(2)	114(4)	25(3)	23(3)	22(2)
C(63A)	67(6)	85(7)	135(13)	53(9)	25(9)	50(6)
C(63B)	67(6)	85(7)	135(13)	53(9)	25(9)	50(6)
N(71)	90(4)	60(3)	103(4)	0(3)	46(3)	20(3)
C(72)	55(3)	40(2)	86(4)	4(2)	29(3)	10(2)
C(73)	99(5)	65(4)	129(6)	16(4)	32(4)	6(3)
O(1W)	110(7)	102(6)	87(6)	58(5)	35(5)	36(5)
O(2W)	96(6)	86(6)	73(5)	31(4)	22(4)	20(5)

Table S5. Hydrogen coordinates ($\times 10^4$) and isotropic displacement parameters ($Å^2 \times 10^3$) for *ap28_sq*

Atom	x	y	z	U(eq)
H(1)	2370	373	1710	36
H(2)	3437	25	899	42
H(3)	5230	433	1522	46
H(4)	5900	1142	2967	45
H(7)	6393	2007	4677	38
H(8A)	6755	2720	6287	40

H(8B)	5782	2339	6558	40
H(9A)	6121	3859	6286	38
H(9B)	5193	3488	6606	38
H(10A)	6387	3710	7850	37
H(10B)	7344	4014	7525	37
H(11)	8079	5664	8098	36
H(14)	8819	7409	8837	42
H(15)	9184	8861	9516	45
H(16)	7836	9380	9791	41
H(17)	6167	8453	9390	37
H(18)	2895	-517	2877	40
H(19)	2524	-1725	3130	49
H(20)	1767	-1765	4182	54
H(21)	1395	-579	4950	48
H(24)	997	906	5663	44
H(25A)	513	2306	6210	43
H(25B)	509	2792	5604	43
H(26A)	2286	3072	6919	41
H(26B)	2338	3522	6284	41
H(27A)	1207	4224	6767	39
H(27B)	1037	3723	7349	39
H(28)	2433	4443	8860	36
H(31)	3885	5343	10432	41
H(32)	5302	6158	11633	43
H(33)	6691	7140	11572	40
H(34)	6659	7293	10337	36
H(35)	788	-348	2385	40
H(36)	-797	-630	1462	47
H(37)	-1292	465	1260	49
H(38)	-138	1842	1985	43
H(41)	1394	3347	2943	35
H(42A)	2925	4747	3789	34
H(42B)	4039	4616	3961	34
H(43A)	3998	4670	5284	39

H(43B)	2849	4739	5111	39
H(44A)	4669	5976	5212	34
H(44B)	3523	6041	4987	34
H(45)	3101	6947	6279	34
H(48)	2722	7919	7682	45
H(49)	2506	8608	8967	50
H(50)	3422	8491	10143	46
H(51)	4523	7691	10012	39
H(53A)	103	7438	152	152
H(53B)	801	8010	1088	152
H(53C)	1299	7505	437	152
H(63A)	8978	4499	1470	107
H(63B)	8174	3979	1790	107
H(63C)	8195	3587	853	107
H(63D)	8763	4192	2471	107
H(63E)	8127	3882	1518	107
H(63F)	9180	4660	1921	107
H(73A)	2676	1104	8177	162
H(73B)	2948	348	7575	162
H(73C)	3846	1220	8145	162
H(1WA)	933	-291	6440	111
H(1WB)	251	189	6572	111
H(2WA)	8093	5536	-82	105
H(2WB)	8149	6320	507	105

Table S6. Selected torsion angles (°) for for *ap28_sq*

C(6)-N(2)-N(3)-N(4)	0.0(3)
Fe(1)-N(2)-N(3)-N(4)	-178.0(2)
N(2)-N(3)-N(4)-C(7)	-0.1(3)
N(2)-N(3)-N(4)-C(8)	-179.8(2)
C(11)-N(5)-N(6)-N(7)	0.1(3)
C(10)-N(5)-N(6)-N(7)	179.2(2)
N(5)-N(6)-N(7)-C(12)	-0.2(3)
N(5)-N(6)-N(7)-Fe(2)	179.1(2)

C(23)-N(10)-N(11)-N(12)	-0.1(3)
Fe(1)-N(10)-N(11)-N(12)	-177.9(2)
N(10)-N(11)-N(12)-C(24)	0.5(3)
N(10)-N(11)-N(12)-C(25)	178.0(2)
C(28)-N(13)-N(14)-N(15)	0.1(3)
C(27)-N(13)-N(14)-N(15)	-177.3(2)
N(13)-N(14)-N(15)-C(29)	-0.1(3)
N(13)-N(14)-N(15)-Fe(2)	179.5(2)
C(40)-N(18)-N(19)-N(20)	0.1(3)
Fe(1)-N(18)-N(19)-N(20)	-168.0(2)
N(18)-N(19)-N(20)-C(41)	0.0(3)
N(18)-N(19)-N(20)-C(42)	179.7(2)
C(45)-N(21)-N(22)-N(23)	0.5(3)
C(44)-N(21)-N(22)-N(23)	-178.1(2)
N(21)-N(22)-N(23)-C(46)	-0.4(3)
N(21)-N(22)-N(23)-Fe(2)	166.00(19)
C(5)-N(1)-C(1)-C(2)	0.1(4)
Fe(1)-N(1)-C(1)-C(2)	-177.2(2)
N(1)-C(1)-C(2)-C(3)	-0.7(5)
C(1)-C(2)-C(3)-C(4)	1.2(5)
C(2)-C(3)-C(4)-C(5)	-1.1(5)
C(1)-N(1)-C(5)-C(4)	0.1(4)
Fe(1)-N(1)-C(5)-C(4)	177.7(2)
C(1)-N(1)-C(5)-C(6)	-179.0(2)
Fe(1)-N(1)-C(5)-C(6)	-1.5(3)
C(3)-C(4)-C(5)-N(1)	0.4(5)
C(3)-C(4)-C(5)-C(6)	179.4(3)
N(3)-N(2)-C(6)-C(7)	0.1(3)
Fe(1)-N(2)-C(6)-C(7)	178.48(19)
N(3)-N(2)-C(6)-C(5)	179.1(2)
Fe(1)-N(2)-C(6)-C(5)	-2.5(3)
N(1)-C(5)-C(6)-N(2)	2.5(4)
C(4)-C(5)-C(6)-N(2)	-176.6(3)
N(1)-C(5)-C(6)-C(7)	-178.8(3)

C(4)-C(5)-C(6)-C(7)	2.1(6)
N(3)-N(4)-C(7)-C(6)	0.2(3)
C(8)-N(4)-C(7)-C(6)	179.8(3)
N(2)-C(6)-C(7)-N(4)	-0.1(3)
C(5)-C(6)-C(7)-N(4)	-178.8(3)
C(7)-N(4)-C(8)-C(9)	118.0(3)
N(3)-N(4)-C(8)-C(9)	-62.4(4)
N(4)-C(8)-C(9)-C(10)	-176.8(3)
N(6)-N(5)-C(10)-C(9)	64.4(4)
C(11)-N(5)-C(10)-C(9)	-116.7(3)
C(8)-C(9)-C(10)-N(5)	175.2(3)
N(6)-N(5)-C(11)-C(12)	0.1(3)
C(10)-N(5)-C(11)-C(12)	-178.9(3)
N(6)-N(7)-C(12)-C(11)	0.3(3)
Fe(2)-N(7)-C(12)-C(11)	-179.2(2)
N(6)-N(7)-C(12)-C(13)	-177.4(2)
Fe(2)-N(7)-C(12)-C(13)	3.1(3)
N(5)-C(11)-C(12)-N(7)	-0.2(3)
N(5)-C(11)-C(12)-C(13)	176.7(3)
C(17)-N(8)-C(13)-C(14)	-0.2(4)
Fe(2)-N(8)-C(13)-C(14)	-178.9(2)
C(17)-N(8)-C(13)-C(12)	178.2(3)
Fe(2)-N(8)-C(13)-C(12)	-0.6(3)
N(7)-C(12)-C(13)-N(8)	-1.6(4)
C(11)-C(12)-C(13)-N(8)	-178.3(3)
N(7)-C(12)-C(13)-C(14)	176.7(3)
C(11)-C(12)-C(13)-C(14)	0.0(6)
N(8)-C(13)-C(14)-C(15)	0.9(5)
C(12)-C(13)-C(14)-C(15)	-177.3(3)
C(13)-C(14)-C(15)-C(16)	-0.7(5)
C(14)-C(15)-C(16)-C(17)	0.0(5)
C(13)-N(8)-C(17)-C(16)	-0.7(4)
Fe(2)-N(8)-C(17)-C(16)	177.9(2)
C(15)-C(16)-C(17)-N(8)	0.8(5)

C(22)-N(9)-C(18)-C(19)	-0.1(4)
Fe(1)-N(9)-C(18)-C(19)	179.6(2)
N(9)-C(18)-C(19)-C(20)	-0.7(5)
C(18)-C(19)-C(20)-C(21)	0.3(5)
C(19)-C(20)-C(21)-C(22)	0.8(5)
C(18)-N(9)-C(22)-C(21)	1.3(4)
Fe(1)-N(9)-C(22)-C(21)	-178.5(2)
C(18)-N(9)-C(22)-C(23)	-178.3(3)
Fe(1)-N(9)-C(22)-C(23)	1.9(3)
C(20)-C(21)-C(22)-N(9)	-1.7(5)
C(20)-C(21)-C(22)-C(23)	177.9(3)
N(11)-N(10)-C(23)-C(24)	-0.3(3)
Fe(1)-N(10)-C(23)-C(24)	177.9(2)
N(11)-N(10)-C(23)-C(22)	178.9(2)
Fe(1)-N(10)-C(23)-C(22)	-2.9(3)
N(9)-C(22)-C(23)-N(10)	0.6(4)
C(21)-C(22)-C(23)-N(10)	-179.0(3)
N(9)-C(22)-C(23)-C(24)	179.4(4)
C(21)-C(22)-C(23)-C(24)	-0.2(6)
N(11)-N(12)-C(24)-C(23)	-0.7(3)
C(25)-N(12)-C(24)-C(23)	-177.8(3)
N(10)-C(23)-C(24)-N(12)	0.6(3)
C(22)-C(23)-C(24)-N(12)	-178.3(4)
N(11)-N(12)-C(25)-C(26)	-70.8(4)
C(24)-N(12)-C(25)-C(26)	106.2(4)
N(12)-C(25)-C(26)-C(27)	175.7(3)
N(14)-N(13)-C(27)-C(26)	74.5(3)
C(28)-N(13)-C(27)-C(26)	-102.3(4)
C(25)-C(26)-C(27)-N(13)	174.3(3)
N(14)-N(13)-C(28)-C(29)	0.0(3)
C(27)-N(13)-C(28)-C(29)	177.1(3)
N(14)-N(15)-C(29)-C(28)	0.2(3)
Fe(2)-N(15)-C(29)-C(28)	-179.54(19)
N(14)-N(15)-C(29)-C(30)	178.4(2)

Fe(2)-N(15)-C(29)-C(30)	-1.3(3)
N(13)-C(28)-C(29)-N(15)	-0.1(3)
N(13)-C(28)-C(29)-C(30)	-177.8(3)
C(34)-N(16)-C(30)-C(31)	1.8(4)
Fe(2)-N(16)-C(30)-C(31)	-178.4(2)
C(34)-N(16)-C(30)-C(29)	-176.7(2)
Fe(2)-N(16)-C(30)-C(29)	3.1(3)
N(15)-C(29)-C(30)-N(16)	-1.3(4)
C(28)-C(29)-C(30)-N(16)	176.2(3)
N(15)-C(29)-C(30)-C(31)	-179.7(3)
C(28)-C(29)-C(30)-C(31)	-2.2(6)
N(16)-C(30)-C(31)-C(32)	-0.7(5)
C(29)-C(30)-C(31)-C(32)	177.6(3)
C(30)-C(31)-C(32)-C(33)	-0.3(5)
C(31)-C(32)-C(33)-C(34)	0.1(5)
C(30)-N(16)-C(34)-C(33)	-2.0(4)
Fe(2)-N(16)-C(34)-C(33)	178.2(2)
C(32)-C(33)-C(34)-N(16)	1.1(5)
C(39)-N(17)-C(35)-C(36)	-0.1(5)
Fe(1)-N(17)-C(35)-C(36)	175.6(3)
N(17)-C(35)-C(36)-C(37)	-1.0(5)
C(35)-C(36)-C(37)-C(38)	0.8(6)
C(36)-C(37)-C(38)-C(39)	0.4(5)
C(35)-N(17)-C(39)-C(38)	1.3(5)
Fe(1)-N(17)-C(39)-C(38)	-175.0(3)
C(35)-N(17)-C(39)-C(40)	-178.7(3)
Fe(1)-N(17)-C(39)-C(40)	5.0(3)
C(37)-C(38)-C(39)-N(17)	-1.4(5)
C(37)-C(38)-C(39)-C(40)	178.6(3)
N(19)-N(18)-C(40)-C(41)	-0.2(3)
Fe(1)-N(18)-C(40)-C(41)	170.5(2)
N(19)-N(18)-C(40)-C(39)	-178.9(2)
Fe(1)-N(18)-C(40)-C(39)	-8.2(3)
N(17)-C(39)-C(40)-N(18)	2.0(4)

C(38)-C(39)-C(40)-N(18)	-178.0(3)
N(17)-C(39)-C(40)-C(41)	-176.2(3)
C(38)-C(39)-C(40)-C(41)	3.8(6)
N(19)-N(20)-C(41)-C(40)	-0.2(3)
C(42)-N(20)-C(41)-C(40)	-179.7(3)
N(18)-C(40)-C(41)-N(20)	0.2(3)
C(39)-C(40)-C(41)-N(20)	178.6(3)
N(19)-N(20)-C(42)-C(43)	-66.4(4)
C(41)-N(20)-C(42)-C(43)	113.2(3)
N(20)-C(42)-C(43)-C(44)	-176.1(3)
C(45)-N(21)-C(44)-C(43)	-114.0(3)
N(22)-N(21)-C(44)-C(43)	64.5(3)
C(42)-C(43)-C(44)-N(21)	176.7(3)
N(22)-N(21)-C(45)-C(46)	-0.5(3)
C(44)-N(21)-C(45)-C(46)	178.1(3)
N(22)-N(23)-C(46)-C(45)	0.1(3)
Fe(2)-N(23)-C(46)-C(45)	-168.95(19)
N(22)-N(23)-C(46)-C(47)	177.3(2)
Fe(2)-N(23)-C(46)-C(47)	8.2(3)
N(21)-C(45)-C(46)-N(23)	0.2(3)
N(21)-C(45)-C(46)-C(47)	-176.1(3)
C(51)-N(24)-C(47)-C(48)	-0.3(4)
Fe(2)-N(24)-C(47)-C(48)	174.2(2)
C(51)-N(24)-C(47)-C(46)	-179.5(3)
Fe(2)-N(24)-C(47)-C(46)	-5.0(3)
N(23)-C(46)-C(47)-N(24)	-1.9(4)
C(45)-C(46)-C(47)-N(24)	174.1(3)
N(23)-C(46)-C(47)-C(48)	178.9(3)
C(45)-C(46)-C(47)-C(48)	-5.1(6)
N(24)-C(47)-C(48)-C(49)	0.3(5)
C(46)-C(47)-C(48)-C(49)	179.4(3)
C(47)-C(48)-C(49)-C(50)	-0.1(5)
C(48)-C(49)-C(50)-C(51)	-0.1(5)
C(47)-N(24)-C(51)-C(50)	0.1(4)

Fe(2)-N(24)-C(51)-C(50)	-173.6(2)
C(49)-C(50)-C(51)-N(24)	0.1(5)

Note: All e.s.d.'s (except the e.s.d. in the dihedral angle between two l.s. planes) are estimated using the full covariance matrix. The cell e.s.d.'s are taken into account individually in the estimation of e.s.d.'s in distances, angles and torsion angles; correlations between e.s.d.'s in cell parameters are only used when they are defined by crystal symmetry. An approximate (isotropic) treatment of cell e.s.d.'s is used for estimating e.s.d.'s involving l.s. planes.